GUGGENHEIM AERONAUTICAL LABORATORY

CALIFORNIA INSTITUTE OF TECHNOLOGY



HYPERSONIC RESEARCH PROJECT

Memorandum No. 62
July 1, 1961

# DEVELOPMENT AND CALIBRATION OF A COLD WIRE PROBE FOR USE IN SHOCK TUBES

by

Walter H. Christiansen

ARMY ORDNANCE CONTRACTS
NO. DA-04-495-Ord-1960 and 3231

GUGGENHEIM AERONAUTICAL LABORATORY
CALIFORNIA INSTITUTE OF TECHNOLOGY
Pasadena, California

HYPERSONIC RESEARCH PROJECT

Memorandum No. 62

July 1, 1961

# DEVELOPMENT AND CALIBRATION OF A COLD WIRE PROBE FOR USE IN SHOCK TUBES

by

Walter H. Christiansen

Clark B. Millikan, Director
Guggenheim Aeronautical Laboratory

ARMY ORDNANCE CONTRACTS NO. DA-04-495-Ord-1960 and 3231

## ABSTRACT

The use of a fine unheated wire for making shock tube flow measurements is investigated. The operation of the instrument depends on the transient nature of the shock tube flow. The wire is referred to here as a cold wire; it operates in a non-steady manner which is completely different from the usual hot wire operation. This report describes the construction and calibration of the cold wire.

The experimental law for the rate of gain of heat to the wire in air is determined over a range of Mach numbers from 0.4 to 1.9 and a range of Reynolds numbers from 0.035 to 3,500 based on the wire diameter and the conditions in the hot flow following the initial shock wave. Similar measurements are reported for argon. The heat transfer measurements cover the continuum region, the slip and transitional regions, and extend into the free-molecule flow region. The dimensionless results are compared with hot wire measurements obtained in wind tunnels and are found to differ slightly. A difference exists because the cold wire gains heat from the fluid while the hot wire loses heat to the fluid. The measurements are very repeatable and self-consistent, and they indicate that the wire can be used to give an accurate flow measurement in the shock tube.

Some potential applications of the wire for the study of shock-tube flows are presented. It is concluded that the fine unheated wire is a versatile tool that can be used to great advantage in the shock tube.

## ACKNOWLEDGMENT

I wish to acknowledge Dr. Anatol Roshko for his assistance and encouragement during the course of this project. I also wish to express my appreciation to my wife, Joan, for typing the manuscript and to Mrs. Betty Wood for preparing the figures.

TABLE OF CONTENTS

TABLE OF CONTENTS (cont'd.)

LIST OF FIGURES

LIST OF FIGURES (cont'd.)

# LIST OF SYMBOLS

| | |
|---|---|
| $\mathcal{R}$ | Aspect ratio $\ell/d$ |
| a | Speed of sound |
| c | Specific heat |
| $c_v$ | Specific heat at constant volume |
| $c_p$ | Specific heat at constant pressure |
| C | Capacitance |
| $\bar{c}$ | Mean molecular speed |
| d | Diameter of wire or diameter of shock tube, depending on context |
| E | Oscilloscope voltage |
| h | Specific enthalpy |
| I | Current |
| k | Thermal conductivity |
| Kn | Knudsen number, $\Lambda/d$ |
| $\ell$ | Length of wire |
| m | Mass of wire $\frac{\pi d^2 \ell}{4} \rho$ |
| M | Mach number |
| N | Number of particles per unit volume |
| Nu | Nusselt number $\frac{qd}{k\Delta T}$ |
| P | Pressure |
| Pr | Prandtl number $c_p \mu / k$ |
| Q | Heat transfer rate, $q\pi d\ell$ |
| q | Heat transfer rate per unit area |
| R | Resistance or gas constant, depending on context |
| $R_s$ | Series resistance |

| | |
|---|---|
| $R_p$ | Parallel resistance |
| Re | Reynolds number, $\frac{\rho u d}{\mu}$ |
| s | Molecular speed ratio, $u/\overline{c}$ |
| s' | Laplace transform of time |
| St | Stanton number, $\frac{Nu}{Pr\,Re}$ |
| t | Time |
| T | Temperature |
| U, u | Velocity |
| V | Battery voltage |
| x | Distance from shock tube diaphram |
| $\alpha$ | Thermal coefficient of resistivity or energy accommodation coefficient, depending on context |
| $\gamma$ | Ratio of specific heats, $c_p/c_v$ |
| $\delta$ | Some characteristic length |
| $\eta$ | $T_r/T_t$ |
| $\lambda$ | Non-dimensional length, $\frac{Nuk_a}{kw}\left(\frac{\ell}{d}\right)^2$ |
| $\Lambda$ | Mean free path of the gas |
| $\mu$ | Viscosity |
| $\nu$ | Kinematic viscosity, $\frac{\mu}{\rho}$ |
| $\xi$ | Reciprocal of Knudsen number |
| $\rho$ | Density |
| $\sigma$ | Specific resistance |
| $\tau$ | Two-dimensional time constant of wire, $\frac{d^2\rho_w c_w}{4Nuk}$ |
| $\tau'$ | Temperature loading of wire, $\frac{T_w - T_r}{T_r}$ |

## Subscripts

| | |
|---|---|
| a | Air |
| i | Some initial condition |
| r | Recovery temperature of wire |
| s | Shock wave |
| t | Stagnation conditions |
| w | Wire |
| 1 | Conditions in the shock tube before arrival of primary shock wave |
| 2 | Conditions in the region immediately following primary shock wave |
| 5 | Conditions behind assumed bow shock wave on wire in region 2 for $M_2 > 1$ |

## Superscript

| | |
|---|---|
| — | Mean or normalized quantity |

Other symbols are defined as they appear in the text.

# I. INTRODUCTION

The possibility of measuring flow velocity by measuring the heat loss of an electrically heated wire appears to have been first suggested by Kennelly (Ref. 1). Subsequent work by King (Ref. 2) theoretically predicted and experimentally verified the heat loss from a heated cylindrical wire. His analysis, although based on an inaccurate heat transfer mechanism, predicts a functional relationship between heat transfer and flow velocity in an incompressible fluid. Largely through his efforts, the hot wire anemometer has become a standard technique for measuring mean velocities in a fluid. Using suitable electronic compensation to eliminate the thermal inertia of the wire, Dryden and Kuethe (Ref. 3) developed the measurement technique to the point where the hot wire could be used to measure fluctuating flow velocities.

Interest in compressible flows has resulted in a re-examination of the hot wire anemometer as a flow instrument. Compressibility introduces additional complications (e.g., there are now three parameters of the flow that control wire response instead of only the velocity), and the effective use of the hot wire in compressible flows is a result of many experimenters' efforts, notable among which are the works of Kovasznay (Ref. 4) and Laufer and McClellan (Ref. 5). Their researches helped to establish an experimental law for the loss of heat from a wire in a compressible fluid.

The relative word "hot" has to be defined with respect to a temperature. A wire is "hot" if its temperature exceeds that of the recovery temperature of the wire, that is, the temperature of an

unheated wire when it is in equilibrium with the flow. For incompressible flow (M = 0), this temperature is known to be the total temperature of the flow (which is equal to the static temperature). For compressible flow, however, the recovery temperature is not the total temperature of the flow. Experimentally it is found that this temperature depends appreciably on the flow Mach number and Reynolds number. For a monatomic gas, for example, this temperature may range from 0.94 $T_t$ ($T_t$ = total temperature) to 1.25 $T_t$ depending on the flow conditions (see section V.4).

The hot wire will run hot with respect to the recovery temperature under all conditions of operation. Hence, the heat transfer corresponding to the joule heating of the wire will always be represented as a heat loss from the wire. All experimental work with hot wires represents the results of heat loss from wires.

Recently, various experimenters have used the hot wire anemometer in the shock tube (Refs. 6, 7, and 8). Shock tubes are operated so that there is no mean flow initially and the flow field is established instantaneously behind a moving shock wave. Because of its finite thermal lag, the wire responds to this transient flow situation in a non-steady manner. To use the wire as a hot wire anemometer in this case, the non-steady response of the wire has to be corrected for or be eliminated. This is done by using suitable electrical compensation to eliminate the problem of thermal lag. If this correction is suitably accomplished, the wire operates as if it were in a steady flow, and the steady state techniques and all the experimental information regarding the use of hot wires in wind tunnels can be used.

Accurate compensation is difficult to accomplish when using the constant current hot wire since proper compensation must be known prior to each shot. In cases of unknown flows or where the shock Mach number is somewhat random, this compensation is impossible to accomplish with any precision, since the compensation depends on the flow.

However, the main disadvantage of the hot wire is that it cannot be used at high shock Mach numbers because of the high total temperature in the flow behind the shock wave. For example, at a shock Mach number of only 2 in argon, the total temperature of the flow is 750°C. The hot wire must run at a temperature exceeding this value, since the recovery temperature is given approximately by the total temperature. At higher temperatures, standard hot wire operation is not feasible because the wire would burn out. Thus, the hot wire can be used only at low shock speeds. Dosanjh (Ref. 6) limited himself to low shock speeds ($M_s < 1.2$), and did measure stagnation temperature and mass flow jumps across the shock wave. He also successfully developed the hot wire as a means of detecting weak shock waves for timing and triggering purposes.

The process of heat loss from a wire can be reversed if the wire operates in a non-steady (uncompensated) fashion. In this case, the wire temperature is less than the recovery temperature of the flow, and the heat is transferred into the wire in contrast to hot wire operation. Such a non-steady wire operation can exist in the transient flow in the shock tube. The time required for a wire to come to equilibrium with its surroundings is measured by its time constant (a measure of

the thermal lag of the wire). A wire that is operating within this characteristic time behaves in a non-steady fashion when exposed to the instantaneous flow field established in the shock tube. The wire can be maintained in a non-steady operation for the whole duration of the hot flow if its time constant is sufficiently large.

A particularly simple case occurs when the joule heating of the wire is practically zero and all the heating is caused by the flow. Then the joule heating of the wire does not contribute or interact with the heat being convected to the wire, and this fact makes the signal output of the wire easier to interpret. A wire operating under these conditions will be referred to as a "cold wire". The purpose of this research is to investigate the experimental law governing the gain of heat to cold wires over as wide a range of running conditions as possible and to investigate the potentialities of the wire as a shock tube flow instrument.

A photograph of the wire and its mounting is shown in Figure 1. Figure 2 shows the silhouettes of two of the wire probes that were used in this investigation. The larger probe holds a 0.0005 inch diameter wire while the smaller probe holds a 0.00005 inch diameter wire. The probe uses only a small excitation current to produce a voltage signal across the wire. There is essentially no joule heating in the wire, and it practically maintains the temperature of its surroundings before the initiation of the hot flow. After the shock wave passes, the wire and its supports begin to heat up. This heating continues until the wire reaches an equilibrium temperature or until the hot flow ceases. The resulting change of wire temperature produces a resistance change

which is conveniently read as a voltage on an oscilloscope. When the excitation current is adjusted so that there is no appreciable heating of the wire ($\Delta T = T_w - T_i = O(1^{\circ}C.)$), the resulting output signal is approximately 0.25 mv/$^{\circ}$C. This sensitivity is representative of all the wires used in this investigation.

The wire is assumed to be a perfect calorimeter*; that is, all the heat convected to the wire is stored in the wire itself. Actually it is not a perfect calorimeter because, after the passage of the shock wave, the wire supports are not at the same temperature as the wire. However, these support effects are non-steady in nature, and it will be shown that there are some conditions and certain times for which these effects are negligible.

Quantitative heat transfer measurements can be made if the physical constants $\alpha$, $\rho$, c, and the geometrical quantities d and $\ell$ are known. Thus, there are two additional physical constants ($\rho$ and c) to evaluate when this method of measuring heat transfer is used, as compared to steady state measurements with a hot wire. An electrical calibration method is developed to evaluate them. Heat transfer measurements are made over a wide range of Reynolds numbers and Mach numbers in two test gases, air and argon. The results, obtained from the heat transfer measurements made just after the passage of the shock wave, determine an experimental heat transfer law for the gain of heat by a cold wire in a compressible fluid. These results, expressed in standard non-dimensional parameters, are compared with measurements obtained with the use of hot wires in wind tunnels and found to

---

* Calorimetric methods of heat transfer have been used before in shock tubes (Refs. 9 and 10).

differ slightly. A difference is to be expected because the cold wire gains heat from the fluid while the hot wire loses heat to the fluid. This difference depends on the flow conditions and may reduce the Nusselt number (see section V) by as much as twenty per cent from the corresponding value one would obtain if the wire temperature was nearly the recovery temperature.

The measurements are very repeatable and self-consistent, and they indicate that the wire can be used to give a creditable flow measurement in the shock tube.

There are various possibilities of using the wire as an effective flow instrument. A brief critique of some of the more likely uses is presented in section VI together with the pertinent features of the wire response. Whenever possible, the response is illustrated by an oscillograph of the wire under the particular circumstances. Emphasis is placed on the possible study of the structure of a traveling shock wave using the cold wire technique.

# II. EXPERIMENTAL ARRANGEMENT

## 1. Shock Tubes

Two shock tubes were employed in making the measurements. A three-inch square shock tube described in Reference 11 was used for the higher pressure (Reynolds numbers) air measurements. Physically, it remains unchanged except that the nozzle has been replaced by a dump chamber. In its present condition, the leak rate of the low pressure section is less than 100 $\mu$Hg/min, and it can be evacuated to a pressure of 500 $\mu$Hg with a high vacuum Welch Duo-Seal pump. Figure 3 shows the present arrangement of this shock tube.

A two-inch round shock tube (Ref. 12) was used for the lower pressure measurements in air and for the argon measurements. Its vacuum integrity was much better than the square shock tube. A Consolidated Vacuum Corporation MCF 700-04 oil diffusion pump was placed directly on the shock tube dump chamber and, with the Welch pump, produced an ultimate vacuum of approximately 0.1 $\mu$Hg with a leak rate which was less than 1 $\mu$Hg/min after being under high vacuum for some time.

## 2. Measurement of Shock Tube Initial Conditions

The shock speed was measured in standard fashion with two thin film gages placed some distance apart (usually two feet). Some difficulty was encountered in detecting weak shocks at low pressures. The sensitivity for detecting weak shocks was increased by resorting to higher resistance gage elements. Gage resistances of 500 ohms and currents of 50 ma solved the problem. The output of the gages was fed

through high gain amplifiers and then to a Berkeley counter. The gages were wired independently except for attenuation measurements where it was found necessary to run them in series by pairs. The shock Mach numbers that were measured covered a range from 1.25 to approximately 6. The accuracy of this measurement was $\pm$ 0.3 per cent.

The initial pressures in the expansion chamber were measured with an aircraft type manometer for the high pressures and a Wallace and Tiernan 0 - 50 mm Hg gage for the intermediate pressure range. These gages were carefully calibrated with known reference volumes. For the low pressures, a McLeod gage was used for direct measurement. This instrument had two pressure ranges, 0 - 5 mm Hg and 0 - 100 $\mu$Hg. The pressures that were used in the experiment were 0.1, 0.5, 5, 50, and 500 mm Hg. The accuracy of the pressure measurements using the aircraft type manometer and the Wallace and Tiernan gage was better than 1 per cent. The accuracy of the McLeod gage was only $\pm$ 4 per cent.

Because of the sensitivity of the wire to temperature variations, the initial (room) temperature was monitored. To facilitate the reduction of data, this temperature was kept at 300°K $\pm$ 1 per cent for these measurements.

## 3. Range of Shock Tube Operation; Limitations

The shock tube was operated over a wide range of running conditions with two test gases, air and argon. For convenience, the approximate range of some of the important flow quantities for both gases is summarized below.

| | Air | | Argon | |
|---|---|---|---|---|
| | Minimum | Maximum | Minimum | Maximum |
| $M_s$ | 1.3 | 6.5 | 1.5 | 5.5 |
| $M_2$ | 0.4 | 2 | 0.5 | 1.25 |
| $T_t$ | 430°K | 3400°K | 500°K | 4700°K |
| Re | 0.035 | 3500 | 0.055 | 105 |

There are other considerations and limitations using the present shock tube setup. These will be discussed briefly.

(a) Randomness of $M_s$ : The shock Mach number could not be controlled precisely ($\pm$ 20 per cent) with the present shock tubes because the rupturing pressure of the diaphram, determining the shock Mach number, could not be predetermined. Some regulation was maintained by using different driver gases ( $N_2$ and He ) and by using an area reduction section near the diaphram to control the lower $M_s$. The area reduction technique (Ref. 13) proved highly successful, and was the only means available to achieve low $M_s$ at low pressures.

(b) Shock wave attenuation: The probe was placed in the shock tube one foot downstream of the shock-wave-detecting gages in the round tube and two feet downstream of the shock-wave-detecting gages in the square tube. The shock wave attenuation in the round tube was measured using argon and air as test gases to see if the shock speed could change significantly between the measured value upstream of the

probe and the actual value at the probe itself. Measurements were made only in the smaller round tube because it was felt that this shock tube would represent the case of the largest attenuation. From the results, it was concluded that, at the test section of the round tube, the attenuation was small since $\frac{\Delta M_s}{M_s \Delta x} \sim 0.005$ where $\Delta x$ is measured in feet. The maximum change in shock Mach number is then 1/2 per cent for a one-foot distance. This change was neglected. In Appendix B the results of the attenuation measurements are given.

(c) Decrease in testing time: Ideally, the Reynolds number range could have been extended if the operating pressures ($P_1$) could have been lowered. However, the boundary layer in the shock tube acts as a mass-loss mechanism between the contact surface and shock wave which appreciably shortens the flow duration at low pressures (Ref. 14). No heat-transfer measurements were made when the testing time was shorter than 50 $\mu$sec (usually the testing time was approximately 500 $\mu$sec). Measurements of heat transfer using helium as a test gas were attempted during this investigation, but because of the severe decrease in testing time (testing times of the order of 20 $\mu$sec) they had large scatter and were thought to be inconclusive. Therefore, they are not presented.

## 4. Construction of the Probe

The wires can be made of practically any metal such as nickel, aluminum, or platinum. The maximum signal output, tensile strength, and commercial availability should be kept in mind. In the heat transfer investigations, platinum, a platinum-rhodium alloy, and tungsten wires were used with diameters comparable to those of hot wires – roughly

0.00001 inch to 0.001 inch (see section III.3 for the selection of wires and Table 1 for the actual diameters used). These are readily available from commercial firms. Each wire gives a good signal due to a flow in the shock tube, but tungsten has the obvious advantage of high tensile strength. However, it is available only in limited sizes.

The wire is conveniently supported by two sewing needles (or jeweler's broaches for the smaller wires) held in a bakelite wedge (see Figs. 1 and 2). The wedge is attached to a side wall plug with electrical leads and inserted into the shock tube. For heat-transfer measurements, the wire is placed perpendicular to the flow and centered on the shock tube axis to minimize any shock tube boundary layer and wall effects. The wedge is removable from the plug for convenience in replacing broken wires or installing wires of different diameters. The electrical connections are made with the pin connectors from Winchester plugs such as type MRE 20S. These are gold plated and make good electrical contact.

The platinum or platinum-alloy wires are directly soldered to the supports while tungsten must be copper plated first. In the latter case, a thin layer of copper is deposited on the whole length of wire using a copper sulphate solution. It is then soldered to the supports. The plating process then is reversed to leave the wire bare. Spot welding the tungsten wire to the supports is another method of attaching it to the needles. Some damage is done to the supports and wire with this method, but it is more convenient and requires less time than copper plating. Both methods result in good electrical connections.

The construction of the gage provided for a fairly large aspect ratio ($\ell/d$) to minimize any aerodynamic interference of the supports. This aspect ratio was held between 600 and 1200. For constant aspect ratio, the completed gage has a characteristic resistance proportional to the inverse of the diameter

$$R_w = \frac{\sigma \ell}{\frac{\pi d^2}{4}} = \frac{4 \sigma AR}{\pi} \left(\frac{1}{d}\right)$$

The gage resistances varied from 2 ohms to 1000 ohms at room temperature.

## 5. Probe Operating Conditions; Circuitry

A Wheatstone bridge (see Fig. 4) measured the initial resistance of the gage elements and also supplied the necessary d. c. excitation current. It could measure any resistance between 0 - 1000 ohms to an accuracy of better than one per cent.

In making the heat transfer measurements, great care was exercised in monitoring the gage resistance between shock tube runs. If it changed appreciably, that is, approximately one per cent, from its resistance prior to use in the shock tube, it was discarded on the basis that the wire calibration constant had changed. This did not occur often. For example, the tungsten wires have an amazing durability if carefully built. Wires made from 0.005 inch tungsten have lasted more than twenty consecutive runs in the shock tube at $M_s \sim 4$ and $p_1 \sim 10$ mm Hg.

The wire was operated at constant current as shown in Figure 4. The probe excitation current was monitored with a precision ($\pm$ 1/10

per cent) one ohm resistor and a Leeds and Northrup potentiometer. The excitation current was set so that difference between the initial temperature of the surroundings and the wire temperature was less than $1^{\circ}C$. Figure 5 shows an estimate of the current necessary to heat a wire moderately in still air as a function of the ratio of the mean free path of the gas to the wire diameter. This curve was based on some experimental results using a 0.0005 inch diameter tungsten wire heated to $10^{\circ}C$. in the two inch shock tubes. Dimensional analysis suggested the relevant parameters for a fixed test medium at moderate wire temperature to be

$$\frac{I^2 \sigma}{d^2 k_a (T_w - T_a)} = f\left(\frac{\Lambda}{d}\right)$$

where $\sigma$ is the specific resistance of the wire material at the wire operating temperature. Included in this figure are some results derived from the basic heat transfer data of Billington (Ref. 7) for a 0.0001 inch platinum wire in still air. A few points using argon are included for comparison. The results, agreeing well with one another, indicate that the correct parameters were chosen.

## 6. Oscilloscope and Method of Obtaining Data

The gage output was fed to a Tektronix 535 oscilloscope with a 53C/54D preamplifier that had a maximum sensitivity of $10^{-3}$ v/cm. At this maximum sensitivity, the band width of the scope was 300 KC, but increased as the sensitivity was lowered. This band width did not affect the gage signals to any appreciable extent. The noise level of the signal was less than 100 microvolts. The scope was externally

triggered using one of the signals from a thin film gage in conjunction with a delay pulse generator.

The wire response was photographed for each shot using a Polaroid Land camera, and a calibration of the oscilloscope (both voltage and time) was usually added to the record. The sweep speed and gain of the scope was adjusted so that only the initial portion of the wire response was filmed. This was the only portion of the wire response which was of interest for the heat transfer measurements. By doing this, maximum sensitivity was obtained, and the response appeared nearly linear (see section III). Under such conditions, the initial slope, proportional to the heat transfer rate to the wire (see section III. 2), is easily read as $\left.\frac{\Delta E}{\Delta t}\right|_{t = 0}$. The over-all accuracy of this portion of the measurement is one to five per cent depending on the magnitude of the slope.

# III. COLD WIRE CHARACTERISTICS

## 1. Cold Wire Response and Time Constants

When a fine wire is suddenly subjected to a hot or cold flowing fluid, it strives to achieve thermal equilibrium with the flow. The manner in which it does this is the subject of this section.

Before discussing the nature of the cold wire response, it is necessary to define a time (not the characteristic time required to establish equilibrium) of the instrument below which the transient response of the wire is dominated, not by the standard thermal lag of the wire, but by the readjustment of the flow over the wire or by a readjustment of the temperature distribution within the wire itself. The response of the instrument is then limited by two characteristic times: (1) the characteristic time it takes to set up flow around the wire, and (2) the characteristic time it takes to heat the wire uniformly throughout its volume.

(1) The time required to establish flow over the wire is less than $10\ d/U$. For a 1 mil diameter wire and a velocity equal to 1000 ft/sec, this time is approximately 1 $\mu$sec.

(2) The effective time for penetration of a pulse of heat is

$$t \sim \frac{\rho_w c_w \delta^2}{k_w}$$

If $\delta$ is taken to be equal to the radius of the wire, then this characteristic time is $t \sim 6.4$ $\mu$sec for a 1 mil platinum wire and 2.8 $\mu$sec for a 1 mil tungsten wire. Hence, under most conditions in the shock tube, even those that involve testing times of the order of 100 $\mu$sec,

a fine wire ($d \lesssim 0.001''$) can be considered to be in steady flow and uniform in temperature. For smaller wires, of course, these times are much smaller.

To derive the equation of the wire response, an energy balance of the wire is used*.

Heat Stored =

Heat Produced in Interior + Heat Convected + Heat Conducted (1)
(Joule Heat) (Forced Convection) (To Supports)

In Appendix A, the solution of this equation is obtained for a cold wire ($I^2 R \approx 0$). The solution indicates that for certain conditions and times, the support heat losses are small and can be neglected for all practical purposes. In particular, the analysis shows that initially (i.e., just after the arrival of the shock wave) there is no heat lost to the supports. Therefore, for the following analysis the assumption is made that the wire does not have any heat conduction losses to the supports. Then there will be no spatial variation of temperature in the wire. For a cold wire, the joule heat term is zero and thus

$$\frac{d}{dt} mc_w(T_w - T_i) = Q_{\text{forced convection}} \qquad (2)$$

This equation can be integrated with the assumption of constant material properties and a functional dependence of $Q$ on $T_w$,

---

*At very low densities, radiation may have to be taken into account. Note, however, that initially there are no radiation losses for a cold wire because $T_w$ equals the temperature of the surroundings before the initiation of the hot flow.

$$\int_{T_i}^{T_w} \frac{\pi d^2 \ell \rho_w c_w}{4} \frac{dT_w}{Q} = \int_{T_i}^{T_w} \frac{\frac{\pi d^2 \ell}{4} \rho_w c_w dT_w}{q \pi d} = \int_0^t dt$$

$$\frac{d \rho_w c_w}{4} \int_{T_i}^{T_w} \frac{dT_w}{q} = t \qquad (3)$$

For the fine wire calorimeter gage, the heat transfer q is not constant since the temperature difference between the wire and flow decreases as the wire heats up. Hot wire results (Ref. 5) show that the Nusselt number is reasonably constant for fixed flow conditions and all heat transfer rates, especially at the higher Reynolds number flows*. Define

$$Nu = \frac{Q}{\pi k \ell (T_r - T_w)} = \frac{qd}{k(T_r - T_w)}$$

Substituting into equation 3, we get

$$\frac{d \rho_w c_w}{4} \int_{T_i}^{T_w} \frac{dT_w}{\frac{Nuk}{d}(T_r - T_w)} = t = \frac{d^2 \rho_w c_w}{4Nuk} \int_{T_i}^{T_w} \frac{dT_w}{T_r - T_w}$$

and

$$T_w = T_r - (T_r - T_i) e^{-\frac{4Nukt}{d^2 \rho_w c_w}} \qquad (4)$$

The time constant for this idealized case is the intercept of the initial

---

* This assumption is actually good for small temperature jumps where the temperature loading of the wire does not change appreciably. At higher $M_s$, these jumps are large and probably affect Nu.

slope of the response with $T_r$. This gives for the response time (a measure of the time for thermal adjustment of the wire),

$$\tau = \frac{d^2 \rho_w c_w}{4Nuk} \tag{5}$$

Typical time constants range from 0.1 to 10 msec. Usually for the larger wire diameters, these times are longer than the uniform flow times encountered in the shock tube. The time constant of a 1 mil tungsten wire in the hot flow following the initial shock wave was calculated as a function of the initial pressure and shock Mach number for air based on experimental heat transfer measurements and free molecule theory with $\alpha = 1$. It is shown in Figure 6. The predominant behavior noticed from the curves is the large decrease in time constant with increasing Mach number and pressure. For example, increasing the shock Mach number from 2 to 8 at a fixed pressure reduces the time constant by a factor of 10. Variations in diameter result in a varying time constant, and this effect can be estimated. It may be shown that, for Reynolds number flows greater than 20, the time constant varies as $d^{3/2}$, while for Reynolds numbers less than 0.2, the time constant varies as $d$ when the flow conditions are fixed.

## 2. Calculation of Probe Outputs

In achieving equilibrium, a temperature rise of the wire is accompanied by a resistance variation of the wire;

$$R_w = R_i(1 + \alpha_i(T_w - T_i)) \tag{6}$$

The subscript i denotes some initial conditions where the properties of the wire are known. If a current is passed through the wire, the voltage drop across it is equal to

$$IR_w = E = IR_i(1 + \alpha_i(T_w - T_i)) \tag{7}$$

The variation in voltage will be $\Delta E$ .

$$\Delta E = \Delta I R_w + I \Delta R_w \tag{8}$$

If the voltage source has a high impedance compared to the wire, the current will be essentially constant. This will simplify the computations and reduction of data although it is not a necessary simplification*. Then

$$\Delta E = I \Delta R_w = I R_i \alpha_i (T_w - T_i) \tag{9}$$

A typical element made of tungsten with a diameter of 0.0005 inches and length of 0.5 inches has a resistance of approximately 6 ohms. With I = 10 ma and $\alpha_i$ = 0.004 / $^{o}$C, a voltage of 0.24 mv/ $^{o}$C is obtained. This seems like a small signal, but it should be remembered that large temperature differences are encountered in the shock

---

* Platinum-rhodium wires used in this report with a diameter of 0.00001 inches had an approximate resistance of 1000 ohms. Changes in resistance of 1000 ohms are not uncommon. The impedance load of the heating circuit used was 7500 ohms, and therefore the wire could not be operated at constant current. Corrections for the finite impedance voltage source have to be made for this case, i.e.,

$$\Delta E = \frac{V R_s}{(R_s + R_i)^2} \Delta R \left[ 1 - \frac{\Delta R}{R_s + R_i} + \left( \frac{\Delta R}{R_s + R_i} \right)^2 + \ldots \right]$$

tube and the heat content of the wire is small. The wire may heat up many hundreds of degrees during a test, resulting in a signal of many millivolts.

With the voltage change depending linearly on the temperature change, the wire response after the passage of the initial shock wave is given by a combination of equations 4 and 9. Figure 7 depicts three different operating conditions that can be encountered when using the fine wire in the shock tube. If the time constant is large compared to the flow duration, the response is linear. If the flow time is long compared to the time constant, the response is exponential. At sufficiently long flow times, the response appears as a step function.

The forced convection heat transfer rate to the wire is related to the rate of increase of temperature by the equation

$$Q = q\pi d\ell = \frac{\pi d^2 \ell}{4} \rho_w c_w \frac{dT_w}{dt}$$

Since $\Delta T = \Delta E / I R_i \alpha_i$ (constant current operation), then

$$q = \frac{d\rho c}{4}_i \frac{1}{I R_i} \frac{dE}{dt} \qquad (10)$$

Hence, the heat transfer per unit area is directly proportional to the time rate of change of the voltage across the wire. At an initial pressure of 50 mm Hg and $M_s = 4$ in air, the heat transfer rate to a 0.005 inch wire is 725 cal/cm$^2$ sec (see Fig. 15). For the tungsten wire described previously, this gives a rate of voltage change equal to 830 volts per sec. If the testing time is 40 $\mu$sec ($t/\tau = 0.1$), the change in voltage across the wire is 33 millivolts.

3. Selection of Wires Used

The wires that were chosen for the experiments had diameters less than 0.001 inch. These wires satisfied the requirement that the transient response of the wire has to be dominated by the standard thermal lag (see section III. 1). That is, the characteristic times $\frac{10d}{U}$ and $\delta^2 \rho_w c_w / k_w$ must always be much less than the testing times. The actual diameters that were used are summarized in Table 1. These diameters provided a wide range of time constants and permitted testing over a broad range of Reynolds numbers and shock Mach numbers ($1.25 < M_s < 6.5$).

The wires were constructed from either tungsten, platinum, or platinum 10 per cent rhodium. These materials are superior to most other metals for maximum signal output. This is shown by consideration of the voltage signal

$$\dot{E} = I\dot{R}_w = IR_i \alpha_i \dot{T}_w$$

Assuming the wire to be a perfect calorimeter, $\dot{T}_w$ can be written in terms of heat transfer

$$Q = \frac{\pi d^2 \ell}{4} \rho_w c_w \dot{T}_w$$

With $R = \frac{\sigma \ell}{\frac{\pi d^2}{4}}$, we get

$$\dot{E} = \frac{IQ}{(\frac{\pi d^2}{4})^2} \left(\frac{\sigma \alpha}{\rho c}\right)_w \qquad (11)$$

I, Q, and d are fixed by the geometry and flow conditions. Therefore, for maximum $\dot{E}$, $\left(\frac{\sigma \alpha}{\rho c}\right)_w$ must be a maximum. Table II lists ten

metals in their relative position with respect to this parameter*. Tungsten, platinum, and platinum 10 per cent rhodium are among the best five materials in regards to this parameter.

* The physical properties are principally from Reference 15.

# IV. CALIBRATION OF THE PROBE

If the instrument is to be used for quantitative heat transfer measurements, the physical and geometrical properties must be known. If only crude heat transfer measurements are to be made, handbook values of physical constants and manufacturers' specifications on the geometry would be acceptable. However, if more accurate results are desired, individual calibration is necessary since the above method is good only to $\pm$ 20 per cent.

The separate quantity $\alpha$ was determined by measuring the resistance of the wire between melting ice and boiling water. A two bath system was used. The wire sample was suspended in a silicon oil bath in a test tube which was encased in a porous metal container. This apparatus was in turn put into the water bath and heated to various temperatures. Thermometers (readable to $0.2^{\circ}C$) were used in each container, and equilibrium was assumed to have been reached when they read the same. The resistance of the sample was then read on the same bridge network that was used in the experiments. Two samples from each spool were calibrated this way, and the results were assumed to apply to the rest of the spool. This method was believed to give $\alpha$ to within one or two per cent for the larger diameter wires. No attempt was made to calibrate the wire over a broader range of temperature because the measurements of initial heat transfer involve wire temperature less than $100^{\circ}C$. The higher order coefficients in the resistance-temperature relation were not needed. In most cases, the measured $\alpha$ was considerably lower than that quoted in handbooks.

An optical comparator (Kodak contour projector model 2A) was used to determine the length of the wire used on the gage. This was done to good precision ($\pm$ 0.1 per cent) and, at the same time, made possible a close inspection of the wire itself. Wires that showed defects or non-uniformities were discarded before the calibration was continued.

The diameter of the wire is a most important quantity in the measurement of heat transfer because it enters as a squared quantity in the reduction of the data. At first the diameter was measured optically on a 600 x microscope that had a high precision calibrated moving crosshair eyepiece. Optical diffraction was a problem in measuring the smaller diameters (less than 0.001 inch). Using diameters from the optical measurements, it was not possible to obtain heat transfer results that showed consistency between small and large diameters, and it was concluded that ordinary optical means could not be used to measure wire diameters less than 1 mil.

Therefore, an attempt was made to infer the diameter of the wires by weighing them. A quartz fiber torsional balance (Ref. 16) was used to weigh samples of the wires. This balance is extremely simple, very stable, and sensitive. This balance is the original one illustrated in Reference 16. It has a sensitivity of 0.123 $\mu$gm/division. Suitable lengths were chosen to give the desired accuracy in weighing. At least two samples from each spool were chosen. The density was assumed to be that given in the handbooks. With the length, weight, and density known, the diameter was calculated. The results of these samples were applied to the rest of the wire still on the spool. The

resistance per unit length of each element was measured after completion of the probe, and, if it differed from the average resistance per unit length by more than a few per cent, it was discarded. In this way it was felt that the samples used in determining the wire diameter were adequate. Table I indicates the averaged calibration results.

There was a limitation in the weighing of the wires. This limitation was due to free convection currents set up inside the apparatus resulting in low Reynolds number flow over the wire. Convection currents, even as small as $10^{-2}$ cm/sec, can cause drag forces comparable to the weight of the very small wires. Lengthening the wire sample to increase its weight accomplishes nothing since the drag force is proportional to the length. This limitation was apparently reached at a wire diameter of 1/20 mil since the drift was appreciable here, even though the balance was encased in a glass box to minimize the currents*. It was not possible to evacuate it. A cool (fluorescent) light was used to minimize thermal currents. Sufficient time elapsed between measurements to allow the convection currents to subside (approximately 15 minutes). The diameter, as determined by the weighing technique, was used for the reduction of the heat transfer data since this gave the most consistent results.

The last constant to check is the combination $\rho c$ ; in case we can assume $\rho$ to be the handbook value, the problem is reduced to a determination of $c$ . An electrical means of calibration was chosen because it is fast, convenient, and accurate and offers the convenience

---

* Wire diameters smaller than this require a bootstrap technique of overlapping the experimental heat transfer rates to infer the diameter. No heat transfer measurements were made using wires that had a diameter less than 1/20 mil.

of easily checking the physical constants between shock tube runs. The method is to use a known heat input (by joule heating), measure the gage output and thereby determine the quantity $\rho c$ .

A constant voltage discharge was obtained by utilizing a capacitor in a network that would give a time constant (RC the order of 10 msec) that was much longer than the testing time. A Wheatstone bridge was utilized for the circuit (Ref. 11). It was necessary to resort to a balanced bridge network in order to eliminate the d. c. component of the resulting network signal, so that only the a. c. component is displayed on the oscilloscope. The circuit and its characteristics are displayed in Figures 8 and 9. Stable (small temperature coefficient) resistors must be used for the bridge arms so that the only signal comes from the changes in gage resistance. When possible, the calibration was done in air under atmospheric conditions. With the assumption of no end losses to the supports and no heat conduction to the surrounding fluid, the equation that governs the response becomes:

$$\frac{d}{dt} mc_w(T_w - T_i) = I^2 R_w \tag{12}$$

The assumption of no heat conduction to the surrounding medium is weak. The heat loss to the surrounding fluid is a strong function of time and diameter. In Appendix A an attempt is made to evaluate this assumption. When necessary the calibration was carried out in a vacuum.

The heating current I is given by

$$I = \frac{V}{R_2 + R_w} \tag{13}$$

where $R_w$ is the actual resistance of the gage at any time. The bridge discharge current (equation 13) was experimentally verified. Substituting into equation 12 gives:

$$\frac{\pi d^2 \ell}{4} \rho_w c_w \frac{dT_w}{dt} = \frac{V^2 R_w}{(R_2 + R_w)^2} = \frac{V^2 R_i \left[1 + \alpha_i (T_w - T_i)\right]}{(R_2 + R_i)^2 \left[1 + \frac{R_i \alpha_i (T_w - T_i)}{R_2 + R_i}\right]^2} \tag{14a}$$

If $\alpha \Delta T << 1$ (small times), the right side of the equation can be expanded:

$$\frac{\pi d^2 \ell}{4} \rho_w c_w \frac{dT_w}{dt} = \frac{V^2 R_i}{(R_2 + R_i)^2} \left[1 + \frac{R_2 - R_i}{R_2 + R_i} \alpha_i \Delta T + \ldots\right] \tag{14b}$$

The solution of this equation with the initial conditions $T_w = T_i$ at $t = 0$ gives for small times

$$T_w - T_i = \frac{4V^2 R_i t}{\pi d^2 \ell \rho_w c_w (R_2 + R_i)^2} + \ldots \tag{15a}$$

or

$$\Delta R = -\frac{4\alpha_i}{\pi d^2 \ell \rho_w c_w} \frac{V^2 R_i t}{(R_2 + R_i)^2} \tag{15b}$$

The voltage output $\Delta E$ of the bridge due to the heating of the wire can be shown to be

$$\Delta E = \frac{V R_2 \Delta R}{(R_2 + R_i)^2} \tag{16}$$

In the derivation of this equation, both the changing current and resistance in the bridge have been taken into account. This gives

for $\rho c$ *

$$\rho_w c_w = \frac{V^2 R_2 R_i^2 \alpha_i t}{\frac{\pi d^2 \ell}{4} (R_2 + R_i)^4 E} \tag{17}$$

Figure 9 shows that, for small testing times, the response is indeed a straight line.

The technique will also give an effective measure of this constant for wires made of composite materials (e.g., enamel coated wires).

Care was taken in measuring the volumes, resistances, and voltages as accurately as the present equipment permitted. The voltages were measured by two methods: (1) a 1/4 per cent, 150 volt, d. c. Weston meter for the larger voltages, and (2) for the smaller voltages, a potentiometer measured the voltage drop across a 1 ohm precision resistor wired in series with the helipot. The resistance

---

* Caution should be used with the electrical discharge technique. The energy produced and stored in the wire must not raise the temperature of the wire more than a few hundred degrees in order not to burn the wire out. The voltage used for calibration must be varied accordingly. In most cases a resistor in series or parallel with the wire is needed to balance the bridge. This resistor complicates the formula for $\rho c$. For convenience, the corresponding equations are mentioned here.

Series Resistance in Circuit ($R_s$)

$$\rho_w c_w = \frac{V^3 R_2 R_i^2 \alpha_i t}{\frac{\pi d^2 \ell}{4} (R_2 + R_s + R_i)^4 E}$$

Parallel Resistance in Circuit ($R_p$)

$$\rho_w c_w = \frac{V^3 R_p^4 R_2 R_i^2 \alpha_i t}{\frac{\pi d^2 \ell}{4} (R_2 R_p + R_i R_p + R_i R_2)^4 E}$$

of the circuit was known to high precision, and Ohm's law was used to calculate the battery voltage. It is felt that the over-all calibration was better than five per cent. The calibration of each gage was repeatable to one per cent. The average values of many samples of wires are shown in Table I along with the other wire properties. The variances of $\rho c$ of each gage were on the order of one to three per cent of the average value. It is felt that most of this variation of $\rho c$ actually represents the variation of the other physical and geometrical properties of the wire, since these were determined by spool values rather than individual calibrations. The results show that the quantity $\rho c$ increases appreciably with a decrease in the diameter. No explanation of this can be presented at this time.

The calibration actually gives the lumped quantity $\frac{d^2 \rho c}{\alpha}$. This quantity also appears in the definition of the Nusselt number. Thus, even if the individual quantities were in error, this over-all constant as given by the electrical calibration would still be correct. (The wire length, voltages, and resistances used in the calibration are assumed to be accurately measured.)

# V. HEAT TRANSFER MEASUREMENTS

## 1. Raw Results

From dimensional arguments it can be shown that the heat transfer rate to the wire expressed in energy per unit area per unit time can be written (Ref. 17)

$$q = \frac{k(T_r - T_w)}{d} f(Re, M, \gamma, Pr, \tau', \ell/d, \ldots) \qquad (18a)$$

If the flow in the shock tube is in equilibrium (or completely frozen), the flow behind the shock wave can be simply determined from $M_s$, $P_1$, and $T_1$, given the test gas. The heat transfer rate can then be written in terms of these quantities. It depends only on three groups of variables: (1) the gas variables ($\gamma$, Pr, ...), (2) the wire variables such as d, $\ell/d$, $T_w$ (not the wire properties $\rho$, c, $\alpha$), and (3) the shock tube variables, $M_s$, $T_1$, and $P_1$.

The measurements and reduced data presented herein represent heat transfer rates measured at the initial moment when the wire temperature equals the initial temperature. As shown by the calculations in Appendix A, there is no heat loss to the end supports at this moment, and the effect of $\ell/d$ is neglected in correlating the results. The tabulated results of heat gain (q) are presented in Tables III and IV. The results are grouped according to the variables presented above for ease of interpreting and correlating them.

Figures 14 to 17 show the heat transfer measurements that were made in air. (Argon measurements are not presented in any figures, but are just tabulated.) The figures are just the pictorial

representation of the tabulated results for air. In this presentation of the data it is seen that the heat transfer rate (q) depends strongly on the shock Mach number. If it is assumed that the heat transfer is proportional to $M_s^n$ (fixed $P_1$ and $T_1$), n is approximately 4. If the dependency of heat transfer on initial pressure is assumed to be $P_1^m$ (fixed $M_s$ and $T_1$), m is approximately 1/2 to 1. The dependency of heat transfer on the initial pressure is weak compared to the shock Mach number. The experimental results show excellent repeatability and consistency; the scatter is small. The sum of all the heat transfer measurements in air (Figs. 14 to 17) entailed the use of 15 to 20 different wires and materials, but the scatter is well within the bounds of any calibration error, i.e., $\pm$ 5 per cent. The calibration technique gives consistent results. However, the scatter is appreciably increased at the lower pressures. This is predominantly due to the decreased testing time influencing the flow following the shock wave and the inability to read the McLeod gage accurately (see section II.2).

These figures were cross plotted in order to present the systematic variation of the non-dimensionalized variables. This procedure will be explained more fully in section V.4.

## 2. Dimensionless Parameters Used in Data Reduction

From dimensional arguments the heat transfer, expressed in terms of the Nusselt number, depends on the following parameters:

$$Nu = Nu(Re, M, Pr, \gamma, \tau', \ldots) \tag{18b}$$

The heat transfer measurements have been reduced to the above form.

The parameters involved in the preceding equation were chosen to be expressed in terms of conditions in region 2 or region 5, depending on the flow Mach number in region 2. Region 2 is the hot flow following the moving shock wave. This flow may be subsonic or supersonic depending on shock tube operating conditions, e.g., the flow Mach number is supersonic at $M_s > 2.1$ and subsonic at $M_s < 2.1$ for air. If a blunt body is placed in the supersonic stream, a detached bow-shock wave is established in front of the body. At the stagnation region of the body this bow wave is nearly normal to the flow, and the conditions immediately behind this portion of the wave are determined by normal shock relations. Region 5 refers to these conditions. For $M_2 < 1$ there is no normal bow shock on the model, and the parameters are expressed in terms of the free stream conditions 2. For $M_2 > 1$ the parameters are expressed in terms of region 5. At high Mach numbers it will be shown that such a procedure helps to minimize the Mach number effect on the non-dimensionalized form of the heat transfer coefficient. The use of the flow condition behind a normal shock for $M_2 > 1$ to reduce the Mach-number dependence of the Nusselt number was clearly demonstrated by Laufer and McClellan (Ref. 5). It should be noted that such a procedure may lose some of its physical significance at the large Knudsen numbers (say $Kn_2 > 1$) because the shock wave begins to merge with the body. At the limit of large Knudsen numbers, no "real" shock wave exists at all. However, this procedure is used even for the larger Knudsen numbers since it gives consistent correlations.

In summary, the following definitions are used to represent the reduced data.

Subsonic Case

$$Nu_2 = Nu_2(Re_2, M_2, \tau', \ldots)$$

$$Nu_2 = \frac{qd}{k_2(T_r - T_w)} \; ; \; Re_2 = \frac{(\rho u)_2 d}{\mu_2} \; ; \; M_2 = \frac{u_2}{a_2} \; ; \; \tau' = \frac{T_w - T_r}{T_r}$$

Supersonic Case

$$Nu_5 = Nu_5(Re_5, M_5, \tau', \ldots)$$

$$Nu_5 = \frac{qd}{k_5(T_r - T_w)} \; ; \; Re_5 = \frac{(\rho u)_2 d}{\mu_5} \; ; \; M_5 = \frac{u_5}{a_5} \; ; \; \tau' = \frac{T_w - T_r}{T_r}$$

3. Temperature Loading

The wire temperature loading has been defined as

$$\tau' = \frac{T_w - T_r}{T_r} \tag{19}$$

This definition is the one that was used by Laufer and McClellan. In hot wire work this temperature loading is positive and usually ranges from 0 to +1. (The upper limit 1 is based on practical limitations.) For $\tau'$ equal to zero, the temperature of the wire is equal to the recovery temperature, while for a value of one the wire temperature is twice that of the recovery temperature.

The same definition was used for these measurements in order to retain a standard definition. For the cold wire case, $\tau'$ is negative and may vary from 0 to - 1. Minus one represents a limit in cold wire operation for which a wire is infinitely cold with respect to the flow ($T_w \ll T_r$). The heat transfer measurements cover a range of $\tau'$ from approximately - 0.15 to - 0.95.

Because of the definition of $\tau'$, the magnitudes of the cold wire temperature loading and the hot wire temperature loading are comparable. However, the actual temperature differences between the wire and the flow are not comparable. For many wind tunnel operations $T_r$ (approximately equal to the total temperature) is nearly $300^{\circ}K$, and the maximum temperature difference between the flow and the wire (i.e., $\tau' = 1$) is only $300^{\circ}K$. For a cold wire at a temperature loading of - 0.95 with the wire operating at $300^{\circ}K$ (the wire temperature used for the measurements), this temperature difference is $5700^{\circ}K$! This tremendous range of the temperature difference makes the specification of the temperature loading parameter very important in the reduction of the shock tube data.

## 4. Basic Considerations for Data Reduction

The problems that are encountered in reducing the heat transfer measurements to non-dimensional form can be classified into three groups and are discussed separately: (1) problems which are associated with the actual gas properties behind the shock wave; (2) thermodynamic properties that cannot be measured or calculated, but have to be inferred from data gleaned from other sources; (3) problems which

are due to the randomness of data taking because of the inherent randomness of $M_s$.

The first problem is most critical and centers primarily on the validity of the assumption of thermodynamic equilibrium behind shock waves when calculating the flow conditions. Under certain conditions in the shock tube, thermodynamic equilibrium will not be reached because of the finite length of time taken for a gas to reach equilibrium, both in composition and distribution of energy between the various degrees of freedom of its constituents. At high gas temperatures more and more of these degrees of freedom are excited (vibration → dissociation → first ionization, etc.). The shock Mach number was deliberately kept low for these measurements so that dissociation and ionization were not present. However, for air the vibration degree of freedom begins to be excited above 300°K ($\Theta_v \sim$ 3000°K), and the effects could not be avoided. Blackman (Ref. 18) has made measurements of the vibrational relaxation time in $N_2$ and $O_2$ in the shock tube. The results show that the relaxation time can be greater than, less than, or equal to the testing time in the shock tube, depending on $P_1$, $M_s$, and $T_1$. The following table shows the vibrational relaxation times for air based on the results of Reference 18. The relaxation times are given in the laboratory frame of reference. (This is not the relaxation time along particle paths.) Included in the table is the corresponding ranges of test intervals, i.e., the time intervals over which the heat transfer measurements were made.

| $P_1$ | 500 | | 50 | | 5 | | 0.5 | | 0.1 | |
|---|---|---|---|---|---|---|---|---|---|---|
| $M_s$ | t | T | t | T | t | T | t | T | t | T |
| 3 | 3 | 20 | 30 | 40-200 | 300 | 40-200 | | | | |
| 4 | | | 4 | 30-200 | 40 | 30-200 | 400 | 50-200 | | |
| 5 | | | | | 9 | 20-150 | 90 | 50-120 | 450 | 25 |
| 6 | | | | | | | 20 | 50-90 | 100 | 20 |

t = vibration relaxation time in laboratory coordinates ($\mu$sec)

T = approximate range of test intervals used for the heat transfer measurements ($\mu$sec)

The effects of vibration on the thermodynamic quantities become significant at $M_s \sim 3$ for air. In the reduction of the heat transfer data, only two extremes of the effect of vibration were considered, a completely frozen flow and a flow in complete equilibrium. If the flow in region 2 was not in equilibrium, i.e., if the test interval was short compared to the relaxation time for air, then all flow quantities including the transport properties were calculated from frozen flow relations. Fully frozen flow occurred only at an initial pressure of 0.1 mm Hg for the measurements. If the flow in region 2 was in equilibrium, then the flow quantities were calculated on this basis. Further complications arise when calculating the gas properties in regions 5 and the stagnation point of the model. Since the distance between the shock and the body is of the order of a body length (d) which is extremely small,

it is unlikely that the flow ever readjusts to equilibrium here. The flow properties behind the bow wave were calculated on the basis of thermodynamic equilibrium if the flow in region 2 was in equilibrium. A sample calculation showed that the differences between equilibrium and frozen flows in this region were small for the flow Mach numbers encountered.

The Sutherland formula was used to calculate the viscosity coefficient for all the temperatures encountered in making the heat transfer measurements.

$$\mu = \frac{AT^{3/2}}{B + T}$$

With $\mu$ in poises and T in degrees Kelvin, the constants were taken as*

| | A | B |
|---|---|---|
| Air | $145.8 \times 10^{-7}$ | 110.4 |
| Argon | $191.0 \times 10^{-7}$ | 136.6 |

Using these values of viscosity, Reynolds numbers were calculated as a function of $M_s$ for regions 2 and 5 for the various test gases using real gas relations. For air the calculations also include the effects of fully frozen and equilibrium flow. The results, plotted for any wire diameter and initial pressure $(\frac{Re}{dP_1})$, are shown in Figures 10 and 11.

The other transport coefficient used in non-dimensionalizing the results is the thermal conductivity. Since the effects of dissociation

* Where possible, the NBS tables Cir 564 (Ref. 19) were used to determine the constants; otherwise, the American Physics Handbook (Ref. 15) was used.

and ionization on the state properties of the gas were considered negligible, the formulas for predicting the conductivity at the lower temperatures were extended to include the whole temperature range encountered in the shock tube. For air in equilibrium the conductivity is

$$k = \frac{0.6325 \times 10^{-5} T^{3/2}}{245.4 \times 10^{-12/T} + T}$$

For argon it is

$$k = \frac{0.379 \times 10^{-5} T^{3/2}}{179.6 \times 10^{-10/T} + T}$$

The dimensions of k are cal/cm sec $^{o}$K. Appendix B indicates how the transport properties were calculated in the case of frozen flow.

The definition of Nusselt number introduces a temperature difference defined as

$$T_r - T_w = \Delta T$$

$T_r$ is called the recovery temperature and is the temperature that an unheated wire will achieve in equilibrium with the flow. Generally, this temperature does not equal the stagnation temperature for a wire except at $M = 0$. It is usually determined by experiment. In the shock tube this determination is impossible since the wires seldom have time to reach equilibrium. (If they did, they would burn out at high $M_s$.) The only recourse is to use the experimental results for the recovery temperature from wind tunnel experiments with fine wires. Except for the transitional region ($0.1 < Kn < 1$), this data is comprehensive for air. Collis and Williams (Ref. 20) have compiled the results of many experimentalists into a universal curve of the

recovery temperature ratio in air as a function of Mach number and Knudsen number. The latest measurements of Dewey (Ref. 21) agree well with the curve, and these compiled data and this curve were used to infer the recovery temperature of the wire in air. This curve was assumed to be valid even in the case where $\gamma \neq 1.4$, i.e., high temperatures. Changing the specific heat ratio slightly has a small effect on the recovery temperature for air. The maximum change in $T_r/T_t$ can be estimated by using the theory of free molecule flow.

$$\eta = \frac{T_r}{T_t} = \frac{2\gamma}{\gamma + 1} \quad \text{as} \quad M \rightarrow \infty$$

$$\gamma = 1.4 \qquad \eta = 1.165$$

$$\gamma = 1.29 \qquad \eta = 1.13$$

This is most likely the largest change possible for this change in $\gamma$. There is only three per cent difference, and therefore the assumption seems valid. The form chosen for $T_r/T_t$ is illustrated in Figure 12 as a function of Mach number and Knudsen number in region 2.

The recovery temperature for argon is plotted in Figure 13. The experimental measurements of $T_r/T_t$ are fewer in number and scope for argon. The curves in Figure 13 had to be constructed from the recovery temperature measurements in air, theory, and some experimental results from Weltmann and Kuhns (Ref. 22). The construction of the graph predicting the recovery ratio as a function of $M_2$ and $Kn_2$ proceeded as follows. The continuum value (Kn = 0) of the recovery ratio was determined from the recovery temperature measurements made in air. It can be shown that the recovery

temperature of a flat plate is a function only of the square root of the Prandtl number for a laminar boundary layer. This fact is borne out by experiment, including a wide variety of experiments on cones of various included angles (Ref. 23). The Prandtl number of air is very similar to that of argon. It was therefore concluded that the recovery ratio of argon has the samd value as air at equal Mach numbers, and the recovery temperature ratio of air was used for argon in the continuum range. The free molecule ($Kn = \infty$) recovery temperature ratio was determined by using the theory of Stalder et al (Ref. 24) for a monatomic gas ($\gamma = 1.66$) and plotted accordingly. The high Mach number transitional values of the recovery ratio were determined from the results of Weltmann and Kuhns. These experimental points were used to infer all the transitional region recovery temperature ratios. The remaining lines in this figure were drawn from these points.

As previously mentioned, the heat transfer expressed in terms of the Nusselt number depends on the following parameters:

$$Nu = Nu(Re, M, Pr, \gamma, \tau', \ldots) \qquad (18b)$$

The only possible way to derive the functional relationship of the Nusselt number with a parameter is to vary the parameter while the rest remain fixed. However, this is practically impossible to do directly in the shock tube since they are all interrelated and depend on $M_s$, $P_1$, and $T_1$. (The shock speed is somewhat random; see section II.3.) Because the Mach number could not be fixed accurately prior to each measurement, it was necessary to plot the initial heat

transfer results as a function of $M_s$, as in Figures 14 to 17, while the other variables remained fixed. The resulting curves were in turn cross plotted at fixed values of the non-dimensional parameters. This done, the resulting points can in turn be plotted in a more standard fashion, i.e., equation 18b.

The cross plotting was chosen arbitrarily so as to present the Reynolds number as a variable and the flow Mach number as a parameter in the final results. Therefore, the cross plotted heat transfer measurements represent measurements at fixed shock Mach numbers. The following table indicates the values of $M_s$ chosen to be used in the final results. The flow Mach number is also included.

| Air | | Argon | |
|---|---|---|---|
| $M_s$ | $M_2$ | $M_s$ | $M_2$ |
| 1.29 | 0.4 | 1.49 | 0.5 |
| 1.75 | 0.8 | 2.02 | 0.8 |
| 2.44 | 1.2 | 2.67 | 1.0 |
| 3.28 | 1.5 | 4.3 | 1.2 |
| 4.16 | 1.7 | 5.18 | 1.25 |

## 5. Results for Air and Comparison with Hot Wire Data

In this section the non-dimensional heat transfer results are compared to other experimental and theoretical determinations of the Nusselt number as a function of the flow parameters. Before

describing the present results for air, a consideration of the available data is useful as a guide for comparison. Figure 18 is a graphical presentation of this data.

The very low Mach number results were placed on the figure to indicate the upper boundary of the Nusselt number-Reynolds number curve. The contributions of Cole and Roshko (Ref. 25), Collis and Williams (Ref. 26), King (Ref. 2), and the McAdams correlation (Ref. 27) represent the non-dimensional heat-transfer law at $M \tilde{=} 0$ and a temperature loading of zero. As indicated by the figure, the theoretical results of King are considerably higher than the experimental results.

The experimental results of Kovasznay, and Laufer and McClellan are representative of the high Mach number, high Reynolds number range. They do not agree well with one another. The results of Laufer and McClellan are plotted for two temperature loadings, i.e., a temperature loading of zero and a temperature loading of one in terms of the present terminology. These two curves indicate the general trend of the effect of temperature loading on the Nusselt number for a hot wire in this Mach number and Reynolds number range. The apparent effects of temperature loading on the Nusselt number are less pronounced at the high Reynolds numbers than at the lower Reynolds numbers. The Nusselt number is lowered as the temperature loading is increased for $M > 0$ and fixed Reynolds number.

Some experimental results of Tewfik and Giedt (Ref. 28) are also included in the figure. In their experiment, local heat transfer measurements were taken on a rather large diameter pyrex tube

(0.5 inch) in a low density wind tunnel. The model was continually cooled by flowing liquid nitrogen or butyl cellusolve through it. The heat transfer was inferred by measuring the temperature difference between the outer and inner circumference of the tube. The local heat transfer distribution was integrated around the model to determine the average Nusselt number. It is these results that are plotted here. It should be noticed that in the experiment the model was cold with respect to the flow. The Nusselt numbers are lower than for the corresponding hot wire results. The experimental error for this experiment is estimated to be $\pm$ 15 per cent.

In the lower Reynolds number range the hot wire heat transfer results of Cybulski and Baldwin (Ref. 29) at subsonic Mach numbers and those of Dewey at a Mach number of 5.8 are presented. The data of Dewey at a Reynolds number range from 0.6 to 3 agree very well with the work of Laufer and McClellan at $\tau' = 0$.

The free molecule analysis of Stalder et al provides a theoretical estimate of the heat transfer from a fine wire. For a wire of constant temperature and no radiation losses, the formulas are simply

$$Nu = \frac{\gamma - 1}{\gamma} \frac{1}{2\pi^{3/2}} \propto Re\,Pr\,\frac{g(s)}{s}$$

and

$$\frac{T_r}{T_2} = \frac{f(s)}{g(s)}$$

where $g(s)$ and $f(s)$ are functions of the molecular speed ratio ($s = \sqrt{\frac{\gamma}{2}}\,M$) and are given in Reference 24. The analysis predicts the heat transfer relationship as a function of the flow quantities, but

involves an accommodation coefficient $\alpha$ (assumed to be a constant in the analysis) which takes into account the gross effects of the energy exchange mechanism between the gas and the body. As yet this accommodation coefficient remains practically undetermined, both experimentally and theoretically. Considerable variation among heat transfer results obtained under different conditions may be expected because of the inability to fix this coefficient. The free molecule analysis of Stalder et al with an accommodation coefficient of one is plotted in the Reynolds number range where it is approximately applicable. Some experimental results of Weltmann and Kuhns are shown also. Their results indicate an accommodation coefficient of 0.9. The experimental error appears to be $\pm$ 20 per cent.

Some approximate calculations of the heat transfer to a cylinder in nearly free molecule flow were made on the basis of Willis' work (Ref. 30). By assuming that the accommodation coefficient is one and that the molecular model of Krook employed by Willis is the correct physical model, an approximate variation of heat transfer with Reynolds number and Mach number was obtained and plotted in Figure 18 for $M_2 = 1.5$. (See Appendix B for calculations.) Such a calculation is useful to show the effects of nearly free molecule flow on heat transfer. The result gives an extremely small correction in the range plotted and shows the typical asymptotic behavior of the heat transfer from free molecule results.

The non-dimensional heat transfer results for air obtained in the present experiment are shown in Figure 19. The points that are plotted are not the experimental points, but are the cross plotted values

from Figures 14 to 17. The results show a systematic Mach number and Reynolds number variation over the entire flow region that was plotted, $0.035 < Re < 3500$, $0.4 < M_2 < 1.9$. The scatter is $\pm$ 5 per cent which is small for this type of work. In the high Reynolds number range ($Re > 20$) the results have a nearly $\sqrt{Re}$ behavior characteristic of boundary layer theory. At Reynolds numbers less than 0.1 the heat transfer results exemplify the behavior predicted by free molecule theory. Between these two limits, sometimes called slip and transitional flow, the functional relationship of the heat transfer parameter can be represented by

$$Nu = Nu(Re^n, M, \tau', P_1, \gamma) \quad \text{where} \quad \frac{1}{2} < n < 1$$

The results exhibit no apparent Mach number dependency above a Mach number of 1.5. The heat transfer results above this Mach number merged together when the transport coefficients were evaluated at conditions behind the bow shock, at least to the accuracy of the experiment. It should be noticed that along lines of constant $M_2$, i.e., constant $M_s$, the wire is also at a temperature loading ($\tau' = \frac{T_w - T_r}{T_r} = \frac{T_i - T_r}{T_r}$) which is not zero. The temperature loading depends primarily on $M_s$. At $M_s = 1.29$ this factor is small and approximately equal to - 0.18. At the highest value of $M_s$ this factor approaches - 1. The opening statement of this paragraph can now be made more specific by including the effects of temperature loading. The results show no combined Mach number and temperature loading effects above a flow Mach number of 1.5. At these values of $M_2$ the principal independent parameter is the

Reynolds number. At lower values of $M_2$ the effects of Mach number on heat transfer are pronounced.

Comparing the available results with the present work, Figures 18 and 19 respectively, it is noticed that in the high Reynolds number (Re > 100), high Mach number (M > 1.2) range the present results are lower than the hot wire data of Laufer and McClellan ($\tau' = 0$) by 20 per cent. In the same Reynolds number range but at lower Mach number, the results also appear lower than hot wire data ($\tau' = 0$). However, the difference between hot wire results ($\tau' = 0$) and cold wire results seems to be larger at the higher $M_2$.

The results of Tewfik and Giedt ($\tau' \neq 0$, M > 1.2) agree more closely with the present work. In order to supplement and check the integrated values of the local heat transfer rates, some platinum sputtered glass rod elements were made and tested in the shock tube. The sputtered element was then used as a thin film heat transfer gage (Ref. 11). The elements were sputtered uniformly around the circumference of the rod. The voltage output of the gage then represents the total heat transfer to the rod. Therefore, these elements simulated a wire. (Note that the internal temperature is not uniform as in the case of a metal wire.)

Some results of six runs using a rod of diameter 0.277 cm are shown in Figure 19, together with the cold wire results. The data accrued from this technique were crude in comparison to the cold wire data (probably no better than $\pm$ 10 per cent). Figure 20 compares the response of the thin film gage with that of a cold wire. The response of the thin film gage does not reproduce the ideal parabolic response

well and indicates why these heat transfer results could not be repeated to better than 10 per cent. However, the results (i.e., the magnitude of Nu at a given Re and $M_2$) agree with those of Tewfik and Giedt (to an accuracy of $\pm$ 10 per cent) and compare with the cold wire results.

In the range $0.6 < Re < 100$, the high $M_2$ results begin to approach the results of Laufer and McClellan and Dewey at $\tau' = 0$. The results of Dewey differ by only a few per cent from the results obtained in the shock tube.

At the very lowest Reynolds numbers, the present data (Fig. 19) approach the theoretical solution of Stalder et al with an accommodation coefficient of nearly 1. The minimum Reynolds number results in Figure 19 represent frozen flow heat transfer data normalized using the conditions set forth in section V.4. The flow Mach number for these results was lower than the corresponding equilibrium flow Mach number ($M_{2_{equilibrium}} \simeq 1.7$, $M_{2_{frozen}} \simeq 1.5$).

6. Results for Argon

The argon measurements are shown in Figure 21. Qualitatively they appear similar to the air measurements and cover a Reynolds number range of $0.1 < Re < 100$ and a Mach number range of $0.5 < M_2 < 1.25$. Again the main independent parameter is the Reynolds number with the flow Mach number and temperature loading of the wire playing a secondary role.

At high Reynolds numbers the heat transfer coefficient exhibits no Mach number dependency above a Mach number of 1.0, even though

the temperature loading is not constant at the different Mach numbers. At $M_2 = 1.0$ the temperature loading is already quite large and equals - 0.75. Unfortunately, the limitation on the flow Mach number in the shock tube precluded making heat transfer measurements at Mach numbers in excess of approximately 1.3 for a monatomic gas. Therefore, direct comparison cannot be made with the high $M_2$ results in air. The high Reynolds number heat transfer results are slightly lower than the air results at the same Mach number and Reynolds number.

At Reynolds numbers below 8, the Mach number dependency on heat transfer becomes more apparent. The results again approach the theory of Stalder et al ($\gamma = 1.66$) with an accommodation coefficient of 1 and agree with the heat transfer calculations under nearly free molecule conditions. For convenience and comparison, these theoretical estimates of the heat transfer coefficient are also plotted in Figure 21.

7. Effect of Temperature Loading on Heat Transfer to Fine Wires

Comparing Figures 18 and 19, it is seen that the experimentally determined heat transfer coefficient of a wire in the shock tube is lower than the corresponding hot wire results obtained in wind tunnels for Reynolds numbers greater than 1*. At Reynolds numbers greater than 100 and a Mach number greater than 1.2, the cold wire results are almost 20 per cent lower than Laufer and McClellan's hot wire

* The work of Tewfik and Giedt, who did not use heated wires, but used cylinders cold with respect to the flow in a low density wind tunnel, compares favorably with the cold wire results.

results at $\tau' = 0$. The difference between the cold wire and hot wire heat transfer coefficients is larger at the higher Reynolds numbers than at the lower Reynolds numbers. In particular, at Reynolds numbers below 1 there is no difference between the hot wire results of Dewey ($\tau' = 0$) and the cold wire.

It is suggested that the difference between hot wire and cold wire heat-transfer coefficients is principally an effect of temperature loading $(\frac{T_w - T_r}{T_r})$ such that for $Re > 1$ the Nusselt number decreases as the algebraic value of the temperature loading is increased. An effect of temperature loading is plausible since effects of temperature loading are also noticed experimentally for hot wires, namely, as the wire is heated appreciably above the flow recovery temperature, the Nusselt number decreases. (At very low Mach numbers, the Nusselt number increases as the temperature loading is increased.) It is also noticed experimentally that, as the Reynolds number is reduced, the effect of temperature loading on a hot wire is increased. See Laufer and McClellan's results in Figure 18 as an example of this effect.

However, free molecule analysis predicts that there will be no effect of temperature loading on the heat transfer coefficient. Using free molecule theory as a guide, one would expect that the temperature loading effect (if there is one) would be reduced as the hot or cold wire operation approaches the free molecule range. This expectation is in direct contrast with experiments with the hot wire, because the trend is reversed. However, it agrees most favorably with the cold wire results since the apparent effects of temperature loading are continually diminished as the wire approaches the free molecule range from the

continuum range of heat transfer. This suggests that the temperature loading effect as measured by using hot wires in the low Reynolds number region is possibly an extraneous result, i.e., erroneous end loss corrections or variations in the accommodation coefficient.

The effects of temperature loading at the large Reynolds numbers were examined using laminar-boundary-layer analysis at the stagnation point. It has been demonstrated experimentally (Refs. 11 and 28) that the major portion of the heat transfer to a cylindrical body occurs at the stagnation point – at least for high $M$. The boundary layer heat transfer and, through it, the effect of temperature loading are dependent on the distribution of $\rho\mu$ within the boundary layer. The stagnation-point heat-transfer analysis of Fay and Ridell (Ref. 31) which uses the exact $\rho\mu$ relationship for air was used. Their analysis indicates that there is an effect of wall conditions on heat transfer, but this effect is small. For the cold wire it amounts to approximately 5 per cent at $\frac{T_r}{T_w} \sim 5$ and does not explain the difference between the hot wire and cold wire results.

An attempt was made to verify experimentally a temperature loading effect by using a heated wire at low $M_s$. Unfortunately, at low $M_s$ the effects were too small to be detected within the experimental accuracy since the heated wire involved large end loss corrections. The experiment was inconclusive, and it was abandoned.

The difference between the hot wire and cold wire heat transfer coefficients at high Reynolds numbers has not been resolved. Future work is necessary in order to explain this difference. A comparison with hot wire heat transfer data using argon as a test gas may be useful

in explaining this. No suitable hot wire measurements using argon are available. If such measurements are made and compare favorably with the cold wire data (Fig. 21), then the difference between the heat transfer coefficients in air may be attributed to the possibility that the vibrational energy of the heated gas is not fully transmitted to the wire.

8. Accommodation Coefficient

Forced convection heat transfer measurements can be used to infer the accommodation coefficient ($\alpha$) when compared to the theory of Stalder et al. As mentioned in sections V.5 and 6, the heat transfer measurements gave $\alpha \cong 1$ for air and argon using platinum or platinum-rhodium wires. It should be mentioned that the wire elements underwent no special cleaning procedure before use. The wires were etched in a solution of nitric acid and water and then flushed clean with acetone. The resulting elements were then exposed to a high vacuum for five or ten minutes before use, but were not overheated. No attempt was made to specify the surface condition of the wires accurately for this experiment.

A survey of the literature reveals that the accommodation coefficient can differ widely under apparently similar circumstances. Values of $\alpha$ range from less than 0.1 to 1. A good many of these measurements are probably in error due to one of the following three reasons: (1) the experimenter did not work in the free molecule range, and transitional effects are present; (2) there were erroneous and excessive radiation and end loss corrections which markedly decrease the accuracy of the experiments; (3) there was a failure to specify the

surface condition of the element accurately in the experiment. Heat transfer measurements in the shock tube can easily determine the accommodation coefficient to the accuracy of the heat transfer measurements*. The heat transfer measurements made in the shock tube can easily avoid errors introduced by (1) and (2) by working at sufficiently high Knudsen numbers (say $Kn > 50$ ) and taking only initial heat transfer measurements when there are no end loss corrections. The forced convection heat transfer can be made much larger than any heat transfer due to radiation from the heated gas. The surface conditions are critical, but still have to be specified for any experiment.

The coefficient $\alpha$ should not necessarily be considered a constant dependent only on the material properties of the wire. Various experiments show that $\alpha$ is very dependent on the molecular properties of the gas and surface conditions of the wire. In particular, Nocilla (Ref. 32) has shown that under certain conditions the accommodation coefficient may be a function of the molecular speed. The experimental work of Oliver (Ref. 33) indicates that the accommodation coefficient is a function both of the wire temperature and gas temperature under conditions of no flow. Hence, the experimental values of $\alpha$ are most likely only indicative of the conditions as met in the shock tube, and the value of $\alpha$ should not be interpreted as an absolute invariant quantity. No theoretical study has been able to cope

---

* One must have a knowledge of the recovery temperature to do this. Wind tunnel experiments verifying the theoretical recovery temperature are numerous and well determined since the recovery temperature does not involve the accommodation coefficient. For this reason, the experimental recovery temperature, as measured in the wind tunnel, can be used in reducing the heat transfer data obtained in the shock tube.

successfully with all the apparent independent variables and their effect on the accommodation coefficient. The actual mechanism of energy accommodation does not yet seem to have been adequately described. Perhaps simple forced convection heat transfer measurements made in the shock tube over a wide range of operating conditions can help to clarify the mechanism of energy accommodation. Much difficult theoretical and experimental work has yet to be done in order to evaluate the accommodation coefficient precisely.

# VI. POSSIBLE APPLICATION OF THE COLD WIRE

## 1. Timing Measurements

One of the most useful features of the cold wire is its ability to detect wave phenomena in the shock tube. It has been observed that the heat transfer rate to the wire changes radically with the passage of a shock wave or contact surface. Even an expansion wave can easily be seen if the wire is hot or cold with respect to the flow. Because the signal output of the wire depends on the heat transfer rate, the cold wire can be used in conjunction with an oscilloscope to detect and measure the arrival time of these waves or surfaces. For example, this technique was used in Reference 14 in measuring the duration of the hot flow in the shock tube and is indicative of this possible use of the instrument. The contact surface, or region marking the end of the hot flow (region 2), was indicated by the first discontinuity after the arrival of the shock wave in this study (see Fig. 7).

To illustrate the application to wave detection, measurements were made of the time it takes a shock wave to traverse the distance from a point in the shock tube to an end wall and return, using a cold wire. The measurements were carried out at high pressures (5, 50 mm Hg). The probe was a 0.0005 inch tungsten wire supported by two needles protruding from the side wall of the shock tube and was placed at a distance of 8.44 cm from the end of the shock tube. The oscilloscope with a calibrated sweep speed monitored the output of the wire, and the time between successive discontinuities was measured. A typical response of the wire in the quiescent hot air is quite different

from that in a flow. The experimental results together with the theoretical time to return (based on $\gamma = 1.4$) are shown in Figure 22. At these pressures and $M_s$ the experimental points agree well with the theoretical estimate. The experimental scatter is small.

Another important use of the wire is its ability to infer the incident shock wave speed by measuring the heat transfer to the wire. The possibility of measuring incident shock wave speeds comes from the results of section V.1. It has been shown that the heat transfer to a fine cold wire is very repeatable and consistent. It has also been indicated that the heat transfer is a strong function of the shock Mach number (see Figs. 14 to 17). It follows that the heat transfer to a cold wire can be used to infer the value of $M_s$. A wire that is carefully calibrated can measure the heat transfer to within 5 per cent (the random error of the measurements is even smaller). If the heat transfer can be measured to 5 per cent, $M_s$ can be measured to an even closer degree of accuracy since the heat transfer law may be written as

$$q = q_0 M_s^n$$

$$\frac{1}{n} \frac{\Delta q}{q_0} = \frac{\Delta M_s}{M_s}$$

where $n$ is always greater than 2. At low $M_s$ ($M_s < 2$) where $n$ is greater than 4 or 5, the shock wave Mach number can be measured to better than 1 per cent using this technique. This method of measuring shock speed is advantageous in some instances, since it is a local measurement of $M_s$ rather than an average measurement between

two timing stations. Two cases are apparent when such a method of measuring shock speed is advantageous: (1) if the shock wave is highly decelerating or accelerating, a mean measurement may be too crude; (2) if the distance over which the shock speed must be measured is too small to use ordinary film gages with any precision, the indirect measurement of $M_s$ is preferable.

The cold wire can contribute a great deal to the measurement and timing of wave phenomena in the shock tube with only a minimum amount of equipment.

## 2. Sensitivity Characteristics of the Probe; Separation of Total Temperature and Mass Flow

In wind tunnel work using the equilibrium technique, an unheated wire is simply a resistance thermometer which reaches the equilibrium temperature $T_r$. When it is not at the equilibrium temperature, the unheated wire becomes also a heat transfer meter which is sensitive to mass flow, as is the ordinary hot wire.

To illustrate this point more fully, mass flow and temperature sensitivity coefficients will be derived for the cold wire suddenly subjected to a flow disturbance. These coefficients are analogous to the coefficients derived by Kovasznay for a hot wire (Ref. 4). However, while the basic idea of the calculation is the same, the results are not identical. In general, these coefficients are time dependent for a cold wire while they are constant for hot wire operation.

Consider a heat loss relation given by

$$Nu = \frac{qd}{k(T_r - T_w)} = f(Re) \qquad (20)$$

$$q = \frac{d\rho c}{4\alpha} \frac{1}{RI} \dot{E} = \frac{d\rho c}{4\alpha} \left(\frac{\dot{E}}{E}\right) \tag{10}$$

where $$\dot{E} = \frac{dE}{dt}$$

Substituting into equation 20 gives:

$$\frac{\frac{d^2\rho c}{4\alpha} \frac{\dot{E}}{E}}{k(T_r - T_w)} = f(Re) = \frac{\psi \frac{\dot{E}}{E}}{\eta T_t - T_w}$$

where $\eta = T_r/T_t$ = a constant, $T_t$ = stagnation temperature, and $\psi = d^2\rho c/4\alpha k$. Now, in general, the variation in the voltage output is related to variations in mass flow and temperature by

$$\Delta\dot{E} = \frac{\partial\dot{E}}{\partial(\rho u)} \Delta(\rho u) + \frac{\partial\dot{E}}{\partial T_t} \Delta T_t \tag{21}$$

Then

$$\frac{\partial\dot{E}}{\partial\rho u} = \frac{E(\eta T_t - T_w)}{\psi} f'(Re) \frac{d}{\mu} \tag{22a}$$

$$\frac{\partial\dot{E}}{\partial\rho u} \frac{\Delta\rho u}{\dot{E}} = \frac{f'(Re)}{f(Re)} \Delta Re \quad \text{mass sensitivity coefficient}$$

where $\Delta Re = \frac{d}{\mu} \Delta(\rho u)$

$$\frac{\partial\dot{E}}{\partial T_t} = \frac{E}{\psi} f(Re)\eta \tag{22b}$$

and also $$\frac{\partial\dot{E}}{\partial T_t} \frac{\Delta T_t}{\dot{E}} = \frac{\eta \Delta T_t}{\eta T_t - T_w} \quad \text{temperature sensitivity coefficient}$$

The sensitivity coefficients are simple in the above form. Notice that evaluation of the coefficients in the case of the cold wire requires derivatives of the signal (E), in contrast to the case of the hot wire which requires only the signal itself. However, $T_w$ is a function of time and, in general, these coefficients are not constant. If one substitutes the solution for $\dot{E}$ and $T_w$ (equations 4 and 9) into the above equations and solves for the rate of voltage change, the equations become

$$\Delta\dot{E}\Big|_{T_t = \text{constant}} = \frac{E\alpha(\eta T_t - T_{w_i})}{\tau} e^{-\frac{t}{\tau}} \frac{f'(Re)}{f(Re)} \Delta Re \tag{23a}$$

and

$$\Delta\dot{E}\Big|_{\rho u = \text{constant}} = \frac{E\alpha}{\tau} \eta \Delta T_t \tag{23b}$$

Combining yields

$$\frac{\Delta\dot{E}\Big|_{T_t}}{\Delta\dot{E}\Big|_{\rho u}} = \frac{(\eta T_t - T_{w_i})}{\eta \Delta T_t} e^{-\frac{t}{\tau}} \frac{f'(Re)}{f(Re)} \Delta Re \tag{23c}$$

Therefore, the sensitivity of the cold wire to mass flow variations decreases exponentially with time while its sensitivity to temperature variations remains a constant. This trend is to be expected, since a wire in thermodynamic equilibrium with its surroundings is sensitive only to temperature variations. For the unheated wire, the sensitivity coefficients have the same sign if the wire temperature is less than the recovery temperature. (The signs are opposite if the wire temperature is greater. Such a condition could exist in the cold flow behind the contact surface.) This fact means the flow has the

tendency to help heat the wire. This situation does not exist in hot wire anemometry where the flow has a tendency to cool the wire. The condition of maximum sensitivity to mass flow occurs at $t = 0$, and the ratio of mass flow variations to temperature variations has a maximum there also. For the same percentage deviations of mass flow and total temperature, this function has a maximum of one for $M_s \rightarrow \infty$ and $Re \rightarrow 0$. The equation below summarizes this:

$$\frac{\Delta \dot{E}\big|_{T_t}}{\Delta \dot{E}\big|_{\rho u}} = \begin{cases} 0 & \text{as } t/\tau \rightarrow \infty \\ 1 & \text{as } t/\tau \rightarrow 0 \\ & \text{and } Re \rightarrow 0 \\ & M_s \rightarrow \infty \end{cases}$$

In certain cases of shock tube operation, the experimental determination of the mass flow and total temperature is desirable. The cold wire can give information leading to these two quantities.

In order to separate the mass flow and recovery temperature, it is necessary to run the wire under at least two different operating conditions and use these two conditions to solve simultaneously for the unknowns $T_r$ and $\rho u$. For a hot wire to do this in a shock tube, it is necessary to heat and operate the wire initially at two different temperature loadings for two identical shock tube runs, i.e., same $P_1$, $T_1$, and $M_s$ (see Ref. 6). However, the cold wire has an advantage over the hot wire here. The mass flow and recovery temperature separation can be accomplished simultaneously with only one shock tube run. The basic reason for this property is that the sensitivity coefficients change with time (see equation 22). The changing temperature loadings are obtained from the response of the wire as it

heats up during the hot flow. As the wire progressively gets hotter, each new wire temperature changes the operating condition (and sensitivity coefficients) and permits evaluation of $\rho u$ and $T_r$ (equation 21). This process could just as well take place in a cold flow if the body is hot.

For the purpose of this analysis, consider only a heat transfer relation given by equation 20. Then for the two operating conditions, called conditions 1 and 2 respectively, we have two identical heat transfer relations if the flow is assumed to be steady.

$$\frac{q_1 d}{k(T_r - T_{w_1})} = f(Re) \tag{20a}$$

$$\frac{q_2 d}{k(T_r - T_{w_2})} = f(Re) \tag{20b}$$

Taking the ratio of these equations, one obtains the wire recovery temperature,

$$T_r = \frac{q_1 T_{w_2} - q_2 T_{w_1}}{q_1 - q_2} \tag{24}$$

By virtue of equations 9 and 10, this result is equivalent to

$$T_r = \eta T_t = -\frac{\dot{E}_1\left(\frac{\Delta E_2}{E_i}_i + T_i\right) - \dot{E}_2\left(\frac{\Delta E_1}{E_i}_i + T_i\right)}{\dot{E}_1 - \dot{E}_2} \tag{25a}$$

For simplicity and ease of evaluation of this equation, the quantities at operating condition 1 should be taken at the conditions just after

the arrival of the shock wave, that is,

$$T_w = T_i = T_1 \; ; \quad \Delta E_1 = 0$$

then

$$T_r = \eta T_t = \frac{\dot{E}_1 \left( \frac{\Delta E_2}{E_1 \alpha_1} + T_1 \right) - \dot{E}_2 T_1}{\dot{E}_1 - \dot{E}_2} \tag{25b}$$

and

$$\eta T_t = \frac{\dot{E}_1 \Delta E_2}{E_1 \alpha_1} \left( \frac{1}{\dot{E}_1 - \dot{E}_2} \right) + T_1 \tag{25c}$$

These quantities determining $T_r$ in equation 25 are easily evaluated. Most of the quantities are in fact directly determined by observing the wire response. $T_1$, $\alpha_1$, and $E_1$ are predetermined variables.

The transport coefficients can now be evaluated in terms of the wire recovery temperature (equation 25). When the heat transfer rate, the thermal conductivity, and the difference between the wire temperature and recovery temperature are substituted into equation 20, the Reynolds number is determined if the dependence of the Nusselt number on Reynolds number is known. From the definition of the Reynolds number, the mass flow is determined. The experimental heat transfer results given in Figures 19 and 21, for air and argon respectively, determine such a relationship.

If $T_r$ has not been calculated or is not known, the mass flow may be determined directly from equations 20a and 20b. By subtracting equations 20a and 20b, one gets

$$q_1 - q_2 = \frac{k}{d} f(Re)(T_{w_2} - T_{w_1}) \tag{26}$$

In order to specialize this equation, let

$$f(Re) = A + B(\rho u)^{\zeta} \tag{27}$$

Then

$$\rho u = \left[ \frac{\frac{q_1 - q_2}{T_{w_2} - T_{w_1}} \frac{d}{k} - A}{B} \right]^{\frac{1}{\zeta}} = \left[ \frac{\frac{\dot{E}_1 - \dot{E}_2}{\Delta E_2} E_1 \alpha_1 \frac{d}{k} - A}{B} \right]^{\frac{1}{\zeta}} \tag{28a}$$

A, B, and $\zeta$ are chosen to fit the experimental heat transfer laws. For free molecule flow the relation is especially simple since $\zeta = 1$, $A = 0$,

$$\rho u = \frac{E_1 \alpha_1}{\Delta E_2} (\dot{E}_1 - \dot{E}_2) \frac{1}{C} \tag{28b}$$

where C is a constant independent of the transport properties and is a function only of the gas constant, molecular speed ratio, and accommodation coefficient. Again the equation is easily solved since the response is monitored by an oscilloscope.

A major experimental difficulty occurs if the two operating conditions are chosen so that $\dot{E}_1 \sim \dot{E}_2$, because it is extremely difficult to read the small difference of two large numbers. A small error in the difference between $\dot{E}_1$ and $\dot{E}_2$ leads to a large error in the quantities $\rho u$ and $T_r$. However, this difficulty is overcome when $E_1$ is much different from $E_2$. In other words, the wire operating conditions should be chosen just after the shock wave passes over the

wire and at a later time corresponding to approximately the time constant of the wire. In this case, $\rho u$ and $T_r$ are easily determined. End loss corrections should be made throughout this analysis if the corrections are large enough to affect the signal level.

The experimental determination of mass flow and recovery temperature will be useful in the investigation of the contact region behind the hot flow, the actual measurement of boundary layer profiles in the shock tube, and in regions where the flow conditions are not calculable.

3. Response of Very Fine Wires to the Flow Within a Moving Shock Wave

The precise determination of the structure or thickness of a moving shock wave presents many experimental difficulties, principal among which is the lack of sensitivity and time resolution of any instrument that can give a localized measurement at the required low densities. However, such an investigation, if possible, would be of considerable interest*.

Some experience with very fine wires has been gained in the shock tube. These wires had a nominal diameter of 0.00001 inch (smaller wires can be obtained) and were made from an alloy of platinum and rhodium. The lengths of the wires were approximately 0.008 inch when mounted. If the wires were made slack (length of the wire divided by the sag approximately equal to 10), they withstood

---

* Fine wires using the steady state technique have been used to study shock wave structure in low density wind tunnels (Ref. 34).

the aerodynamic loads extremely well. Figure 7 shows the response of one of these wires in the two-inch round shock tube at an initial pressure of 50 mm Hg and a shock Mach number of 1.5. The calculated time constant is less than 16.7 μsec.

It is believed that these fine wires have a sufficiently fast response so that meaningful heat transfer measurements can be made in the flow within a moving shock wave. (Note: $\frac{10d}{U_s}$ and $\frac{d^2\rho c}{k}$ are the order of 1 m μsec.) To illustrate this point, the response of the wire is estimated in an assumed flow within the wave. It is assumed that: (1) the wire is in free molecule flow, and the ordinary heat transfer laws apply; (2) the wire temperature is constant while the shock wave is passing over the wire, although the derivative of the response $-\frac{dT_w}{dt}$ is not zero; (3) joule heating and radiation play an insignificant role; (4) the velocity distribution is represented by a hyperbolic tangent function symmetrical about the center of the wave; and (5) the energy integral is $c_p T + \frac{u^2}{2}$ = constant in the shock fixed system. An energy balance gives

$$\frac{d}{dt}(T_w - T_i) = \frac{AR\rho u}{(d\rho c)_w} \frac{g(s)}{s} (\eta T - T_w) \qquad (29)$$

where A is a constant, R = gas constant, $\frac{g(s)}{s}$ = function depending on the molecular speed tabulated in Reference 24, and $\eta = \frac{T_r}{T}$ = a function of molecular speed. For strong shocks, s approaches a constant with a maximum not too different from unity in the shock tube, and $\frac{g(s)}{s}\eta$ can be assumed to be a constant since it is not a strong function of s (i.e., between $0.4 < s < 1.2$). Neglecting also $T_w$ in

comparison to $T_r$ for a strong shock, the equation simplifies to

$$\frac{d}{dt}(T_w - T_i) = \frac{Bu^3}{u_s - u} \tag{30}$$

Let

$$u = \frac{u_2}{u}(1 + \tanh \alpha x) \tag{31}$$

where $x$ is measured from the center of the wave. The variables $x$ and $t$ can be related by $x = \delta/2 - u_s t$ where $\delta$ is some shock wave thickness. If the equation is specialized to a monatomic gas $\frac{u_2}{u_s} \rightarrow \frac{3}{4}$ as $M_s \rightarrow \infty$, then

$$\frac{1}{B} \frac{d(T_w - T_i)}{dt} \doteq \frac{(1 + \tanh \alpha x)^3}{1 - \frac{3}{8}(1 + \tanh \alpha x)}$$

and

$$T_w - T_i \doteq \frac{B^2}{\alpha u_s} \int \frac{1}{B} \frac{d(T_w - T_i)}{dt} d(\alpha x) \tag{32}$$

In Figure 23a, the normalized values of the velocity distribution, rate of change of wire temperature, and wire temperature are plotted as a function of $\alpha x$

$$\overline{u} = \frac{u}{u_2}, \quad \Delta\dot{\overline{T}}_w = \frac{\Delta \dot{T}_w}{\Delta \dot{T}_{w\,\alpha x = \infty}}, \quad \Delta\overline{T}_w = \frac{\Delta \overline{T}_w}{\Delta T_{w\,\alpha x = 2}}$$

The results show that the unheated wire responds very rapidly after the first half of the shock wave passes. Initially, the wire does not

change its temperature rapidly because the mass flow and recovery temperature are small. Figure 23b shows the response of the wire if it is heated. While the response is qualitatively the same, it does have some additional features. The first portion of the shock wave can be used to infer the initial mass flow since the wire temperature and recovery temperature are approximately known. At first, the wire cools as it is hotter than the flow, but then later the trend is reversed. At the instant when the wire is neither heating nor cooling ($\frac{dT_w}{dt} = 0$), the recovery temperature of the flow equals the wire temperature. This in turn is very similar to the initial temperature since the wire changes its temperature a very small amount ($\frac{\Delta T_w}{T_i} \ll 1$). The rate of change of wire temperature will be a constant after the shock wave passes. The flow after the shock wave can be used to calibrate the wire under known operating conditions which can in turn be used to reduce the heat transfer results from the flow within the shock wave.

The magnitude of the voltage signals are of prime concern, since these will partly determine whether or not this technique for studying shock wave structure is practical. The maximum voltage signal output, defined as the magnitude of the voltage change of the gage just after the complete passage of the shock wave, can be estimated.

$$\Delta E_{max} \simeq \frac{t}{\tau} T_t I R_i \alpha_i \tag{33}$$

where $t$ = time required for the shock to pass the wire, $T_t$ = total temperature of the flow after the shock wave, and $\tau$ = ideal

two-dimensional time constant taken at conditions after the shock wave. An experiment in argon at an initial pressure of 50 $\mu$Hg and $M_s = 10$ gives $\Delta E_{max} = 0.5$ mv for a 0.00001 inch diameter platinum-rhodium wire for a shock thickness taken equal to one mean free path of the undisturbed gas. This is a small signal, but it is still large enough so that it could possibly be used. The signal output cannot be increased or decreased by changing the initial pressure, since the wire response to a strong wave rests primarily on the diameter and shock wave speed. This can be shown with the help of the preceding equation. Let

$$t \sim \frac{\Lambda_1}{M_s a_1} ; \quad \Lambda_1 \sim \frac{\mu_1}{\rho_1 \bar{c}_1} ; \quad T_t \sim T_1 M_s^2$$

$$\tau = \frac{(d^2 \rho c)_w}{4Nuk} \sim \frac{(d\rho c)_w}{\rho_1 M_s a_1 c_p}$$

Substituting these into the above equation gives

$$\frac{\Delta E_{max}}{IR_i \alpha_i T_i} \doteq \frac{M_s^2}{d} \frac{\mu_1 c_p}{(\rho c)_w \bar{c}_1} \doteq \frac{M_s^2}{d} \left[ \frac{\mu_1}{(\rho c)_w} \sqrt{\frac{R}{T_1}} \right] \qquad (33)$$

The quantity in the bracket is fixed by the choice of test gas and wire material. It does not vary much with different gas properties. Hence, the signal is proportional to the shock speed squared and inversely proportional to the diameter.

It appears that the fine wire may be able to shed some light on the structure or thickness of a strong shock wave. The experimental

difficulties do not seem insurmountable if the experimenter has at his disposal sufficient electronic equipment. The most critical piece of equipment is a high-gain, fast-response oscilloscope which is necessary in order to monitor the probe output.

4. Detection of Flow Non-Uniformities

The variation of the heat transfer to a wire provides a sensitive test for many flow non-uniformities produced in shock tubes. For example, the heat transfer to the wire is very sensitive to the shock wave velocity ($M_s a_1$) as shown by Figures 14 to 17. If the shock wave is accelerating or decelerating, the flow behind the shock wave is continually changing and in turn continually affecting the heat transfer to the wire. If the time constant of the wire is made large with respect to the duration of the hot flow, the response of the wire should ideally appear as a straight line (Fig. 7). Deviations from this straight line indicate that the wire recovery temperature or mass flow is changing. The wire probe must be of sufficient length so that end losses are negligible and do not affect the wire response (see Appendix A).

These heat transfer signals are easy to interpret and detect using the linear portion of the response of a wire. The test is sensitive because deviations from a straight line are easily detected. Tests of flow non-uniformities can also be carried out using thin film gages, but these responses are non-linear and make it difficult to interpret only but the largest flow variations.

# VII. CONCLUSIONS

The fine wire probe employing the calorimetric principle of heat transfer in its operation is shown to be a useful instrument in the shock tube.

The ideal response of the wire is easily interpreted, since the heat transfer rate to the wire is the instantaneous slope of this response. If the wire is operated at small excitation currents so that it remains at the temperature of the surroundings prior to the initiation of the hot flow, the initial heat transfer to the wire does not depend on end loss corrections. The wire then represents a perfect calorimeter.

It has been found necessary to calibrate all the quantities associated with the geometrical and physical properties of the wire ($d$, $\rho c$, $\alpha$) in order to take quantitative heat transfer measurements. The technique of weighing the wire to infer their diameters and using an electrical calibration to evaluate the wire physical constant $\rho c$ has proved successful.

Measurements of heat-transfer rates to cold wires have been made in air and argon in the shock tube. The non-dimensionalized heat transfer results differ slightly from those for hot wires at Reynolds numbers greater than 1 in air. The results show excellent repeatability and consistency.

The wire is extremely useful as a wave detection device, and, if the wire is calibrated, it can also measure local shock speeds ($M_s$) by measuring the heat transfer rate to the wire. This is based on the experimental relation of $q$ versus $M_s$.

The cold wire responds to both mass flow and temperature variations. The relationship between these variations is derived, and it is shown that this relation is a function of time. Using this relation, it is shown that under certain conditions of wire operation the effects of mass flow and temperature on wire response may be separated with a single shock tube run, and the cold wire can be used as a mean flow device.

# REFERENCES


1. Kennelly, A. E., Wright, C. A., and Van Bylevelt, J. S.: The Convection of Heat from Small Copper Wires. Trans. of AIEE, Vol. 28, Part 1, 1909, pp. 363-393.

2. King, Louis Vessot: On the Convection of Heat from Small Cylinders in a Stream of Fluid: Determination of the Convection Constants of Small Platinum Wires with Applications to Hot Wire Anemometry. Philosophical Trans. of Royal Society (London), Series A, Vol. 214, 1914, pp. 373-432.

3. Dryden, H. L., and Kuethe, A. M.: The Measurement of Fluctuations of Air Speed by the Hot Wire Anemometer. NACA Report No. 320, 1929.

4. Kovasznay, Leslie S. G.: The Hot Wire Anemometer in Supersonic Flow. Journal of Aeronautical Sciences, Vol. 17, 1950, pp. 565-572.

5. Laufer, J., and McClellan, R.: Measurements of Heat Transfer from Fine Wires in Supersonic Flows. Journal of Fluid Mechanics, Vol. 1, Part 3, September 1956, pp. 276-289.

6. Dosanjh, Darshan S.: Use of a Hot Wire Anemometer in Shock Tube Investigations. NACA TN 3163, 1954.

7. Billington, Ian J.: The Hot Wire Anemometer and its Use in Non-Steady Flow. University of Toronto, UTIA TN 5, 1955.

8. Dosanjh, Darshan S., Kovasznay, L. S. G., and Clarken, P.: Study of Transient Hot Wire Response in a Shock Tube. CM-725, Department of Aeronautics, The Johns Hopkins University, March 12, 1952.

9. Rose, Peter H., and Stark, W. I.: Stagnation Point Heat Transfer Measurements in Dissociated Air. AVCO Research Report 3, April 1957. Also, Journal of Aero/Space Sciences, Vol. 25, No. 2, 1958, pp. 86-97.

10. Rose, Peter H.: Development of the Calorimeter Heat Transfer Gage for Use in the Shock Tubes. AVCO Research Report 17, February 1958.

11. Rabinowicz, J.: Aerodynamic Studies in the Shock Tube. GALCIT Hypersonic Research Project, Memo. No. 38, California Institute of Technology, June 10, 1957.

12. Evans, Robert C.: Operation and Performance of a Shock Tube with a Heated Driver. GALCIT Hypersonic Research Project, Memo. No. 48, California Institute of Technology, February 1, 1959.

13. Russell, D. A.: A Study of Area Change Near the Diaphragm of a Shock Tube. GALCIT Hypersonic Research Project, Memo. No. 57, California Institute of Technology, July 20, 1960.

14. Roshko, A.: On Flow Duration in Low-Pressure Shock Tubes. Physics of Fluids, Vol. 3, No. 6, November-December 1960, pp. 835-842.

15. American Institute of Physics Handbook. McGraw-Hill Book Company, 1957.

16. Strong, J., Neher, H. V., Whitford, A. E., Cartwright, C. H., and Hayward, R.: Procedures in Experimental Physics. Prentice Hall, 1946, pp. 215-216.

17. Kovasznay, Leslie S. G.: The Hot-Wire Anemometer in Supersonic Flow. Journal of Aeronautical Sciences, Vol. 17, No. 9, September 1950, pp. 565-572.

18. Blackman, Vernon: Vibrational Relaxation in Oxygen and Nitrogen. Journal of Fluid Mechanics, Vol. 1, Part 1, May 1956, pp. 61-85.

19. Hilsenrath, J., et al: Tables of Thermal Properties of Gases. National Bureau of Standards, Circular 564, November 1, 1955.

20. Collis, D. C., and Williams, M. J.: Molecular and Compressibility Effects on Forced Convection of Heat from Cylinders. Aeronautical Research Laboratories, Report A.110, July 1958.

21. Dewey, C. F.: Hot Wire Measurements in Low Reynolds Number Hypersonic Flows. American Rocket Society, 15th Annual Meeting, December 1960.

22. Weltmann, R. N., and Kuhns, P. W.: Heat Transfer to Cylinders in Crossflow in Hypersonic Rarefied Gas Streams. NASA TN D-267, March 1960.

23. Schlicting, H.: Boundary Layer Theory. McGraw-Hill Book Company, 4th Edition, 1960.

24. Stalder, J. R., Goodwin, G., and Creager, M. O.: A Comparison of Theory and Experiment for High-Speed Free-Molecule Flow. NACA TN 2244, December 1950.

25. Cole, J., and Roshko, A.: Heat Transfer from Wires at Reynolds Numbers in the Oseen Range. Proceedings of the Heat Transfer and Fluid Mechanics Institute, 1954.

26. Collis, D. C., and Williams, M. J.: Two-Dimensional Convection from Heated Wires at Low Reynolds Numbers. Journal of Fluid Mechanics, Vol. 6, 1959, pp. 357-384.

27. McAdams, W. H.: Heat Transmission. McGraw-Hill Book Company, 3rd Edition, 1954.

28. Tewfik, O. K., and Giedt, W. H.: Heat Transfer, Recovery Factor and Pressure Distributions Around a Cylinder Normal to a Supersonic Rarefied Air Stream. Part 1, Experimental Data, University of California, HE-150-162, January 30, 1959.

29. Cybulski, R. J., and Baldwin, L. V.: Heat Transfer from Cylinders in Transition from Slip Flow to Free Molecule Flow. NASA Memo. 4-27-59E, 1959.

30. Willis, D. R.: On the Flow of Gases under Nearly Free Molecular Conditions. Princeton University, Department of Aeronautical Engineering, Report No. 442, December 1958.

31. Fay, J. A., and Riddell, F. R.: Theory of Stagnation Point Heat Transfer in Dissociated Air. Journal of Aeronautical Sciences, Vol. 25, February 1958, pp. 73-85.

32. Nocilla, S.: On the Interaction Between Stream and Body in a Free Molecule Flow. Part III, "Relations Between the Interaction Coefficients and the Setting Time of the Molecules on the Surface", Laboratory of Applied Mechanics, Politechnic Inst. of Torino, October 1960.

33. Oliver, R. N.: Experimental Determination of Accommodation Coefficients as Functions of Temperature for Several Metals and Gases. Thesis, California Institute of Technology, 1950.

34. Sherman, F. S.: A Low-Density Wind-Tunnel Study of Shock-Wave Structure and Relaxation Phenomena in Gases. NACA TN 3298, July 1956.

35. Bateman, H.: Bateman Manuscript Project, "Tables of Integral Transforms". McGraw-Hill Book Company, 1953.

36. Carslaw, H. S., and Jaeger, J. C.: Conduction of Heat in Solids. Oxford Clarendon Press, 1947.

37. Hirschfelder, J. O., Curtiss, C. F., and Bird, R. B.: Molecular Theory of Gases and Liquids. John Wiley and Sons, Inc., 1954.

38. Mirels, H.: Attenuation in a Shock Tube Due to Unsteady-Boundary-Layer Action. NACA TN 3278, August 1956.

# APPENDIX A

## 1. Support Influence on the Calorimetric Property of the Wire

It has been previously mentioned that the wire and its supports begin to heat up after the passage of the shock wave. However, the supports do not heat up as rapidly as the wire does because of their larger differences in mass per unit surface area*. This causes a temperature difference to be set up between the wire and its supports. When this occurs, the wire is no longer a perfect calorimeter because some heat is lost in conduction to the supports.

If heat transfer or flow measurements are made at some time after the shock has passed by, some correction will have to be made to correct for this heat loss. It is the purpose of this section to estimate this correction. In formulating the mathematical problem, the following assumptions are made: (1) no radiation effects, (2) no joule heating, (3) the wire's physical parameters are constant, and (4) the Nusselt number does not depend on the heat transfer rates. Consider the heat balance of a small differential element of the wire.

---

* For the case considered here, the ratio of mass to surface area is proportional to the diameter. Usually the support mass per unit surface area is greater than that of the wires by a factor of twenty or more. This indicates that the support has a characteristic response time which is of the order one hundred times that of the wires. It is interesting to note that a platinum sputtered one-dimensional heat transfer gage that has the same resistance per unit length as a 1/10 mil platinum wire has approximately the same mass for the same length (1 $\mu$g/cm). However, their mass to surface area ratio differs by a factor of one hundred, and the characteristic time constants differ by at least this factor, if not more.

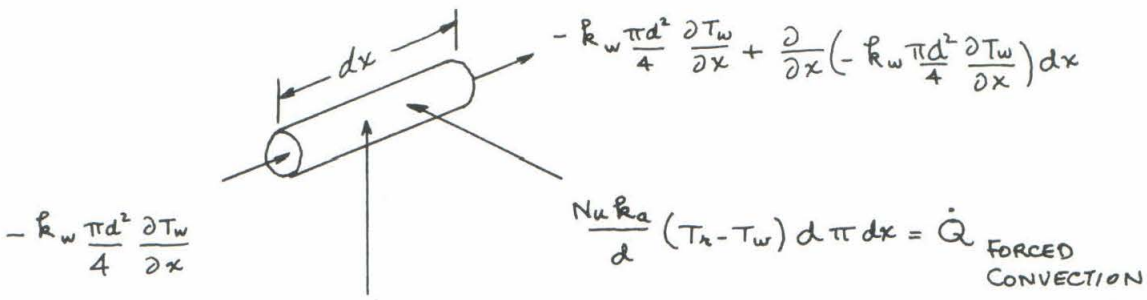


$$\dot{Q}_{STORED} = \frac{\pi d^2}{4} \rho_w c_w \frac{\partial T_w}{\partial t} dx$$

This results in the following differential equation:

$$k_w \frac{d^2}{4} \frac{\partial^2 T_w}{\partial x^2} + Nu\, k_a (T_r - T_w) = \frac{d^2}{4} \rho_w c_w \frac{\partial T_w}{\partial t} \qquad (A\text{-}1)$$

Let

$$\nu = \frac{4\, Nu\, k_a}{d^2 \rho_w c_w} \; ; \quad \kappa = \frac{k_w}{\rho_w c_w} \; ; \quad \Theta = \frac{T_w - T_i}{T_r - T_i}$$

In view of the preceding discussion, the boundary condition of the wire at the supports is assumed to have a fixed initial temperature. The conditions are written as

$$\theta(x, t) = \begin{cases} \theta(x, 0) = 0 \\ \theta(\pm \frac{L}{2}, t) = 0 \end{cases}$$

$$\kappa \frac{\partial^2 \theta}{\partial x^2} + \nu(1 - \theta) = \frac{\partial \theta}{\partial t} \qquad (A\text{-}2)$$

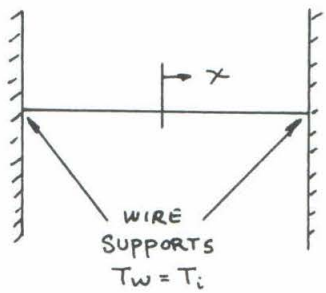


Applying the Laplace transformation to the time variable,

$$\frac{\partial^2 \tilde{\theta}}{\partial x^2} - \left(\frac{\nu + s}{\kappa}\right) \tilde{\theta} = -\frac{\nu}{s + \kappa} \qquad (A\text{-}3)$$

With the transformed boundary condition, the solution to this equation gives

$$\tilde{\theta}(x, s') = \frac{\nu}{s'(\nu + s')} \left[ 1 - \frac{\cosh \sqrt{\frac{\nu + s'}{\kappa}}\, x}{\cosh \sqrt{\frac{\nu + s'}{\kappa}}\, \frac{L}{2}} \right] \qquad \text{(A-4)}$$

This expression is then inverted with the help of Reference 35.

$$\Theta = \frac{T_w - T_i}{T_\infty - T_i} = 1 - \frac{\cosh \sqrt{\lambda}\, \frac{2x}{L}}{\cosh \sqrt{\lambda}} - \frac{2}{\pi} \lambda e^{-\frac{t}{\tau}} \sum_{n=0}^{\infty}{}' \frac{(-1)^n \cos\left[(n+\frac{1}{2})\frac{2\pi x}{L}\right] e^{-(n+\frac{1}{2})^2 \pi^2 \frac{t}{\tau\lambda}}}{(n+\frac{1}{2})\left[(n+\frac{1}{2})^2 \pi^2 + \lambda\right]} \qquad \text{(A-5)}$$

where $\lambda = \frac{Nu\, k_a}{k_w} \left(\frac{\ell}{d}\right)^2$ a non-dimensional length,

$\tau = \frac{d^2 \rho_w c_w}{4\, Nu\, k_a}$ ideal two-dimensional time constant of wire.

From this expression the average temperature $\overline{T}_w$ can be calculated.

$$\frac{\overline{T}_w - T_i}{T_\infty - T_i} = \frac{2}{L} \int_0^{\frac{L}{2}} \frac{T_w - T_i}{T_\infty - T_i}\, dx = 1 - \frac{1}{\sqrt{\lambda}} \tanh \sqrt{\lambda} - \frac{2}{\pi^2} \lambda e^{-\frac{t}{\tau}} \sum_{n=0}^{\infty} \frac{e^{-(n+\frac{1}{2})^2 \pi^2 \frac{t}{\tau\lambda}}}{(n+\frac{1}{2})^2 \left[(n+\frac{1}{2})^2 \pi^2 + \lambda\right]} \qquad \text{(A-6)}$$

This mean wire temperature represents the temperature that is used to calculate the voltage signal.

$$\dot{E} = I\dot{R}_w = I R_i \alpha_i \dot{\overline{T}}_w$$

The measured heat rate takes account only of the heat stored in the wire, and this is equal to $\frac{\pi d^2 \ell}{4} \rho c \dot{\overline{T}}_w$ or:

$$Q_{3D} = \frac{\pi d^2 \ell}{4} \rho_w c_w (T_\infty - T_i) \frac{2}{\pi^2} \frac{e^{-\frac{t}{\tau}}}{\tau} \left[ \sum_{n=0}^{\infty} \frac{e^{-(n+\frac{1}{2})^2 \pi^2 \frac{t}{\tau\lambda}}}{(n+\frac{1}{2})^2} \right] \qquad \text{(A-7)}$$

Ideally,

$$Q_{2D} = \frac{\pi d^2 \ell}{4} \rho_w c_w (T_r - T_i) \frac{e^{-t/\tau}}{\tau}$$

Therefore,

$$\frac{Q_{3D_{\text{measured value}}}}{Q_{2D_{\text{ideal}\ \lambda \longrightarrow \infty}}} = \frac{2}{\pi^2} \sum_{n=0}^{\infty} \frac{e^{-(n+\frac{1}{2})^2 \pi^2 \frac{t}{\tau\lambda}}}{(n+\frac{1}{2})^2} \qquad \text{(A-8a)}$$

If $\frac{t}{\tau\lambda} << 1$, this function can be represented by

$$\frac{Q_{3D}}{Q_{2D}} = 1 - \frac{2}{\sqrt{\pi}} \sqrt{\frac{t}{\tau\lambda}} + \cdots \qquad \text{(A-8b)}$$

$$= 1 - \frac{2}{\sqrt{\pi}} \sqrt{\frac{4 k_w t}{\ell^2 \rho_w c_w}} + \cdots \qquad \text{(A-8c)}$$

It is important to notice that this correction is independent of the flow conditions since $\tau\lambda$ is only a function of the wire properties.

At $t = 0$ the three-dimensional heat transfer rate is identical with that of the two-dimensional case, and no end loss correction is needed. However, because of the functional form of the correction, care must be maintained to keep $t/\tau\lambda$ sufficiently small. In Figure 24 the heat transfer correction is plotted as a function of $t/\tau\lambda$. The initial square-root dependence of the correction very rapidly approaches the function $\frac{8}{\pi^2} e^{-\pi^2/4\ t/\tau\lambda}$ (shown in the figure as a dotted line) which is the first significant term of the series solution of equation A-8a for long times.

The time constant for the three-dimensional case is taken as the intercept of the initial slope of the wire's response with the

equilibrium wire temperature. Since the initial temperature slopes of the two- and three-dimensional wires are the same, the three-dimensional time constant is related to the two-dimensional one by

$$\tau_{3D} = \tau \left( \frac{\overline{T_w} - T_i}{T_r - T_i} \right)_{t \to \infty} \qquad \text{(A-9)}$$

A plot of the equilibrium wire temperature and $\frac{\tau_{3D}}{\tau}$ is given as a function of $\lambda$ in Figure 25. The three-dimensional effects become quite large when $\lambda$ is much less than 100.

Figure 26 illustrates a wire response where $\lambda$ was deliberately made small to show its effect. Associated with the photograph is a graphical representation of the wire's response normalized so that it shows its exponential character. The three-dimensional response appears exponential when referred to the three-dimensional wire recovery temperature. It is not exponential when referred to any other value as shown, for example, by choosing an alternate temperature, the two-dimensional recovery temperature. The actual curve near $t = 0$ is not exponential, but the magnitude of the signal is such that the difference cannot be detected. The results between the calculated three-dimensional values, using previous experimental heat transfer results ( $\lambda$ large), and the measured values are good and are shown in the figure also.

The recovery temperature for a wire of infinite aspect ratio ( $\lambda \longrightarrow \infty$) can be found without a prior knowledge of the flow conditions (i.e., $\lambda$ ) by an integration with time of the three-dimensional wire response.

$$T_r = T_{w_i} + \int_0^{\infty} \dot{T}_w \, dt$$

But

$$\dot{T}_w = \frac{\dot{}}{T}_w \frac{Q_{2D}}{Q_{3D}}$$

Then

$$T_r = T_{w_i} + \int_0^{\infty} \frac{\dot{}}{T}_w \frac{Q_{2D}}{Q_{3D}} \, dt \qquad \text{(A-10)}$$

2. Estimate of Heat Conduction Losses to The Surrounding Media During Calibration

In calibrating the wire, some error is introduced due to the heat conduction to the surrounding medium. Figure 27 shows this effect. The rate at which heat is lost will be a function of the diffusivity of the surrounding medium, time, diameter of the wire, and other physical constants which are usually kept constant during all the calibrations. The ratio of heat conduction rate to the stored heat rate is the error in the calibration due to the presence of this heat loss mechanism

$$\frac{Q_c}{Q_s} = \epsilon \qquad \text{(A-11)}$$

It is this function that is studied here. It is assumed that there are no end loss corrections during calibration because the testing times (less than $\frac{\ell^2 \rho c}{4k_w}$ ) are too short to allow any end losses, but not so short that the heat conduction to the surrounding medium can be neglected.

The value of $Q_c$ requires the complete solution of the heat equation for the surrounding medium in cylindrical coordinates with the appropriate initial conditions.

$$\frac{k_a}{r} \frac{\partial}{\partial r} \left(r \frac{\partial T}{\partial r}\right) = \rho_a c_a \frac{\partial T}{\partial t}$$

No solution of this equation in closed form was found even for the simple case of a step rise in temperature of the wire (Ref. 36).

Dimensional analysis suggests that the heat lost by conduction is represented by

$$q_c = k_a \frac{(T_w - T_a)}{d} f\left(\frac{d^2 \rho_a c_a}{4 k_a t}\right) \qquad \text{(A-12a)}$$

or

$$Q_c = k_a (T_w - T_a) \frac{\pi \ell d}{d} f\left(\frac{d^2 \rho_a c_a}{4 k_a t}\right) \qquad \text{(A-12b)}$$

The stored heat rate is

$$Q_s = \frac{d}{dt}\left[\frac{\pi d^2 \ell}{4} \rho_w c_w (T_w - T_i)\right] = \frac{\pi d^2 \ell}{4} \rho_w c_w \dot{T}_w \qquad \text{(A-13)}$$

Therefore,

$$\frac{Q_c}{Q_s} = \frac{4 k_a (T_w - T_i)}{d^2 \rho_w c_w \dot{T}_w} f\left(\frac{d^2 \rho_a c_a}{4 k_a t}\right) = \epsilon \qquad \text{(A-14a)}$$

In the case of calibration of the wire, $(T_w - T_a)$ is approximately represented by the function $At$, where $A$ is a constant.

$$\frac{Q_c}{Q_s} = \frac{4 k_a A t}{d^2 \rho_w c_w A} f\left(\frac{d^2 \rho_w c_w}{4 k_a t}\right) = \frac{4 k_a t}{d^2 \rho_w c_w} f\left(\frac{d^2 \rho_a c_a}{4 k_a t}\right) \qquad \text{(A-14b)}$$

The empirical form of f is approximated by

$$f = B\left(\frac{d^2 \rho_a c_a}{4k_a t}\right) \qquad \text{(A-15)}$$

Fitting this to the calibration experiments gives

$$B = 1 \pm 20\ \%\ ; \qquad = 0.07 \pm 10\ \%$$

in the range

$$1 < \frac{d^2 \rho_a c_a}{4k_a t} < 100$$

Substituting equation A-15 into equation A-14b gives

$$\epsilon = \left(\frac{4k_a t}{\rho_w c_w d^2}\right)\left(\frac{d^2 \rho_a c_a}{4k_a t}\right)^{0.07} \qquad \text{(A-16a)}$$

The density of the surrounding medium can be written in terms of pressure and temperature with the help of the perfect gas law.

$$\epsilon = \left(\frac{4k_a t}{\rho_w c_w d^2}\right)\left(\frac{d^2 P_a c_a}{4k_a R_a T_a t}\right)^{0.07} \qquad \text{(A-16b)}$$

This formula shows the strong dependence of the calibration error on the diameter of the wire and time, while the pressure has only a slight effect. However, if the calibration is done in a container at sufficiently low pressures, the mean free path becomes comparable to the container dimensions. Then the conductivity is a function of the pressure (Knudsen gas), and, when this occurs, the conduction losses are reduced considerably.

If the allowable error is one per cent, the maximum permissible calibration time is approximately 200 $\mu$ sec for a 1 mil wire and only

2 $\mu$ sec for a 1/10 mil wire under atmospheric conditions. For accurate calibration the calibration time must be reduced drastically with the diameter under these conditions.

# APPENDIX B

## 1. Calculation of Transport Properties in Frozen Flow

The question of gas equilibrium was brought up in section V. 4 in connection with the reduction of the heat transfer measurements taken in air. The diatomic molecules of air undergo an energy redistribution due to the excitation of another internal degree of freedom in the range of measurements.

Only two cases were considered in section V. 4, that of complete equilibrium and that of completely frozen flow. The state properties of the gas and flow velocity u are easily calculated in such cases. For equilibrium flows, the shock tube equations are iterated with known equilibrium gas properties for a solution. Completely frozen flows are more simple to calculate and only require the theoretical solutions with a constant ratio of specific heats ( $\gamma$ ). The specific heat is chosen to correspond to the initial temperature of the flow. The transport properties of the gas are usually tabulated for the case of equilibrium. These values can be extended to include the effects of frozen flow under certain assumptions. Assume that $\mu = \mu(T)$ only and that it is independent of the internal degrees of freedom for a gas that is undergoing vibrational relaxation (Ref. 37). The Eucken approximation is used to relate the viscosity to the conductivity (the internal energy is assumed to be distributed independently of the velocity distribution) by

$$k = \frac{9\gamma - 5}{4} c_v \mu = \frac{9\gamma - 5}{4(\gamma - 1)} R \mu \qquad \text{(B-1)}$$

where R is the gas constant. The equilibrium viscosity can be used

in equation B-1 when the temperature of the flow is calculated (see above). By using the $\gamma$ determined by the initial temperature, the thermal conductivity is then approximately determined. The equilibrium conductivity is in all cases larger than the frozen conductivity when heating the gas. Care must be exercised in calculating the frozen thermal conductivity in region 5 if region 2 is in equilibrium. Here the appropriate $\gamma$ is taken at $T_2$, and $T_5$ is calculated on this basis. The effects are similar but are of a smaller scale and are only slightly displaced from the equilibrium curve.

## 2. Measurements of Shock-Wave Attenuation

Measurements were made of the shock wave attenuation in the two-inch diameter shock tube at the test section. The basic measurement involved the detection and determination of shock-wave speeds using four thin film gages. To measure shock wave velocity, the gages were grouped into two pairs, each pair capable of giving signals to measure shock wave speed when using Berkeley counters. The average shock-wave velocity was measured over approximately a span of two feet. The downstream gage of the first pair was separated by a distance of one foot from the upstream gage of the second pair of thin film shock wave detectors. The midpoint position of these side wall gages was 20.5 feet downstream of the diaphram section.

Two driver gases and two test gases were used in the experiments. Helium and nitrogen were used as driver gases while room air and standard grade argon were used as test gases. The attenuation measurements were carried out at fixed pressures similar to the

pressures used in making the heat transfer measurements ( $P_1$ = 500, 50, 5, 0.5 mm Hg ). The shock-wave Mach number was random.

There are stringent experiment requirements in order to measure shock-wave attenuation accurately. Attenuation is measured by the small difference in two large numbers. Error analysis of such measurements indicate that measuring shock-wave speeds to one per cent is not accurate enough for attenuation measurements. Indeed, the accuracy of the shock speed of one-tenth of one per cent may still involve considerable error in the measurements. The distances were measured to approximately $\pm$ 0.02 inch, and the counter was assumed to give a time accurate to $\pm$ 1 $\mu$sec. Under certain conditions of attenuation, this could still represent twenty-five per cent error, part of which is a systematic error and part is a random error of the counter.

Measurements were made and then reduced to the following form:

$$\frac{\Delta M_s}{M_s} \Delta x$$

where $\Delta M_s$ is the Mach number difference between the two shock speeds, $M_s$ is the average shock Mach number, and $\Delta x$ is the differential distance (in feet) from the midpoint of each of the two shock speed measurements. Only the attenuation measurements in air are presented and are shown in Figure 28. The results are plotted in the above form as a function of $M_s$ with the parameter $P_1$. These results were compared with the theory of Mirels (Ref. 37) for an air to air shock tube with an infinitely long driver. The case of a fully laminar or fully turbulent boundary layer within the shock tube was calculated

in this reference. The effect of the heat conductivity of the shock tube walls also enters into the calculations. The theoretical results also presented in Figure 28 have been derived on the assumption that the walls of the shock tube are perfect heat conductors. The results of Reference 38 were reduced to the form of the experimental results by the following method.

Case I: Laminar boundary layer

From Mirels

$$\frac{\Delta p_2}{p_2}\left(\frac{u_s}{u_2}\frac{d^2}{x}\frac{a_2}{\nu_2}\right)^{\frac{1}{2}} = -\mathcal{L}(M_s) \qquad \text{(B-2)}$$

where $\mathcal{L}(M_s)$ is the tabulated function determining the relationship between the Mach number and the Reynolds number giving the attenuation expressed in terms of the changing pressure immediately behind the shock wave (region 2). Differentiating equation B-2 with respect to x and rearranging gives

$$\frac{\partial}{\partial x}\left(\frac{\Delta p_2}{p_2}\right) = -\frac{\mathcal{L}(M_s)}{2}\left[\frac{M_2\frac{\mu_2}{\mu_1}}{M_2\frac{\rho_2}{\rho_1}}\right]^{\frac{1}{2}}\left(\frac{\mu_1}{\rho_1 a_1 d}\right)^{\frac{1}{2}}\frac{1}{\sqrt{xd}} \qquad \text{(B-3)}$$

The pressure jump across the shock wave and Mach number are related by

$$\frac{p_2}{p_1} = 1 + \frac{2\gamma}{\gamma+1}(M_s^2 - 1)$$

$$\frac{\Delta p_2}{p_2} = \frac{4\gamma M_s \Delta M_s}{2\gamma M_s^2 - (\gamma - 1)} \qquad \text{(B-4)}$$

Substituting this equation into B-3 gives

$$\frac{\Delta M_s}{M_s \Delta x} = -\frac{2\gamma M_s^2 - (\gamma - 1)}{4\gamma M_s^2}\frac{\mathcal{L}(M_s)}{2}\left[\frac{M_2\frac{\mu_2}{\mu_1}}{M_s\frac{\rho_2}{\rho_1}}\right]^{\frac{1}{2}}\left(\frac{\mu_1}{\rho_1 a_1 d}\right)^{\frac{1}{2}}\frac{1}{\sqrt{xd}} \qquad \text{(B-5)}$$

This equation, representing the shock wave attenuation per foot for a laminar boundary layer, was calculated for the initial pressures 5 and 0.5 mm Hg and for the conditions (x = 20.5', etc.) of the experiment. A similar calculation was carried out for the turbulent boundary layer case, and the result is indicated in equation B-6.

Case II; Turbulent boundary layer

$$\frac{\Delta M_s}{M_s \Delta X} = -\frac{2\gamma M_s^2 - (\gamma-1)}{4\gamma M_s^2} \frac{4}{5} T(M_s) \left(\frac{a_2}{a_1}\frac{M_2}{M_s}\right)^{\frac{7}{5}} \left(\frac{\mu_2/\mu_1}{\rho_2/\rho_1\, a_2/a_1}\right)^{1/5} \left(\frac{\mu_1}{\rho_1 a_1 d}\right)^{\frac{1}{5}} \frac{1}{d^{\frac{4}{5}} x^{\frac{1}{5}}} \quad \text{(B-6)}$$

where $T(M_s)$ is analogous to $\mathcal{L}(M_s)$. Calculations were made for the initial pressures of 500 and 50 mm Hg.

The theoretical results compare favorably with the experiment. Under no conditions was any experimental attenuation ( $\Delta M_s/M_s \Delta x$) greater than 0.01. The largest discrepancy between theory and experiment exists at 50 and 0.5 mm Hg. At 50 mm Hg the boundary layer is not completely turbulent. Hence, there would probably be a slight reduction in the attenuation because of the influence of the laminar boundary layer.

## 3. Calculation of Nearly Free-Molecule Flow Heat Transfer

The calculation of the heat transfer to a cylinder under nearly free molecule flow was approached by using the work of Willis (Ref. 30) in order to estimate the effects of the Knudsen number on the heat transfer. Willis has approached the problem of nearly free molecule flow of gases by transforming Boltzmann's equation into an integral form and applying an iterative method of solving for the distribution function under specific assumptions of surface interaction ($\alpha = 1$)

and collision mechanism (a modified Krook's molecular model). Willis has calculated the difference in heat transfer from the free molecule values to a two-dimensional strip as a function of the speed ratio of the gas stream and body temperature.

Assume that the heat transfer distribution and incident molecule distribution of a circular cylinder, as calculated by free molecule flow, remains unchanged under near free molecule conditions ( $\frac{1}{Kn} = \xi \ll 1$). The total heat transfer to a cylinder can then be represented by an equivalent (based on area) two-dimensional strip. Assume also that the recovery temperature does not change as the Knudsen number is increased. A heat balance per unit area of the two-dimensional strip, together with the conservation of mass, gives

$$q_{total} = q_{incident} - q_{reflected} = q_i - N_i \, 2 \, R \, T_w \qquad (B-7)$$

where i represents the actual number of incident molecules. Willis has tabulated values of $\frac{Q_i - Q_{io}}{Q_{io}}$ and $\frac{N_i - N_{io}}{N_{io}}$ for a two-dimensional strip as a function of gas temperature and body temperature. Let

$$\frac{Q_i - Q_{io}}{Q_{io}} \quad \frac{1}{\xi \ln \xi} \quad \frac{\sqrt{\pi}}{2} = \psi$$

$$\frac{N_i - N_{io}}{N_{io}} \quad \frac{1}{\xi \ln \xi} \quad \frac{\sqrt{\pi}}{2} = \chi$$

where io represents the free molecule calculations and $\xi$ is the reciprocal of the Knudsen number. Then

$$Q_t = Q_{io}\left(1 + \psi \frac{2}{\sqrt{\pi}} \xi \ln \xi\right) - \left(1 + \chi \frac{2}{\sqrt{\pi}} \xi \ln \xi\right) N_{io}\, 2R\, T_w$$

(B-8)

$$= (Q_{io} - N_{io}\, 2\, R\, T_w) + \psi \frac{2}{\sqrt{\pi}} \xi \ln \xi\, Q_{io} - \chi N_{io}\, 2\, R\, T_w \frac{2}{\sqrt{\pi}} \xi \ln \xi$$

With the definition of Nusselt number, the equation can be rewritten

$$\frac{Nu}{Re\ Pr} = \frac{Q_{io} - N_{io}\, 2\, R\, T_w}{\rho\, u\, c_p\, \Delta T} + \frac{2}{\sqrt{\pi}} \xi \ln \xi \left( \frac{\psi\, Q_{io} - \chi N_{io}\, 2\, R\, T_w}{\rho\, u\, c_p\, \Delta T} \right)$$

Now the two-dimensional strip heat-transfer coefficient can be related to a cylinder by a constant K by virtue of the first assumption. This equation then represents that of a cylinder if the corresponding free molecule heat-transfer results are used.

$$\frac{Nu}{Re\ Pr} = St = St_{\text{free molecule flow}}$$

(B-9)

$$+ \frac{2}{\sqrt{\pi}} \xi \ln \xi \left[ \psi\, St_{F.M.} + \frac{(\psi - \chi) N_{io}\, 2\, R\, T_w}{\rho\, u\, c_p\, \Delta T} \right]$$

$N_{io}$ can be calculated with the help of Reference 24.

$$St = St_{FM} + \frac{2}{\sqrt{\pi}} \xi \ln \xi \left[ \psi St_{FM} + (\psi - \chi) \frac{N\sqrt{2RT}}{2\sqrt{\pi}} \frac{g^\circ(s)}{2\pi} \frac{2RT_w}{\rho U c_p \Delta T} \right]$$

$$St = St_{FM} \left(1 + \frac{2\psi}{\sqrt{\pi}} \xi \ln \xi\right) + \frac{1}{\pi^2} \xi \ln \xi\, (\psi - \chi) \frac{g^\circ(s)}{s_\infty} \left(\frac{T_w}{T_r - T_w}\right)^{\frac{\gamma - 1}{\gamma}}$$

(B-10)

where $g^o(s)$ is tabulated in Reference 24. Specific examples have been calculated using this formula under the environmental conditions imposed by the shock tube. For argon, the results gave for

$M_s = 4.3$, $M_2 = 1.2$, and $T_w = 300^{\circ}K$.

| Knudsen Number | $St_{calc.}$ | $St_{fm}$ | St | % diff | Re | Nu |
|---|---|---|---|---|---|---|
| 194 | .323 | .325 | -.002 | - .62 | .01 | .0021 |
| 19.4 | .313 | .325 | -.012 | -3.7 | 0.1 | .0207 |
| 1.94 | .294 | .325 | -.031 | -10.5 | 1.0 | .194 |

The equivalent Nusselt number is plotted with the experimental results in Figure 21.

TABLE I

CALIBRATION RESULTS

| Nominal Diameter (Inches) | Material | Diameter * | Diameter ** | $\alpha_{0^oC}$ Handbook | $\alpha_{0^oC}$ Measured | ρc Handbook | ρc Measured * | ρc Measured ** |
|---|---|---|---|---|---|---|---|---|
| 0.001 | W | 0.00103 | 0.001 | 0.0045 | 0.00399 | 0.626 | 0.620 | 0.655 |
| 0.0005 | W | 0.00052 | 0.00048 | 0.0045 | 0.00378 | 0.626 | 0.60 | 0.70 |
| 0.0002 | W | 0.000194 | 0.00018 | 0.0045 | 0.00435 | 0.626 | 0.635 | 0.737 |
| 0.0005 | Pt | | 0.0005 | 0.0039 | 0.0036 | 0.681 | | 0.86 |
| 0.0001 | Pt | 0.000118 | 0.000096 | 0.0039 | 0.00393 | 0.681 | 0.675 | 1.02 |
| 0.00005 | $Pt_{90}Rh_{10}$ | | 0.00005 | 0.0017 | 0.00168 | 0.706 | | 1.07 |
| 0.00001 | $Pt_{90}Rh_{10}$ | | | 0.0017 | | 0.706 | | |

* Diameter based on optical measurements.

** Diameter calculated from the weight of the wire.

TABLE II

MATERIAL PROPERTIES

| Position | Metal | $\sigma \frac{\mu\Omega}{cm}$ | $\frac{\alpha}{^oC}$ | $\rho \frac{g}{cm^3}$ | $c \frac{cal}{g\,^oC}$ | $\frac{\sigma\alpha}{\rho c}$ |
|---|---|---|---|---|---|---|
| 1 | Fe | 9.8 | 0.0065 | 7.9 | 0.106 | 0.075 |
| 2 | Pt | 9.8 | 0.0039 | 21.5 | 0.032 | 0.055 |
| 3 | Ni | 7.2 | 0.0066 | 8.85 | 0.110 | 0.048 |
| 4 | $Pt_{90}Rh_{10}$ | 18.4 | 0.0016 | 21 | 0.034 | 0.041 |
| 5 | W | 5.5 | 0.0045 | 19.3 | 0.032 | 0.040 |
| 6 | Mo | 5.2 | 0.0033 | 10.2 | 0.061 | 0.028 |
| 7 | Al | 2.7 | 0.0045 | 2.7 | 0.226 | 0.020 |
| 8 | Au | 2.4 | 0.0034 | 19.3 | 0.031 | 0.014 |
| 9 | Ag | 1.5 | 0.0041 | 10.5 | 0.057 | 0.010 |
| 10 | Cu | 1.7 | 0.0043 | 8.9 | 0.092 | 0.009 |

# TABLE III

## TABULATED RESULTS OF

## HEAT GAIN TO COLD WIRES IN AIR

nominal diameter = 0.001" $\quad \bar{T}_1 = 300^{\circ}K = T_w$

measured diameter = 0.001" $\quad$ material: tungsten

| $P_1$ mm Hg | $M_s$ | $q \frac{cal}{cm^2 sec}$ | $P_1$ mm Hg | $M_s$ | $q \frac{cal}{cm^2 sec}$ |
|---|---|---|---|---|---|
| 500 | 1.38 | 15.7 | 5 | 1.482 | 2.46 |
| 500 | 1.318 | 11.5 | 5 | 1.406 | 1.84 |
| 500 | 1.447 | 21.3 | 5 | 2.32 | 18.55 |
| 500 | 2.37 | 207 | 5 | 2.56 | 29.2 |
| 500 | 2.02 | 113 | 5 | 3.52 | 89.5 |
| 50 | 1.357 | 4.86 | 5 | 3.29 | 70 |
| 50 | 1.402 | 5.81 | 5 | 3.69 | 108 |
| 50 | 1.371 | 4.88 | 5 | 5.64 | 461 |
| 50 | 1.517 | 9.15 | 5 | 4.77 | 277 |
| 50 | 1.81 | 20.5 | 0.5 | 6.01 | 167 |
| 50 | 2.6 | 101.5 | 0.5 | 4.0 | 39.1 |
| 50 | 2.86 | 141 | 0.5 | 4.52 | 62.2 |
| 50 | 4.21 | 479 | 0.5 | 6.84 | 250 |
| 50 | 3.81 | 385 | 0.5 | 6.63 | 276 |

TABLE III (cont'd.)

nominal diameter = 0.005" $\overline{T}_1 = 300^{\circ}K = T_w$

measured diameter = 0.00048" material: tungsten

| $P_1$ mm Hg | $M_s$ | $q \frac{cal}{cm^2 sec}$ | $P_1$ mm Hg | $M_s$ | $q \frac{cal}{cm^2 sec}$ |
|---|---|---|---|---|---|
| 500 | 1.515 | 42.1 | 5 | 2.52 | 38.5 |
| 500 | 1.333 | 19.5 | 5 | 3.09 | 83 |
| 500 | 1.53 | 41 | 5 | 4.56 | 340 |
| 50 | 1.36 | 7.46 | 5 | 2.16 | 188 |
| 50 | 1.736 | 25.5 | 0.5 | 4.16 | 55.2 |
| 50 | 2.274 | 85.2 | 0.5 | 5.17 | 120 |
| 50 | 3.02 | 261 | 0.5 | 6.54 | 276 |
| 50 | 4.07 | 840 | 0.5 | 2.87 | 11.9 |
| 5 | 1.387 | 2.29 | 0.5 | 2.25 | 4.1 |
| 5 | 1.503 | 3.64 | | | |

nominal diameter = 0.0002" $\overline{T}_1 = 300^{\circ}K = T_w$

measured diameter = 0.00018" material: tungsten

| | | | | | |
|---|---|---|---|---|---|
| 50 | 1.27 | 6.6 | 5 | 3.29 | 141 |
| 50 | 1.54 | 20.5 | 5 | 4.2 | 372 |
| 50 | 2.35 | 169 | 0.5 | 3.75 | 45 |
| 50 | 2.4 | 173 | 0.5 | 5.47 | 175 |
| 50 | 3.07 | 430 | 0.5 | 3.89 | 52 |
| 5 | 1.62 | 6.42 | 0.1 | 4.23 | 12.9 |
| 5 | 2.1 | 21.2 | 0.1 | 4.18 | 12.2 |
| 5 | 1.48 | 39.9 | 0.1 | 4.71 | 19 |
| 5 | 3.04 | 106 | | | |

TABLE III (cont'd.)

nominal diameter = 0.0001" $\overline{T}_1 = 300^{\circ}K = T_w$

measured diameter = 0.000096" material: platinum

| $P_1$ mm Hg | $M_s$ | $q \frac{cal}{cm^2 sec}$ | $P_1$ mm Hg | $M_s$ | $q \frac{cal}{cm^2 sec}$ |
|---|---|---|---|---|---|
| 5 | 1.505 | 5.95 | 0.5 | 4.38 | 81 |
| 5 | 2.11 | 29.2 | 0.5 | 5.34 | 156 |
| 5 | 2.84 | 104 | 0.5 | 3.78 | 43 |
| 5 | 3.04 | 133 | 0.1 | 5.21 | |
| 5 | 4.44 | 588 | 0.1 | 6.74 | 77 |
| 5 | 3.08 | 135 | 0.1 | 4.21 | 14.2 |

nominal diameter = 0.0005" $\overline{T}_1 = 300^{\circ}K = T_w$

measured diameter = 0.0005" material: platinum

| | | |
|---|---|---|
| 5 | 4.45 | 300 |

nominal diameter = 0.00005" $\overline{T}_1 = 300^{\circ}K = T_w$

measured diameter = 0.00005" material: $platinum_{90}\ rhodium_{10}$

| | | | | | |
|---|---|---|---|---|---|
| 5 | 4.08 | 450 | 0.5 | 4.27 | 72 |
| 5 | 3.81 | 366 | 0.5 | 4.1 | 57.5 |
| | | | 0.5 | 5.04 | 129 |

TABLE IV

TABULATED RESULTS OF

HEAT GAIN TO COLD WIRES IN ARGON

nominal diameter = 0.001" $\quad \overline{T}_1 = 300^{\circ}K = T_w$

measured diameter = 0.001" $\quad$ material: tungsten

| $P_1$ mm Hg | $M_s$ | $q \frac{cal}{cm^2 sec}$ | $P_1$ mm Hg | $M_s$ | $q \frac{cal}{cm^2 sec}$ |
|---|---|---|---|---|---|
| 50 | 2.25 | 44.1 | 5 | 1.68 | 4.25 |
| 50 | 2.14 | 38.3 | 5 | 2.67 | 28.2 |
| 50 | 1.54 | 9.6 | 5 | 2.08 | 10.75 |
| 50 | 2.45 | 67.1 | 5 | 4.09 | 145 |
| 50 | 2.74 | 108 | 0.5 | 3.69 | 24.8 |
| 50 | 3.63 | 310 | 0.5 | 3.75 | 25.9 |
| 5 | 2.63 | 26.4 | 0.5 | 4.12 | 42.0 |
| 5 | 3.08 | 52 | 0.5 | 5.15 | |
| 5 | 2.85 | 39.3 | | | |

nominal diameter = 0.0005" $\quad \overline{T}_1 = 300^{\circ}K = T_w$

measured diameter = 0.00048" $\quad$ material: tungsten

| | | | | | |
|---|---|---|---|---|---|
| 50 | 1.57 | 16.9 | 5 | 3.45 | 112 |
| 50 | 1.75 | 27.6 | 5 | 5.98 | 738 |
| 50 | 2.52 | 114 | 5 | 3.54 | 123 |
| 50 | 2.46 | 98.2 | 5 | 3.56 | 120 |
| 50 | 3.90 | 580 | 5 | 4.05 | 194 |
| 5 | 1.69 | 6.2 | 0.5 | 4.14 | 41 |
| 5 | 2.02 | 14.2 | 0.5 | 4.48 | 47.3 |
| 5 | 2.4 | 25.5 | 0.5 | 5.7 | 109 |

TABLE IV (cont'd.)

nominal diameter = 0.0002" $\overline{T}_1 = 300^{\circ}K = T_w$

measured diameter = 0.00018" material: tungsten

| $P_1$ mm Hg | $M_s$ | $q \frac{cal}{cm^2 sec}$ | $P_1$ mm Hg | $M_s$ | $q \frac{cal}{cm^2 sec}$ |
|---|---|---|---|---|---|
| 50 | 2.36 | 135 | 5 | 3.22 | 120 |
| 50 | 2.13 | 92.5 | 5 | 2.18 | 24.5 |
| 50 | 2.35 | 138 | 5 | 2.16 | 23.5 |
| 50 | 1.69 | 34.6 | 5 | 3.65 | 195 |
| 50 | 3.06 | 387 | 0.5 | 4.19 | 42 |
| 5 | 3.22 | 129 | 0.5 | 4.6 | 57 |

nominal diameter = 0.0001" $\overline{T}_1 = 300^{\circ}K = T_w$

measured diameter = 0.000096" material: platinum

| | | | | | |
|---|---|---|---|---|---|
| 5 | 3.52 | 200 | 0.5 | 5.13 | 93.5 |
| 5 | 3.86 | 298 | 0.5 | 5.21 | 96 |
| 5 | 2.0 | 21.4 | 0.5 | 4.99 | 81 |
| 5 | 2.98 | 103 | 0.5 | 4.08 | 39.8 |
| 0.5 | 3.35 | 21.5 | 0.5 | 4.19 | 41.7 |
| 0.5 | 3.37 | 22.5 | | | |

nominal diameter = 0.00005" $\overline{T}_1 = 300^{\circ}K = T_w$

measured diameter = 0.00005" material: $platinum_{90}$ $rhodium_{10}$

| | | | | | |
|---|---|---|---|---|---|
| 0.5 | 4.88 | 77 | 0.5 | 5.1 | 85 |

FIGURE 1

THE PROBE AND ITS MOUNTINGS

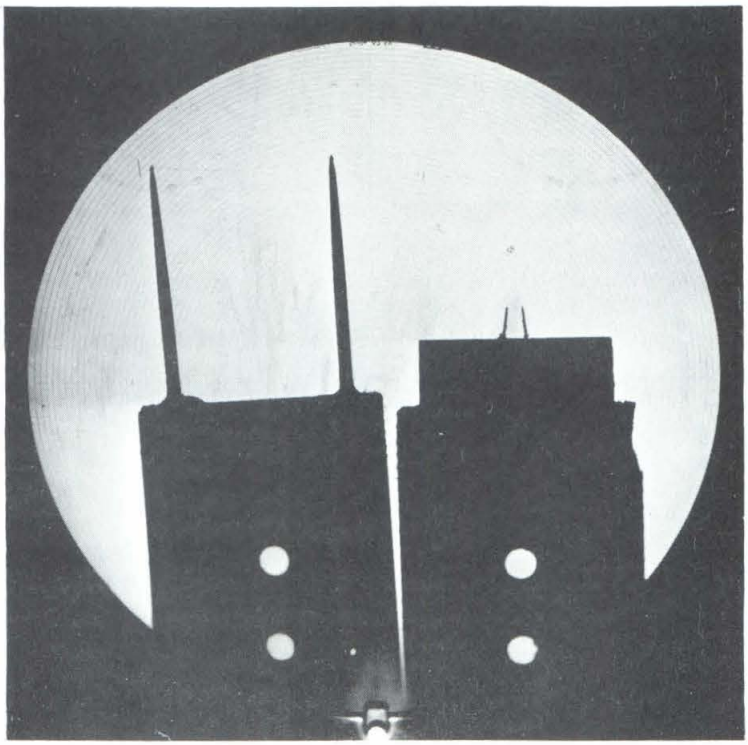

FIGURE 2

SILHOUETTES OF TWO PROBES

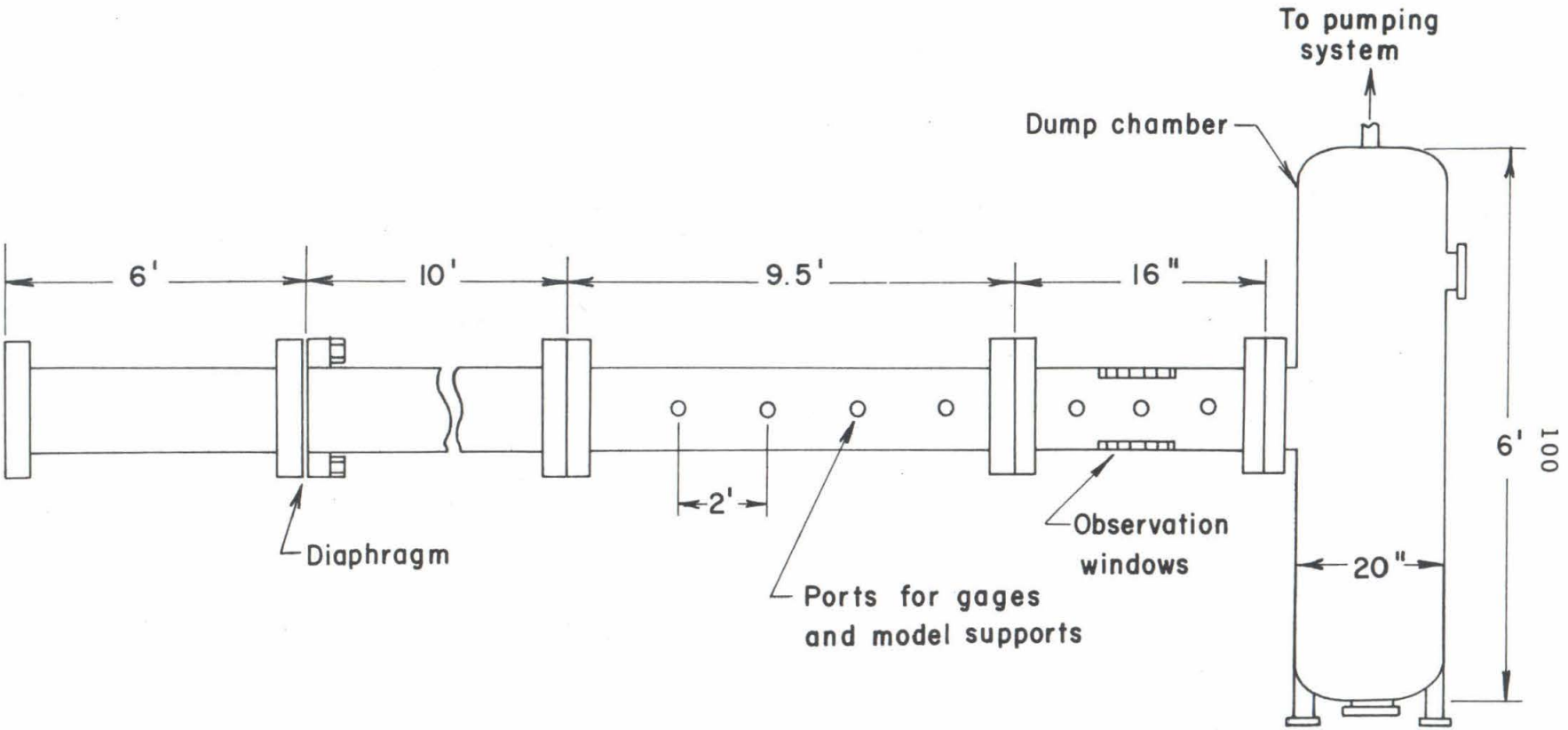


FIG. 3 - PRESENT ARRANGEMENT OF THE THREE INCH GALCIT SHOCK TUBE

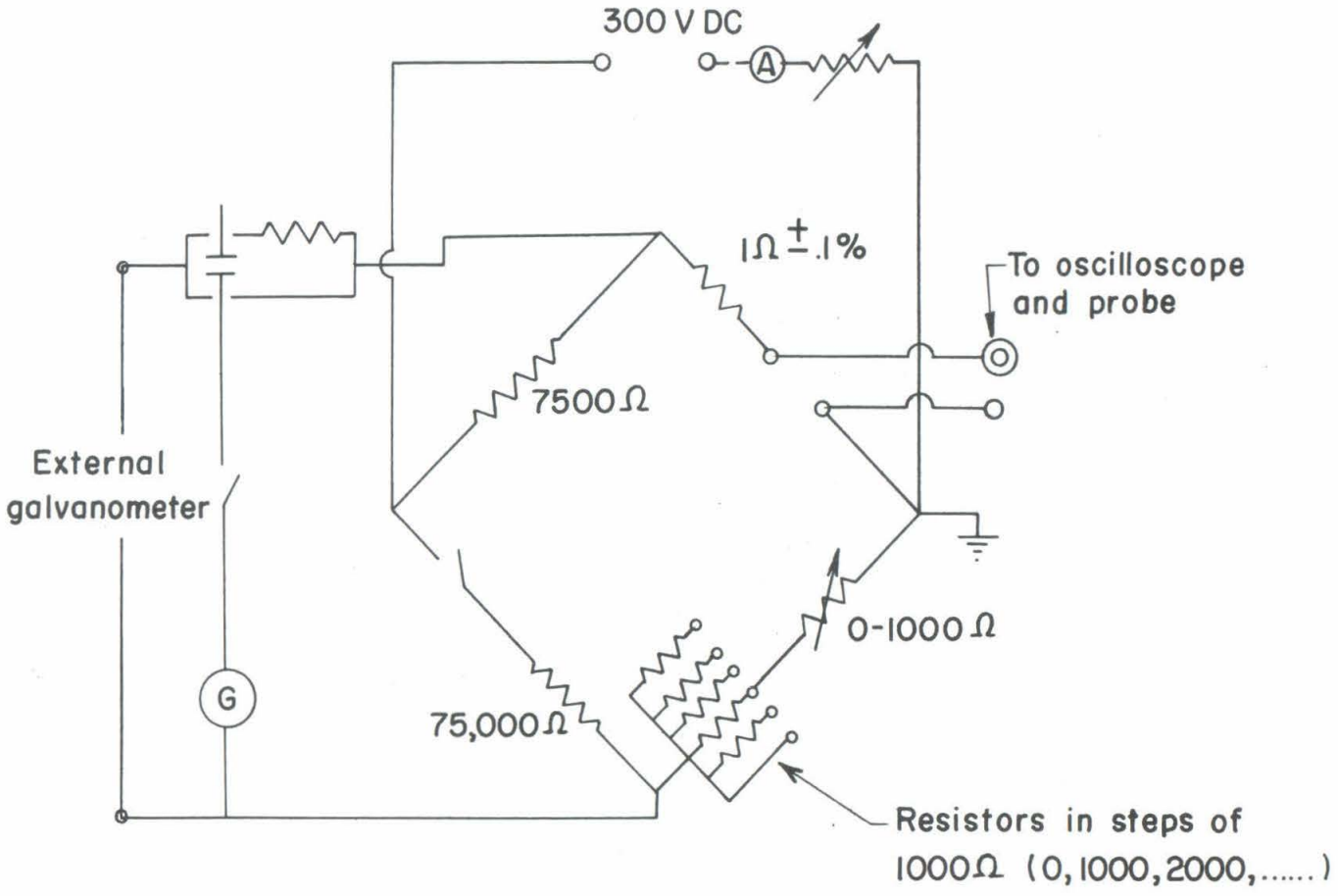


FIG. 4- WHEATSTONE BRIDGE

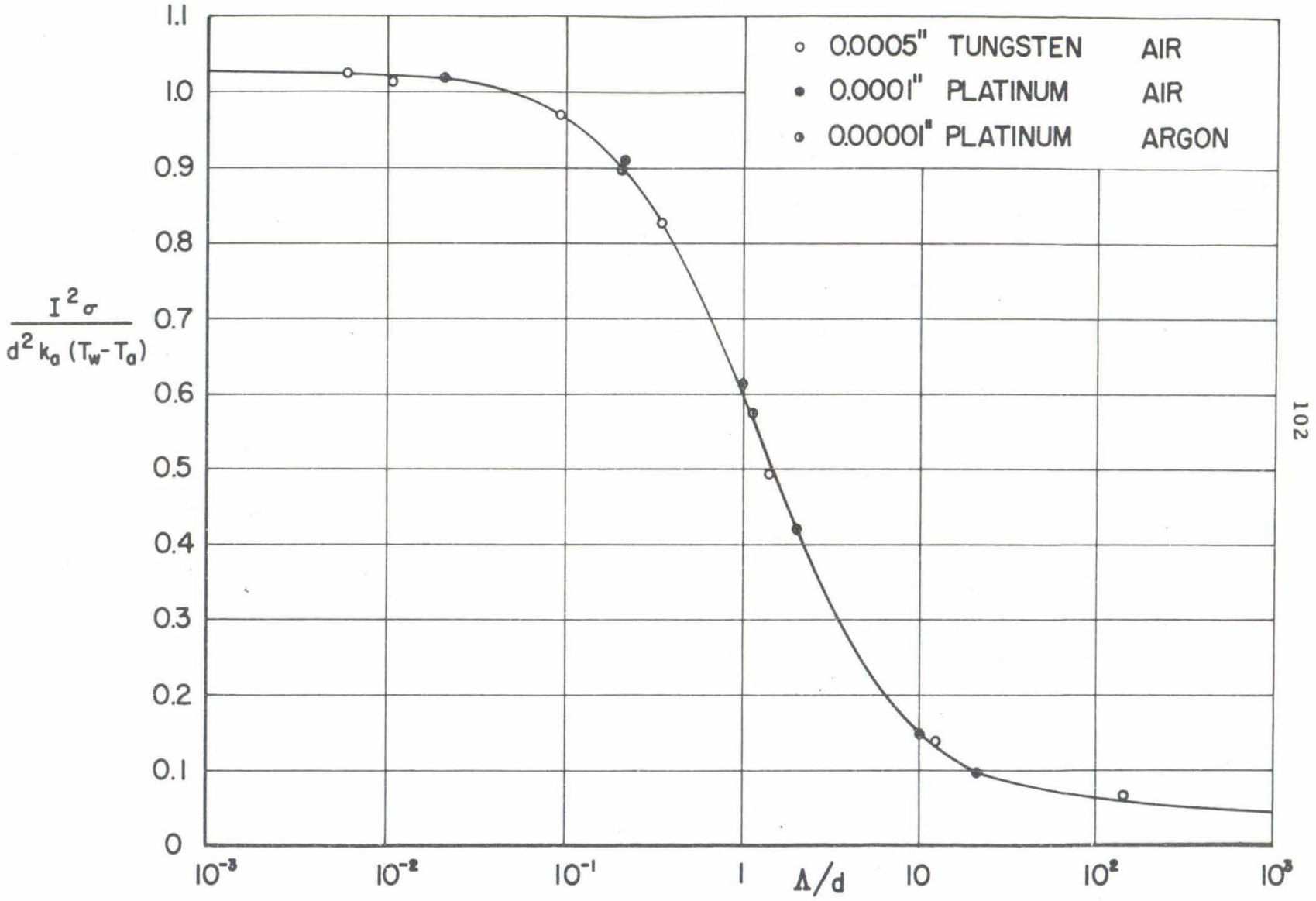


FIG. 5 - CURRENT REQUIRED TO HEAT A WIRE IN STILL AIR

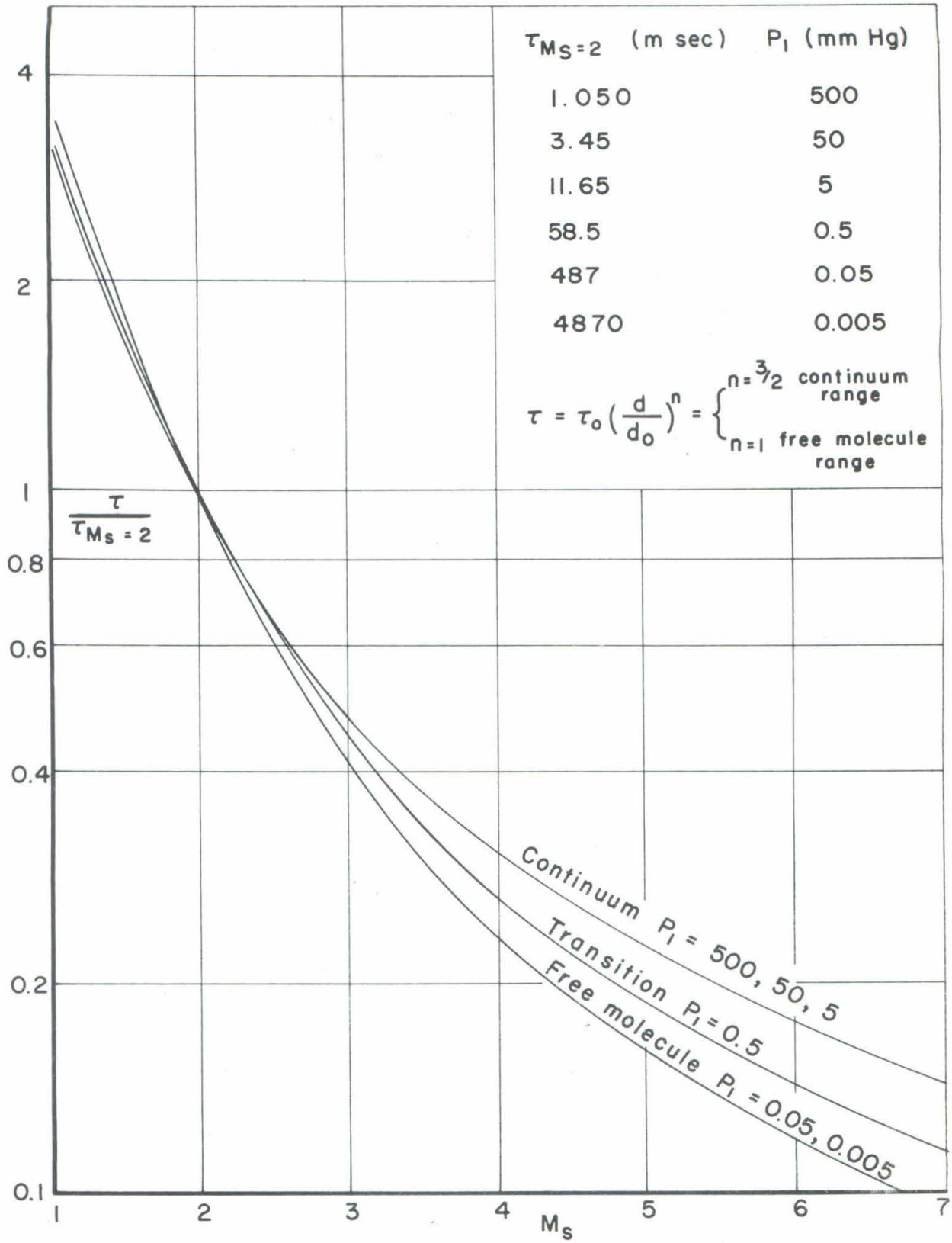


FIG. 6 - TIME CONSTANT OF A ONE MIL TUNGSTEN WIRE IN REGION 2

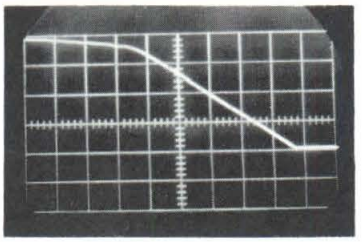

$t/\tau << 1$

Sweep = 100 $\mu$ sec/cm
d = .001"
$P_1$ = 4 mm Hg
$M_s^1$ = 4.06

Flow Duration = 500 $\mu$ sec
$\tau$ = 4000 $\mu$ sec
$t/\tau$ = .125

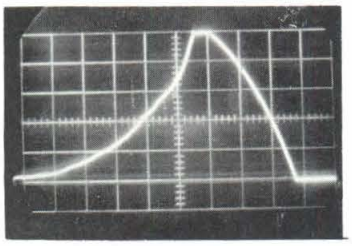

$t/\tau \cong 1$

Sweep = 200 $\mu$ sec/cm
d = .00018"
$P_1$ = 6.5 mm Hg
$M_s^1$ = 4.07

Flow Duration = 520 $\mu$ sec
$\tau$ = 320 $\mu$ sec
$t/\tau$ = 1.62

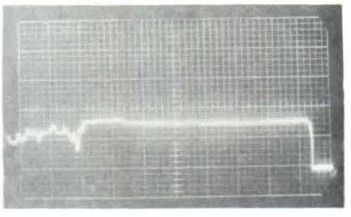

$t/\tau >> 1$

Sweep = 1000 $\mu$ sec/cm
d $\cong$ .00001"
$P_1$ = 50 mm Hg
$M_s^1$ = 1.5

Flow Duration = 7200 $\mu$ sec
$\tau \cong$ 16.7 $\mu$ sec
$t/\tau$ = 430

FIGURE 7

TYPICAL PROBE RESPONSES IN THE SHOCK TUBE

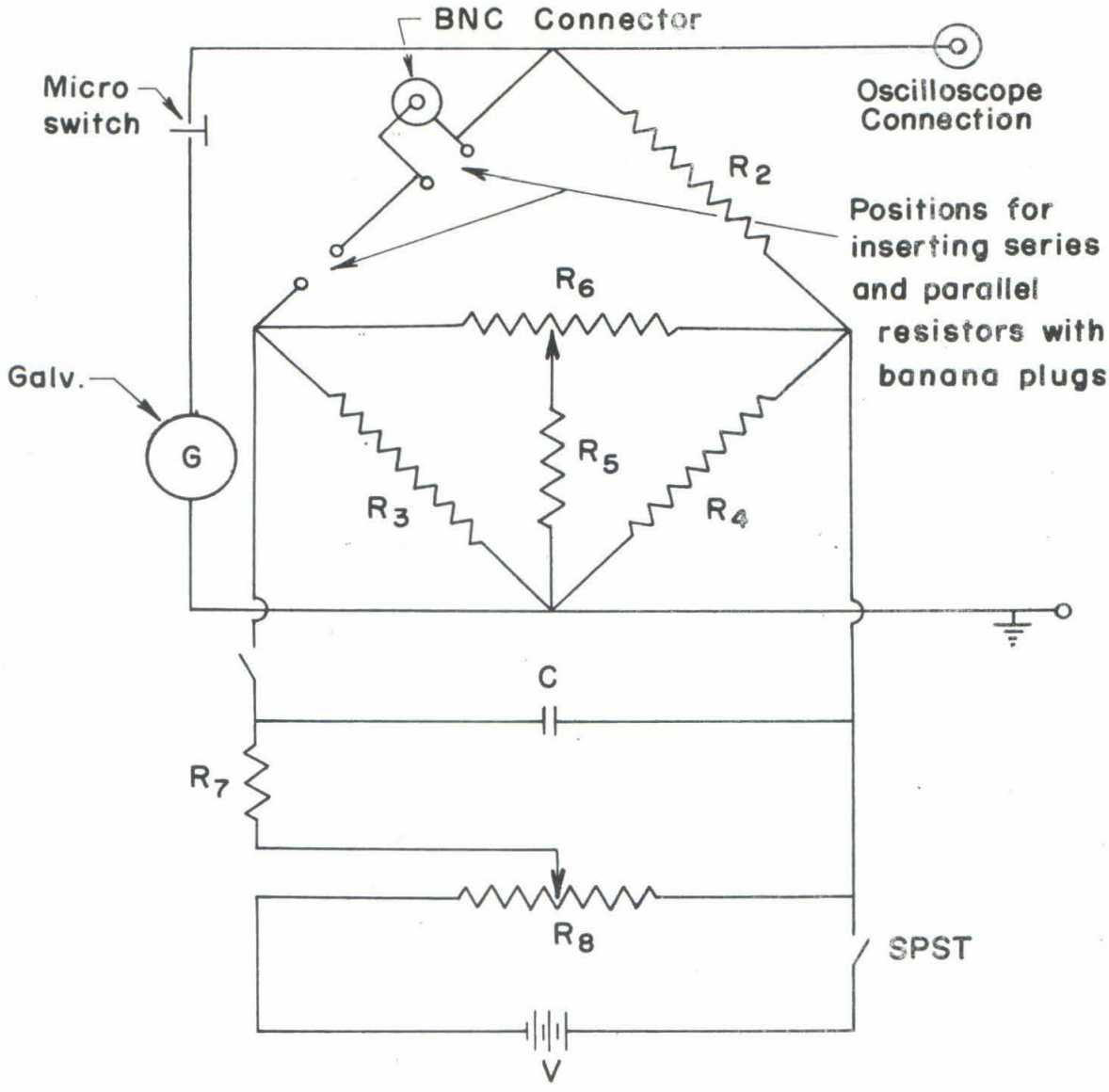


$R_2 = R_3 = R_4 = 50$ ohm

$R_5 = 500$ ohm

$R_6 = 0 - 1000$ ohm

$R_7 = 1000$ ohm

$R_8 = 0 - 1000$ ohm (.25% linearity Helipot)

C = 250 microfarads

FIG. 8 - CALIBRATION CIRCUIT

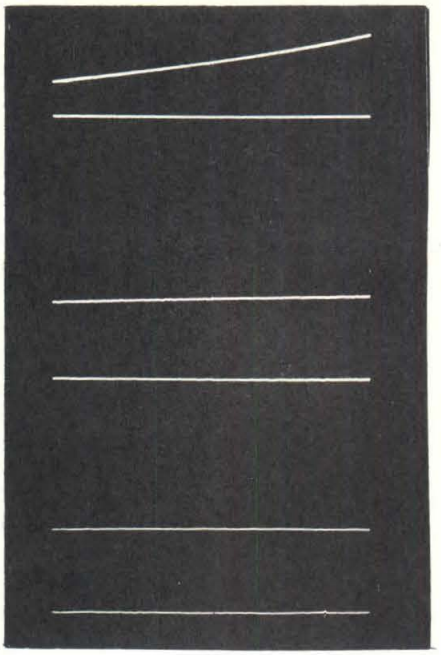


(a) Stable Resistance

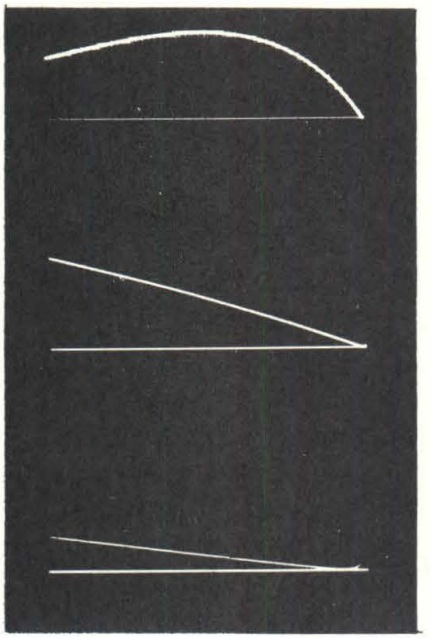


(b) Wire Resistance

FIGURE 9

CHARACTERISTICS OF CALIBRATION CIRCUIT

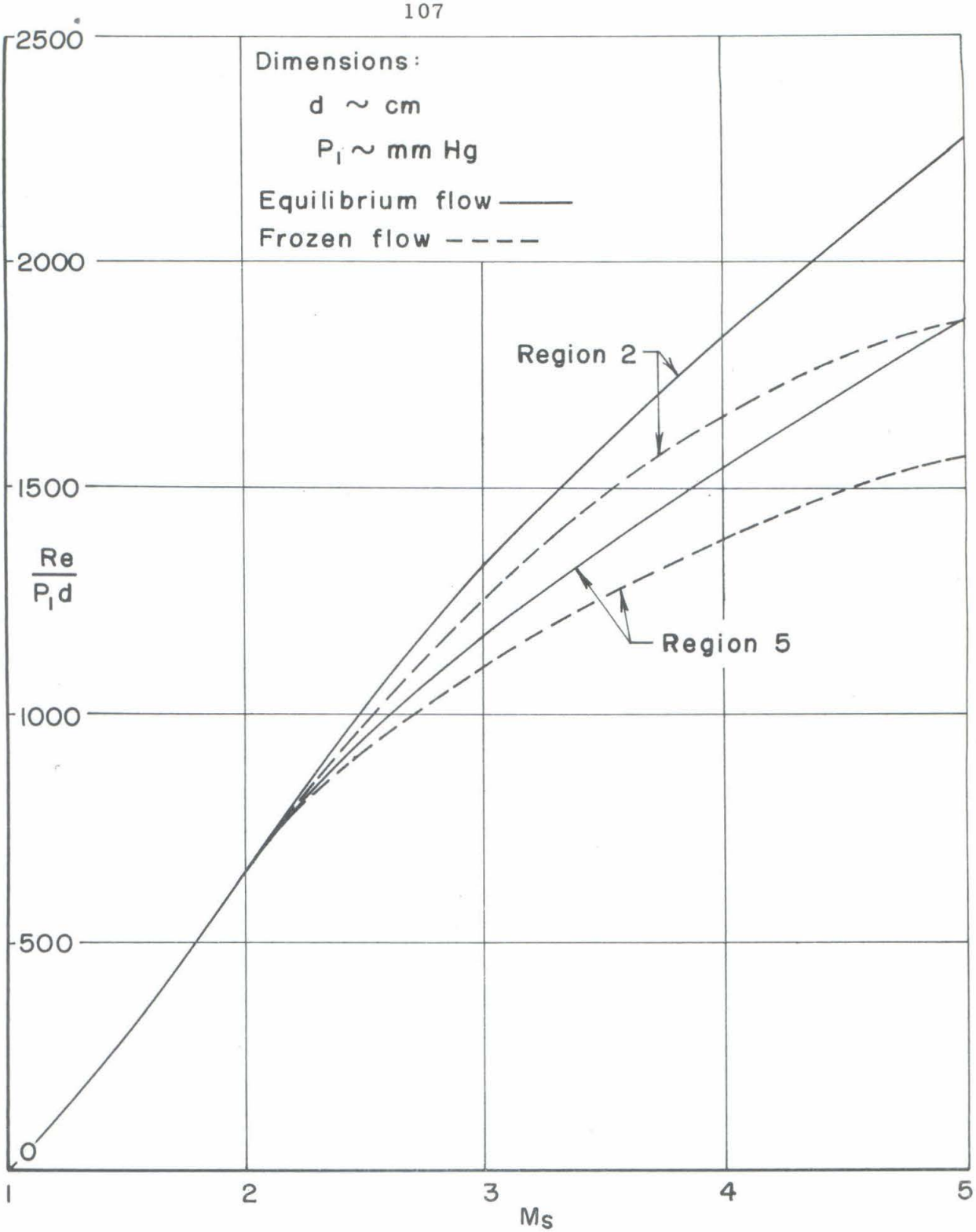


FIG. 10 - REYNOLDS NUMBER FOR EQUILIBRIUM AND FROZEN FLOW IN REGIONS 2 AND 5 FOR AIR

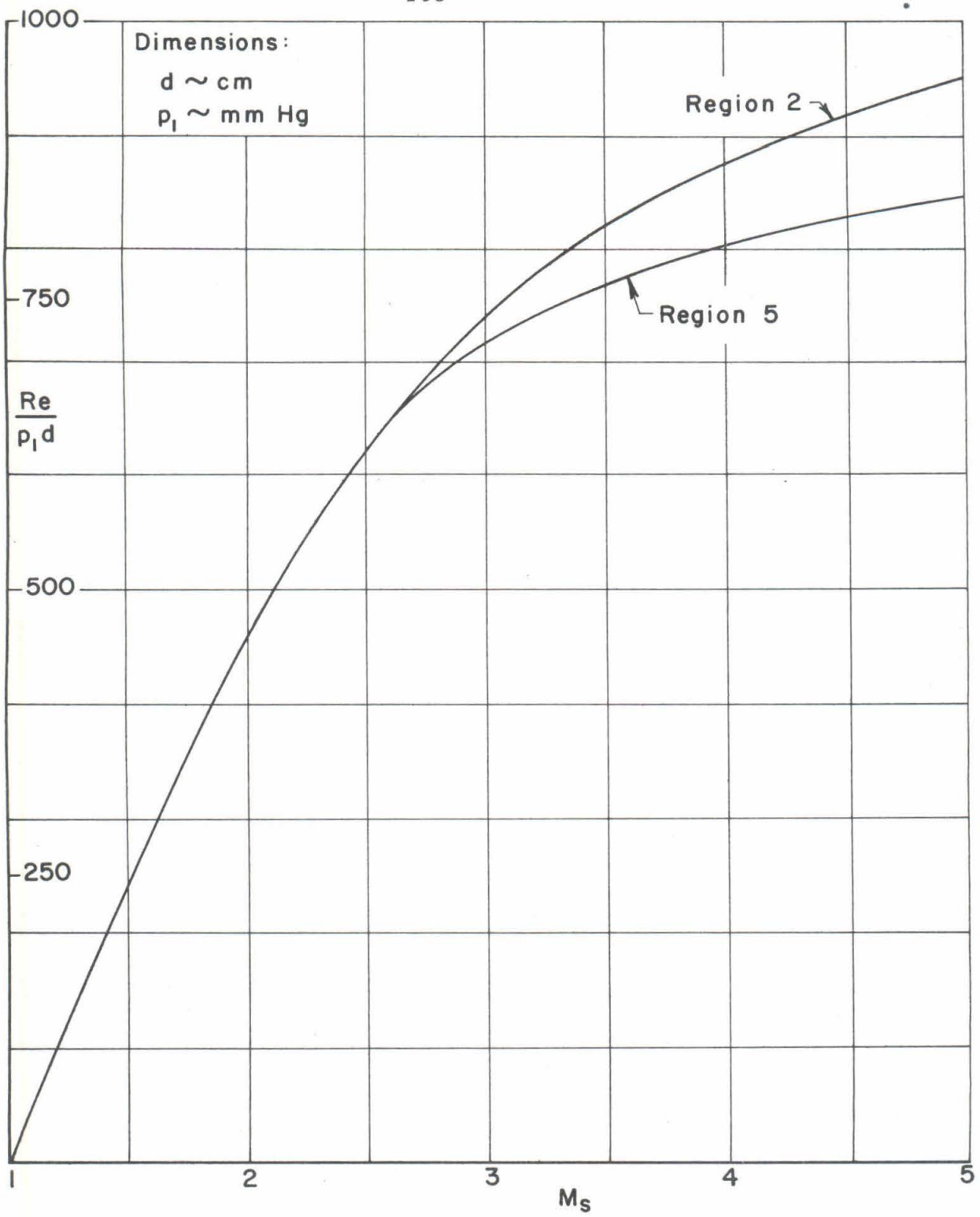


FIG. II – REYNOLDS NUMBER FOR FLOW IN REGIONS 2 AND 5 FOR ARGON

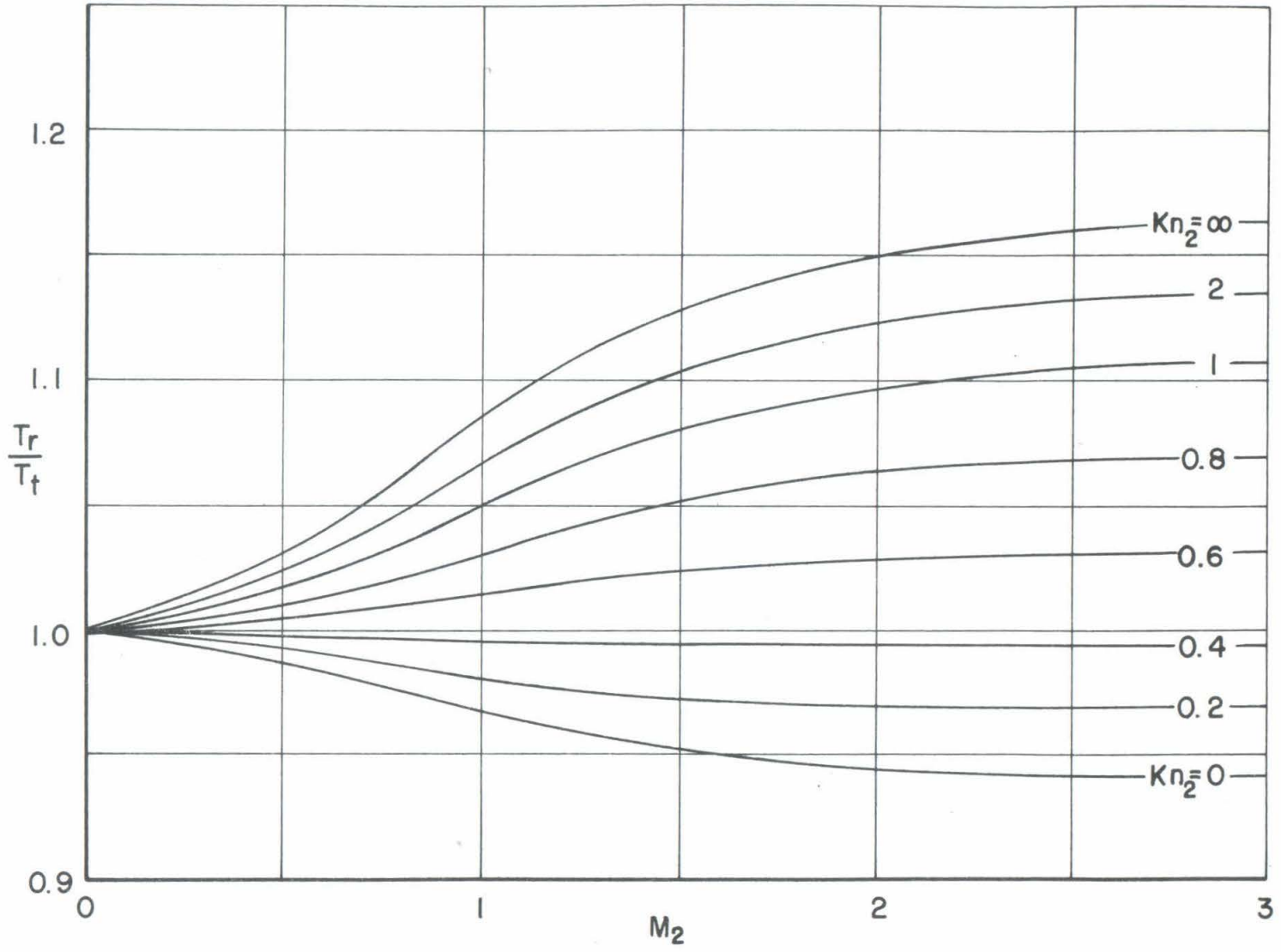


FIG. 12- RECOVERY TEMPERATURE RATIO FOR AIR AS A FUNCTION OF FLOW MACH NUMBER WITH KNUDSEN NUMBER AS A PARAMETER

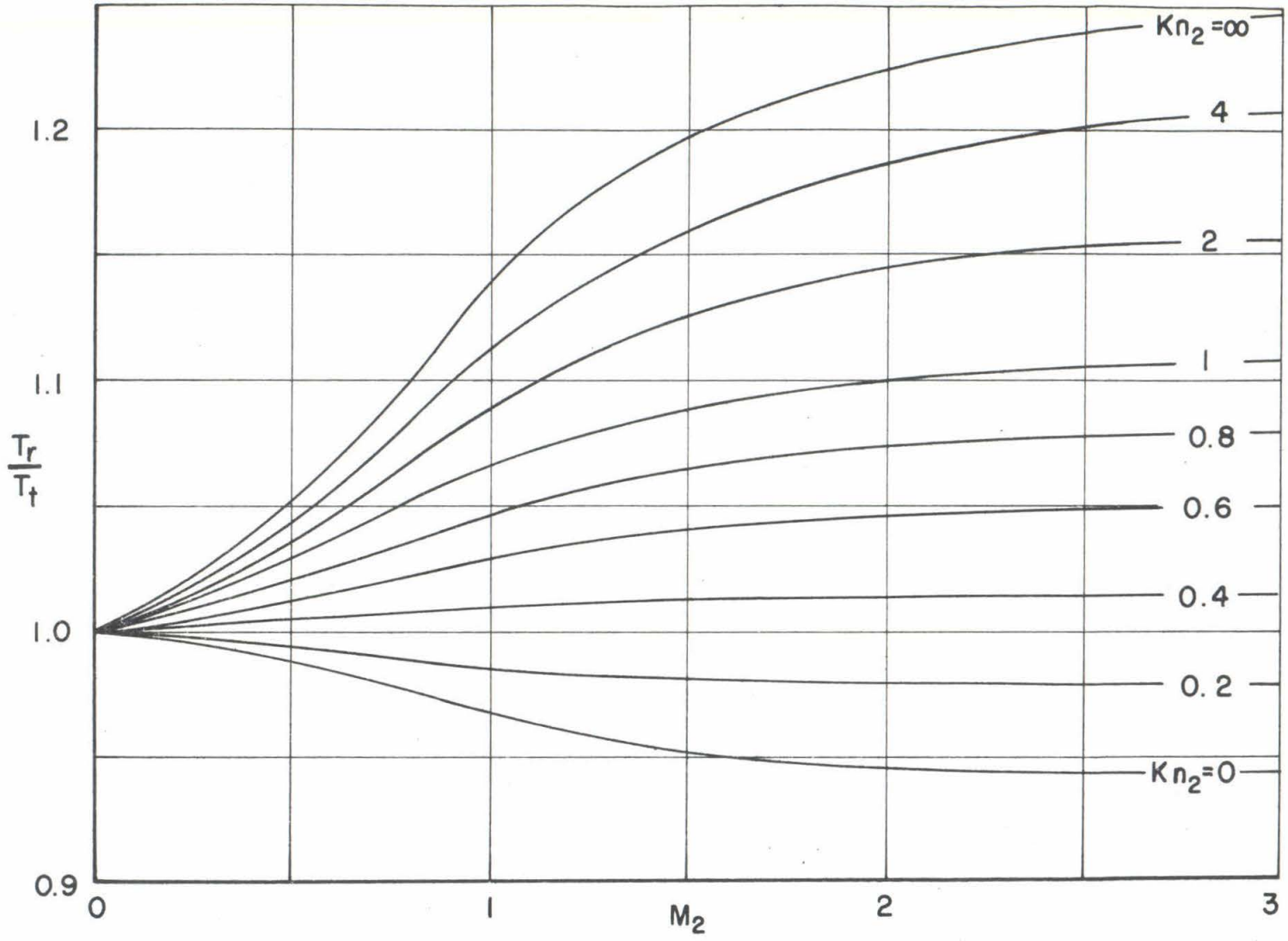


FIG. 13 - RECOVERY TEMPERATURE RATIO FOR ARGON AS A FUNCTION OF FLOW MACH NUMBER WITH KNUDSEN NUMBER AS A PARAMETER

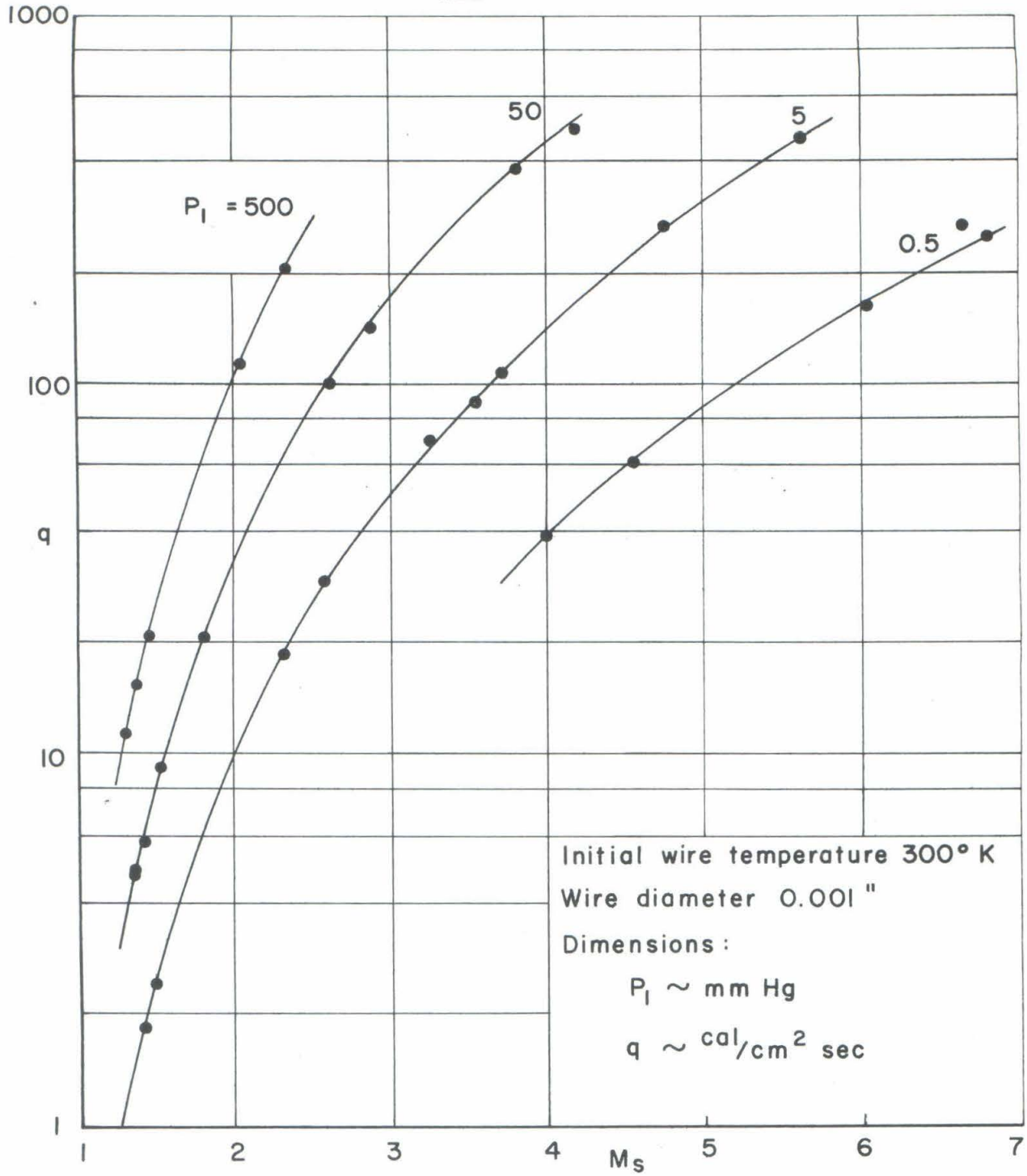


FIG. 14 - HEAT TRANSFER RATE TO A COLD WIRE IN AIR WITH THE INITIAL PRESSURE AS A PARAMETER

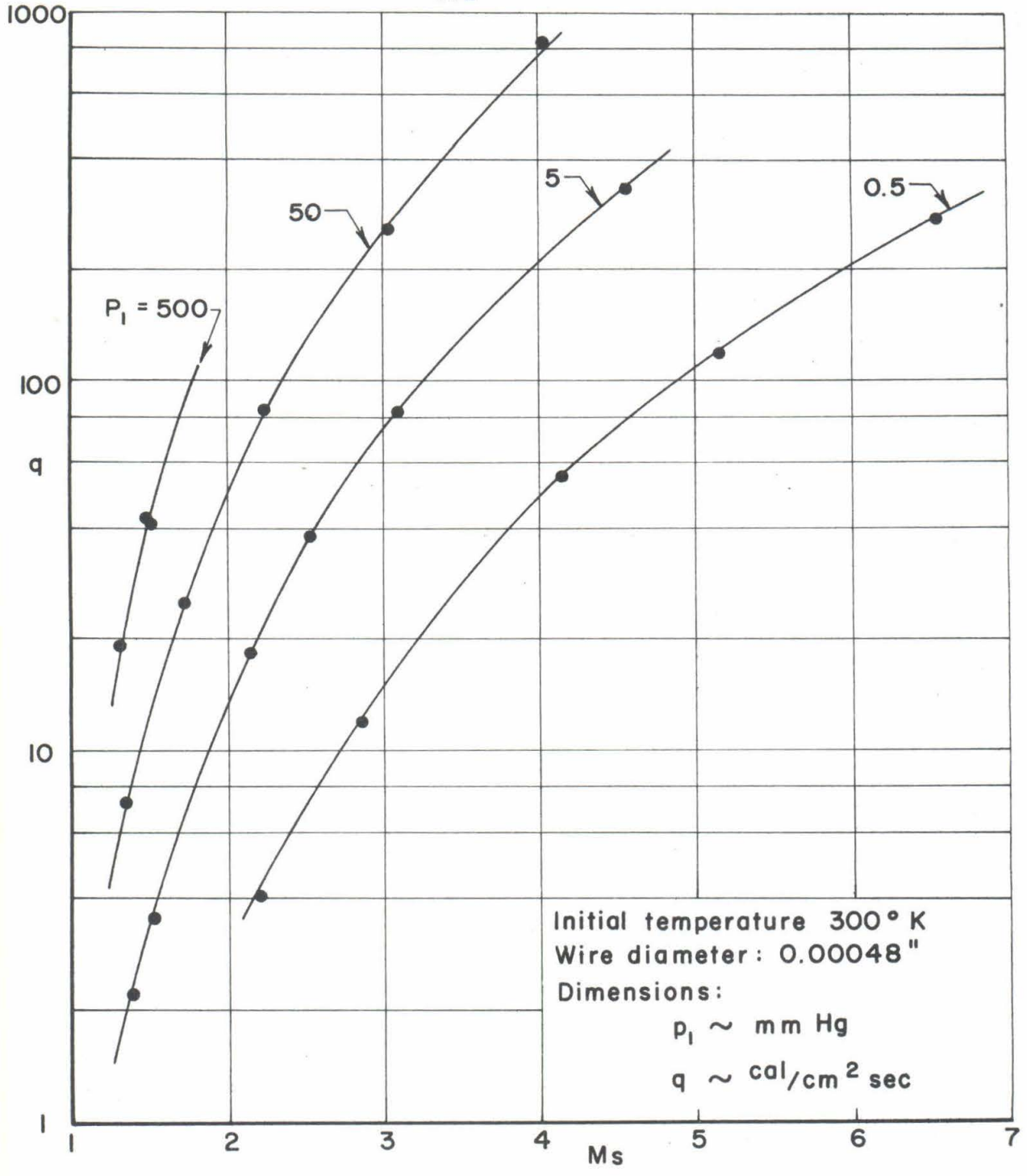


FIG. 15 - HEAT TRANSFER RATE TO A COLD WIRE IN AIR WITH THE INITIAL PRESSURE AS A PARAMETER

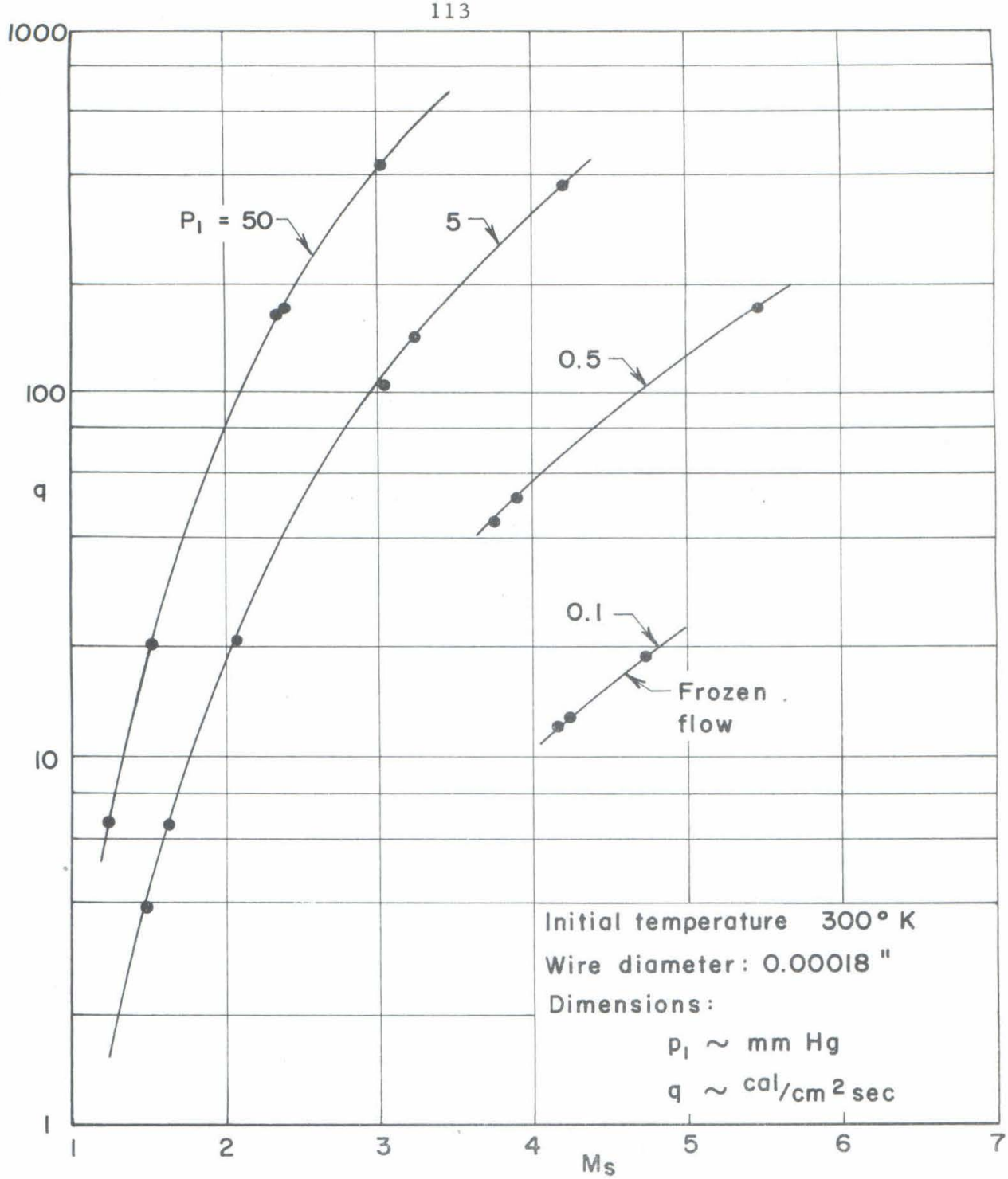


FIG. 16 - HEAT TRANSFER RATE TO A COLD WIRE IN AIR WITH THE INITIAL PRESSURE AS A PARAMETER

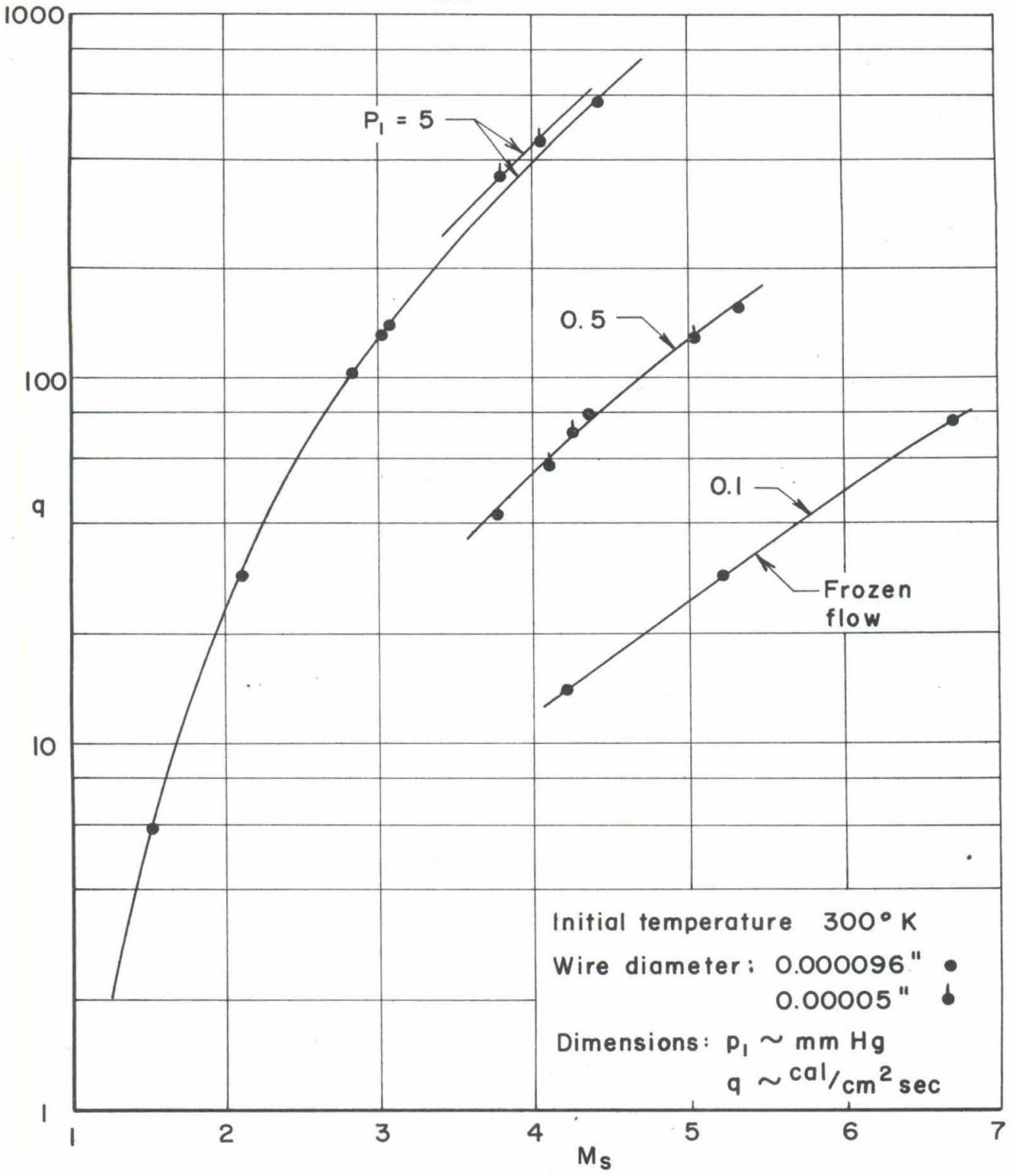


FIG. 17 – HEAT TRANSFER RATE TO A COLD WIRE IN AIR WITH THE INITIAL PRESSURE AS A PARAMETER

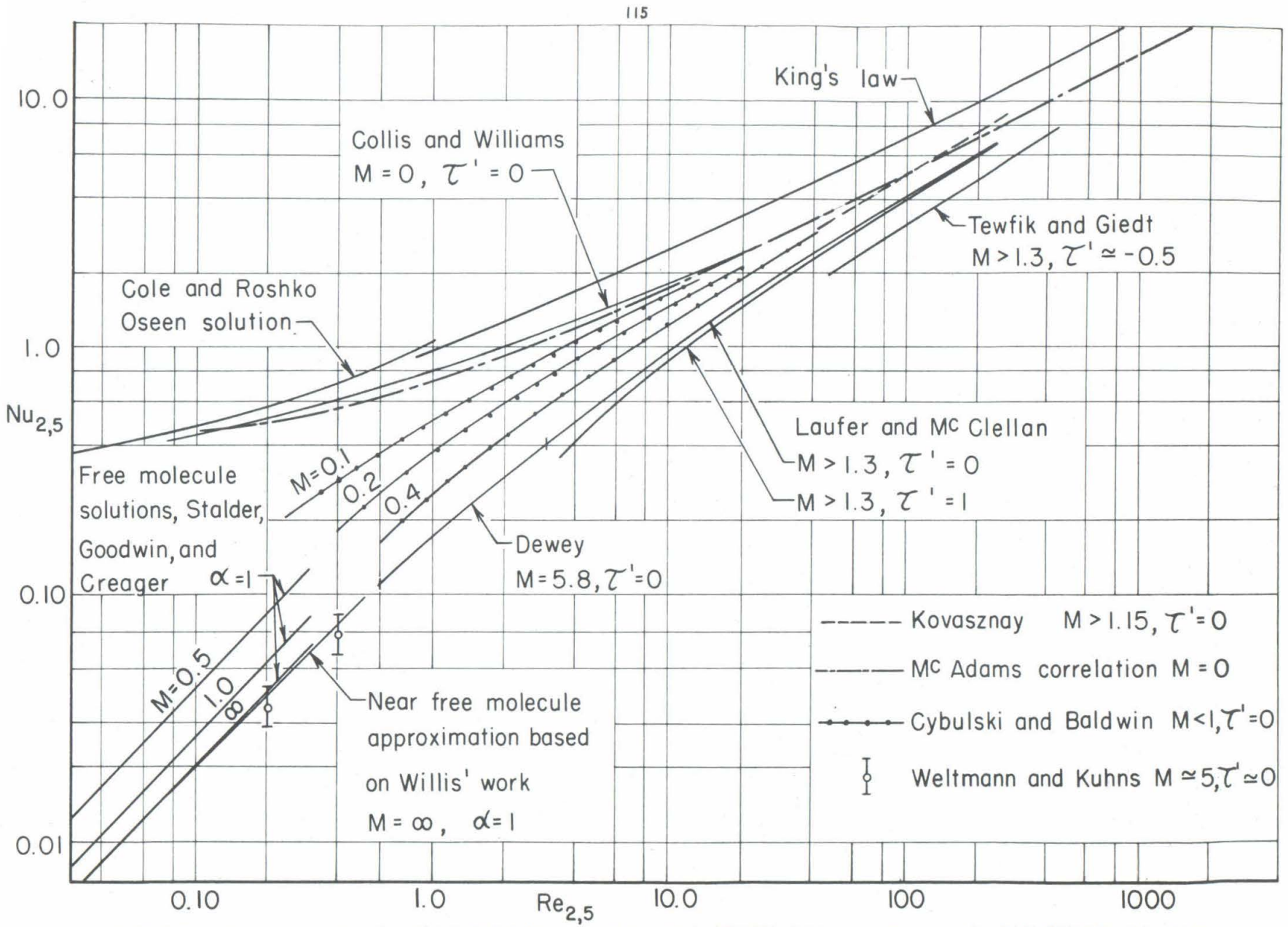


FIG. 18 - CORRELATION OF THE HEAT TRANSFER COEFFICIENTS OF A CIRCULAR CYLINDER IN AIR

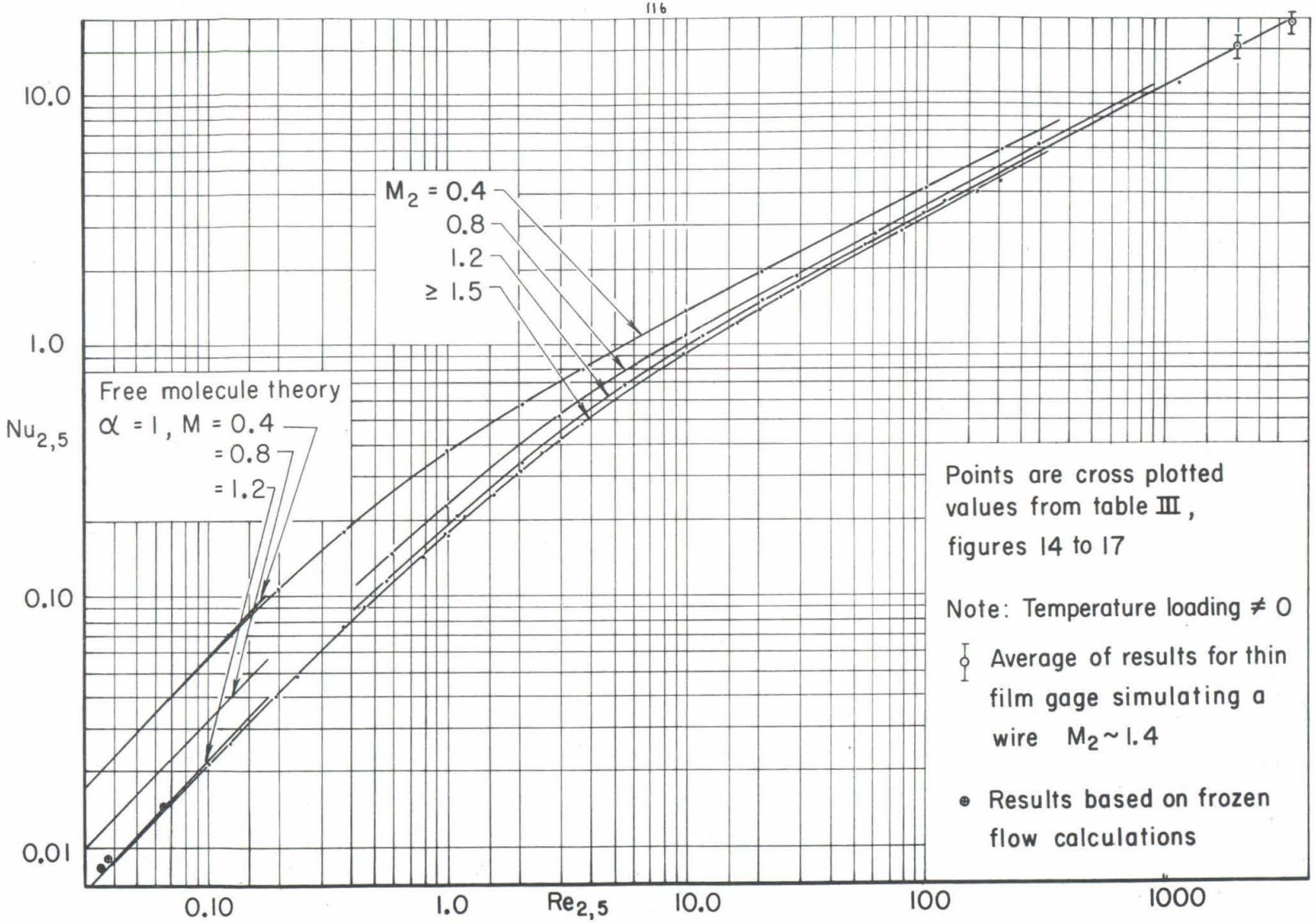


FIG. 19 - DEPENDENCE OF NUSSELT NUMBER ON REYNOLDS NUMBER FOR A COLD WIRE IN AIR

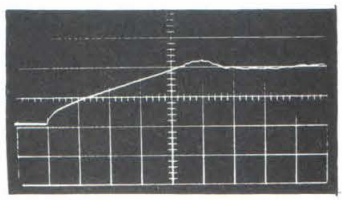

Thin Film Gage Response

$P_1$ = 7 mm Hg

$M_s$ = 3.21

Sweep = 250 $\mu$sec/cm

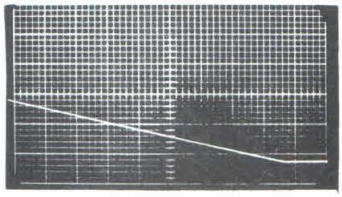

Cold Wire Response

$P_1$ = 5 mm Hg

$M_s$ = 3.69

Sweep = 50 $\mu$sec/cm

FIGURE 20

COMPARISON OF THIN FILM GAGE AND

COLD WIRE RESPONSES

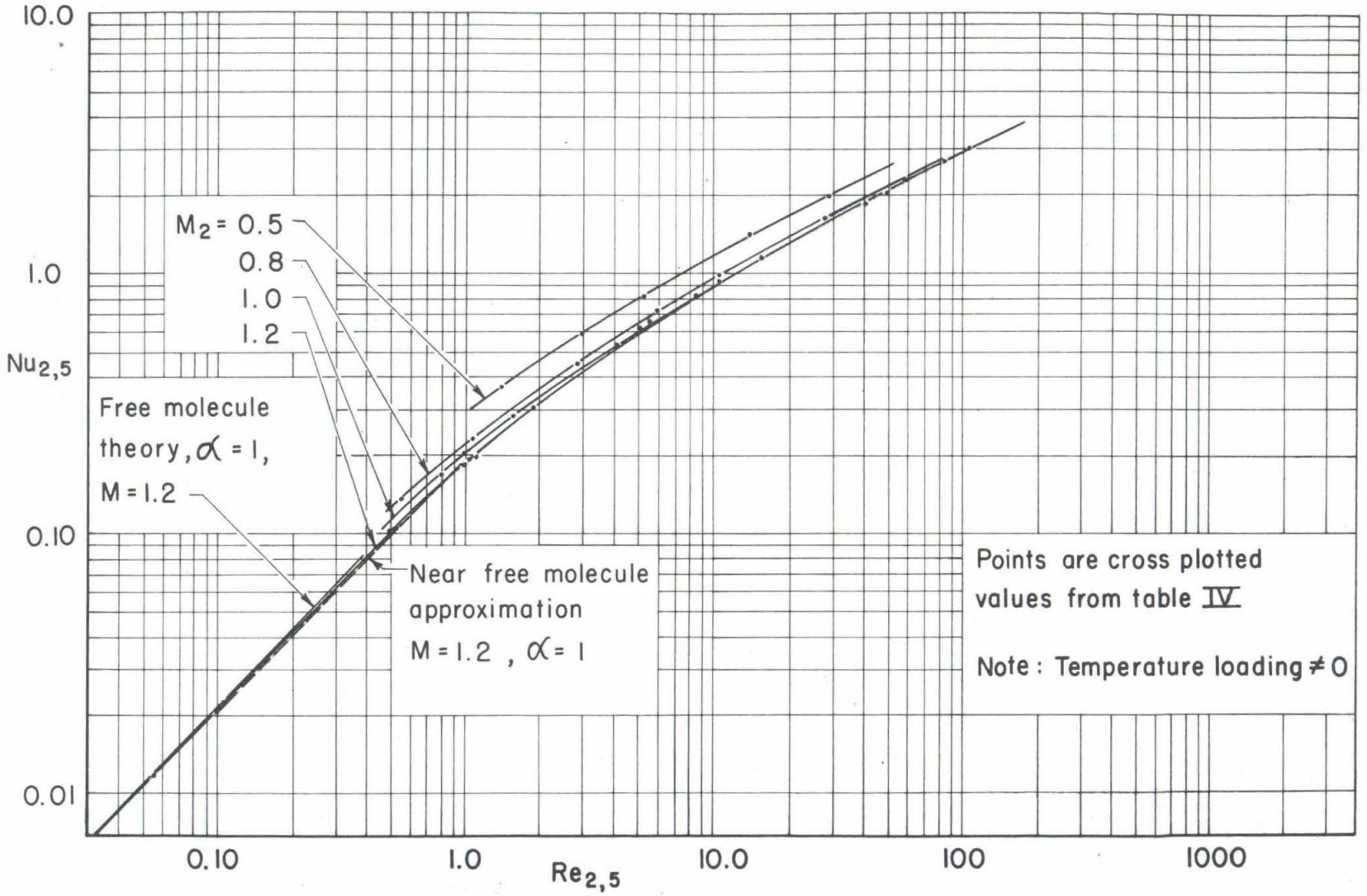


FIG. 21 - DEPENDENCE OF NUSSELT NUMBER ON REYNOLDS NUMBER FOR A COLD WIRE IN ARGON

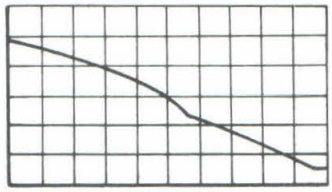

P 250 mm Hg

M 1.72

Sweep 102 $\mu$ sec./cm.

Wire Diameter 0.000048"

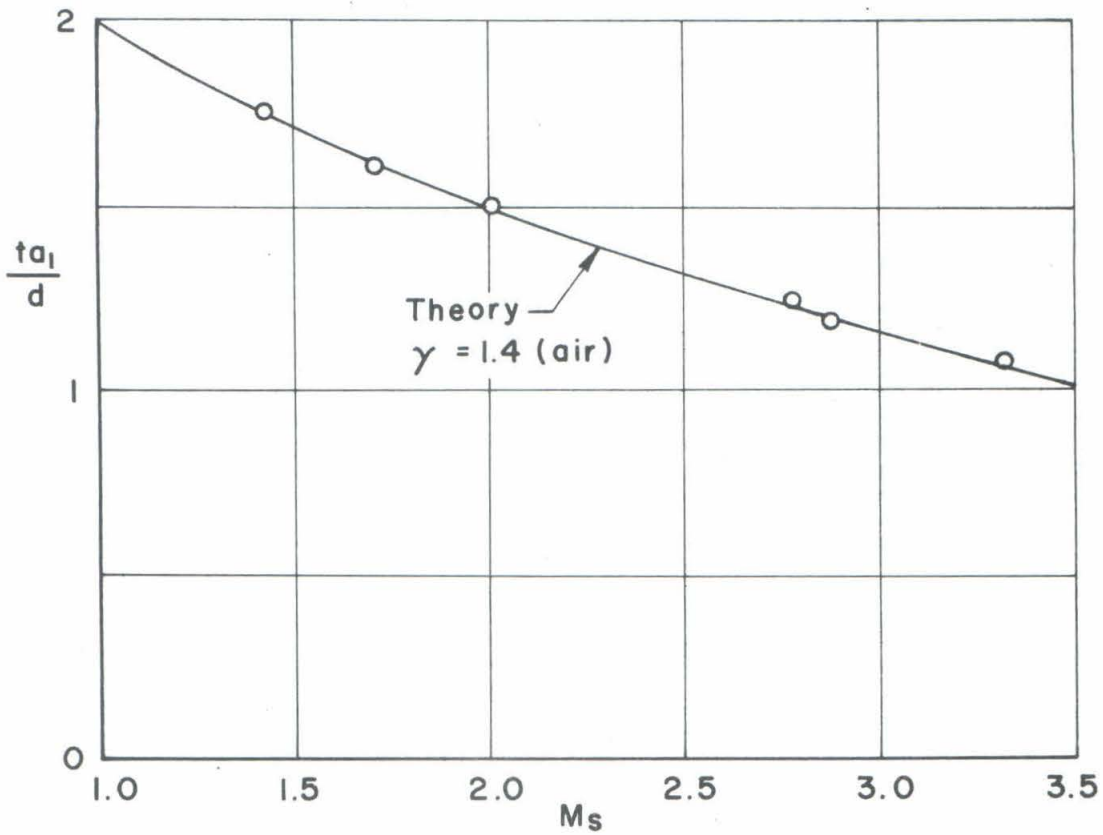


FIG. 22 - TIME REQUIRED FOR A SHOCK WAVE TO REFLECT FROM AN END WALL

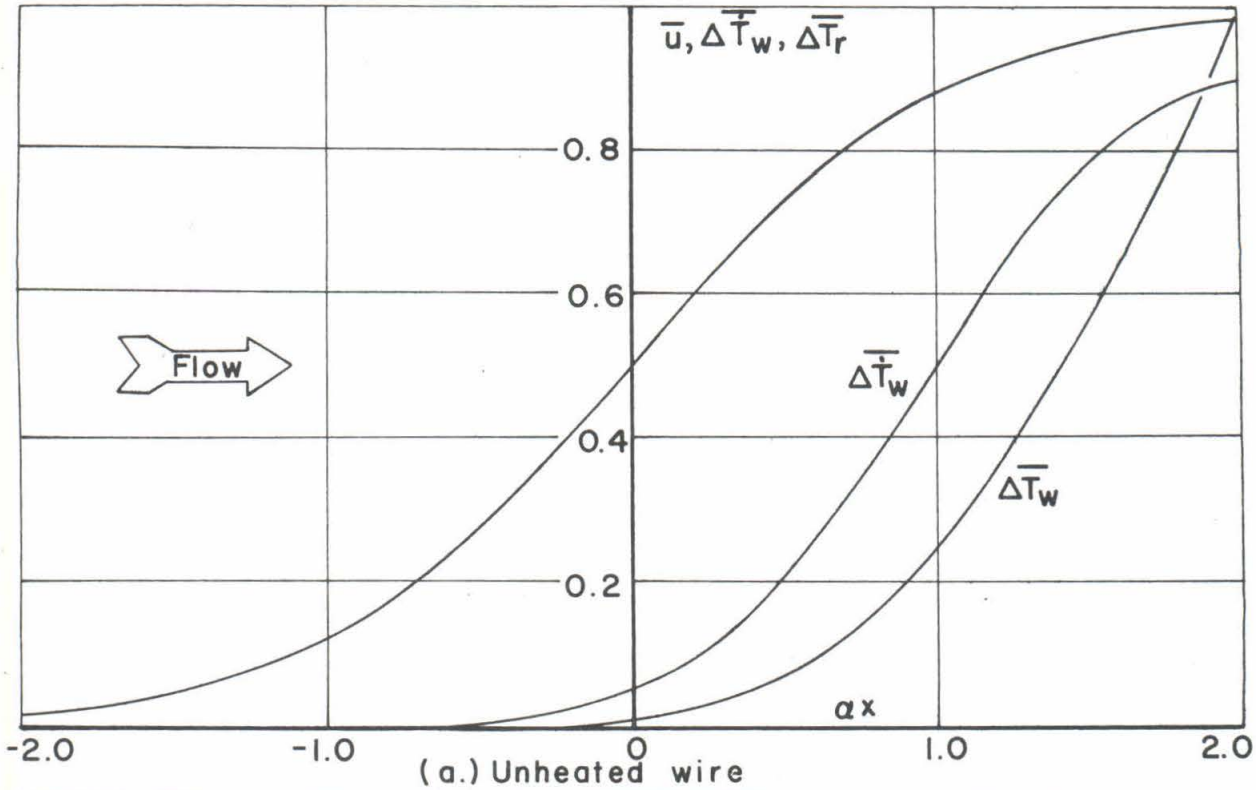


(a.) Unheated wire

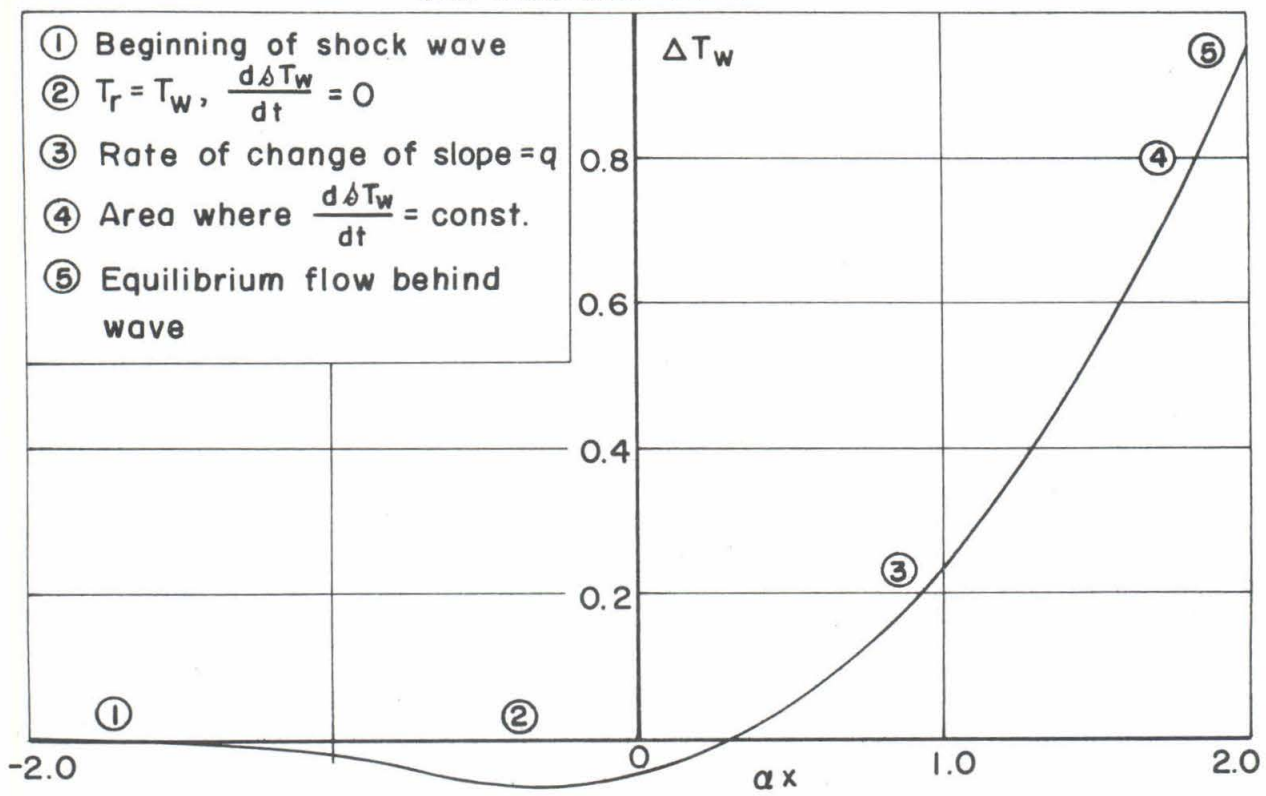


(b.) Heated wire

FIG. 23 - RESPONSE TO THE FLOW WITHIN A SHOCK WAVE

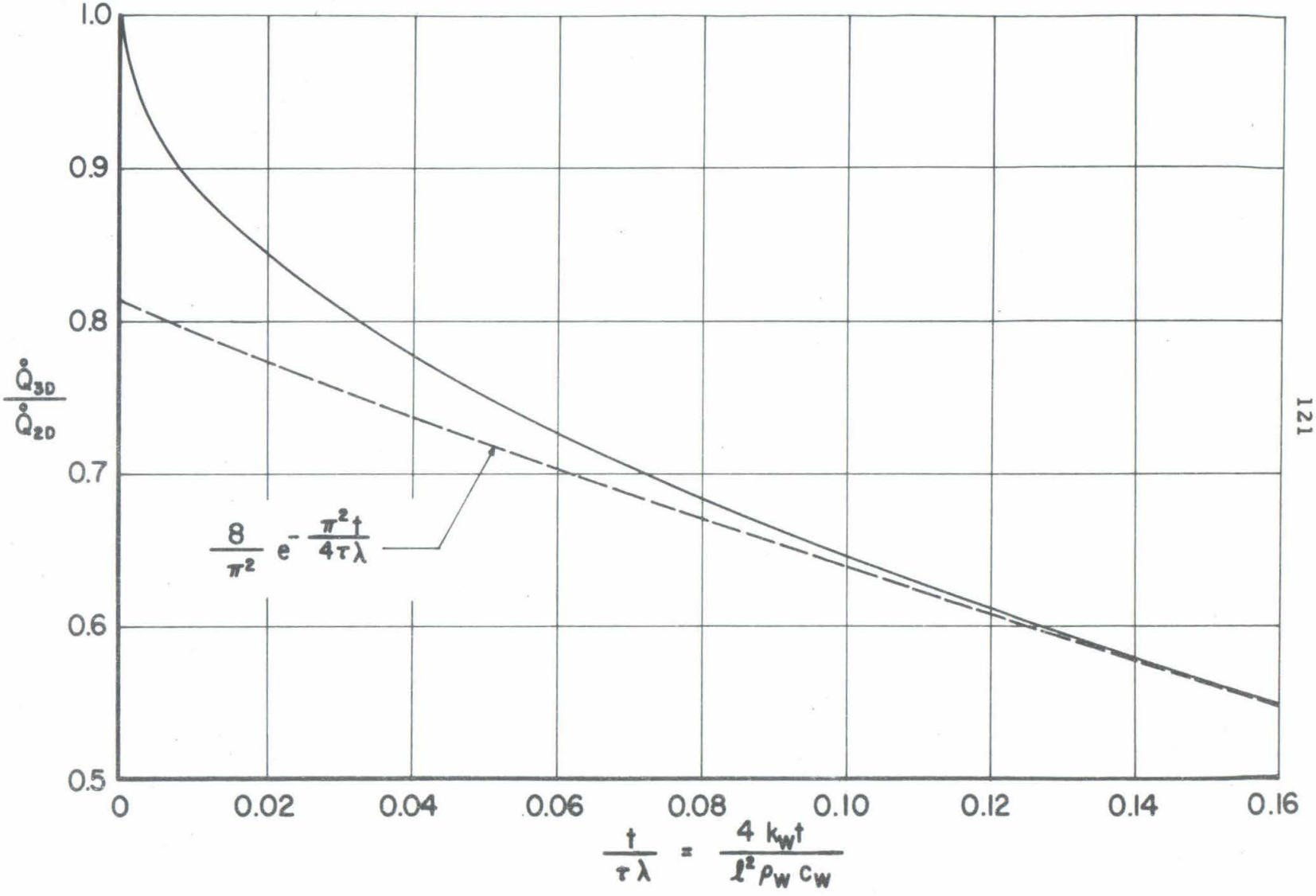


FIG. 24 - HEAT TRANSFER CORRECTION DUE TO SUPPORTS

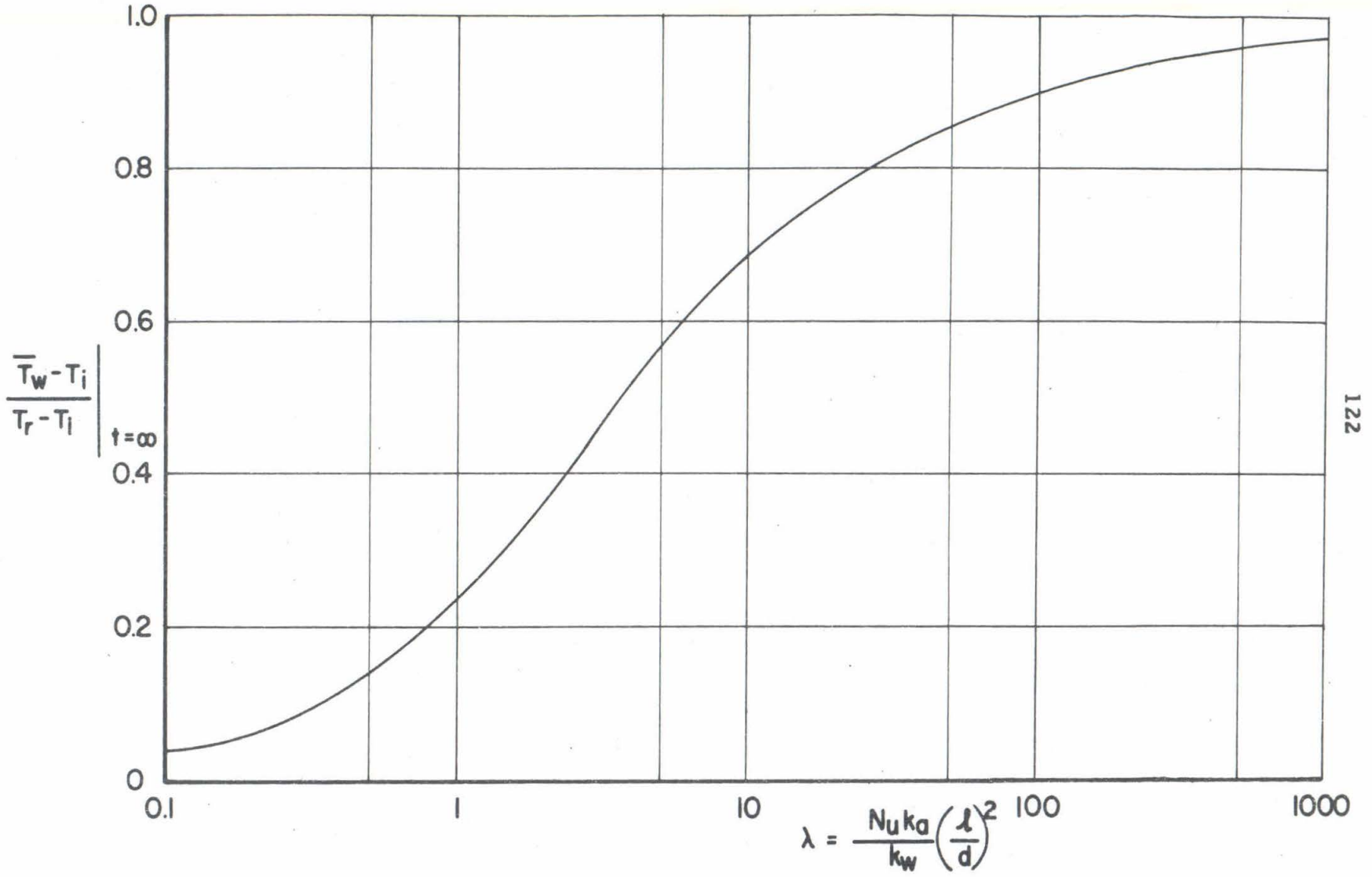


FIG. 25 - EQUILIBRIUM TEMPERATURE OF THE WIRE AS A FUNCTION OF THE WIRE GEOMETRY

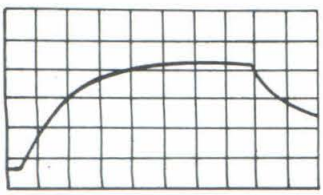

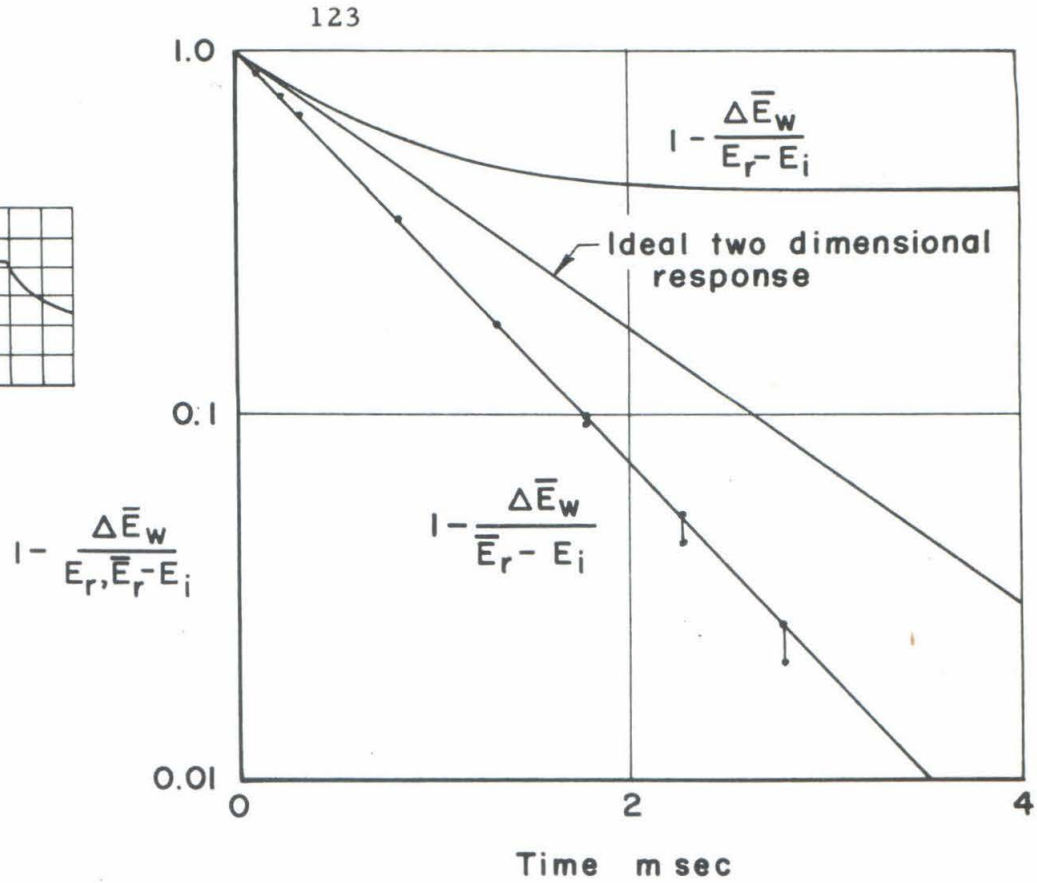


Initial Conditions:

$P_1$ = 5 mm Hg
$T_1$ = 299 °K
$M_s$ = 1.7
$R_i$ = 16.8
I = $10^{-3}$ amps
Sweep = 505 $\mu$sec/cm

d = 0.000096"
$\ell$ = 0.0280"
$\rho c$ = 1.02 cal/cm$^3$ °C
$k_w$ = 0.166 cal/cm sec °C
$\alpha_i$ = 0.00356 / °C
Calib. = 2.08 mv/cm

Calculated Conditions:

$\lambda$ = 6.85
$\tau$ = 1150 $\mu$sec
$\Delta E_r$ = 12.3 mv
$\frac{\bar{T}_{w_{t\to\infty}} - T_i}{T_r - T_i}$ = 0.635
$\tau_{3D}$ = 725 $\mu$sec
$\Delta\bar{E}_r$ = 7.8 mv

Measured Quantities:

$\tau$ = 750 $\mu$sec
$\Delta\bar{E}_r$ = 7.7 mv

FIG. 26- EXAMPLE OF THE SUPPORT INFLUENCE ON WIRE RESPONSE

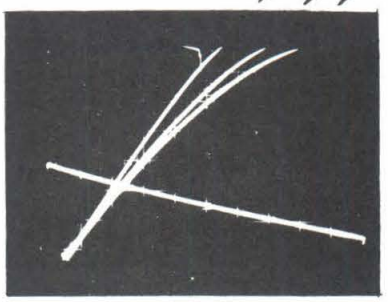


| | |
|---|---|
| Wire Material: | Platinum |
| Diameter: | 0.0005" |
| Sweep: | 500 μsec/cm |
| Calibration: | 50 mv/cm |

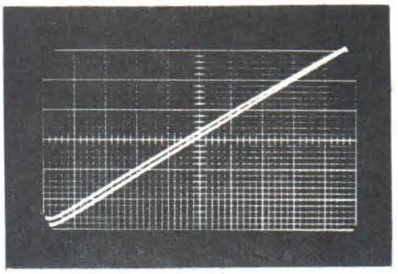


| | |
|---|---|
| Wire Material: | Tungsten |
| Diameter: | 0.001" |
| Sweep: | 100 μsec/cm |
| Calibration: | 10 mv/cm |

FIGURE 27

EFFECT OF SURROUNDING MEDIA ON

GAGE OUTPUT DURING CALIBRATION

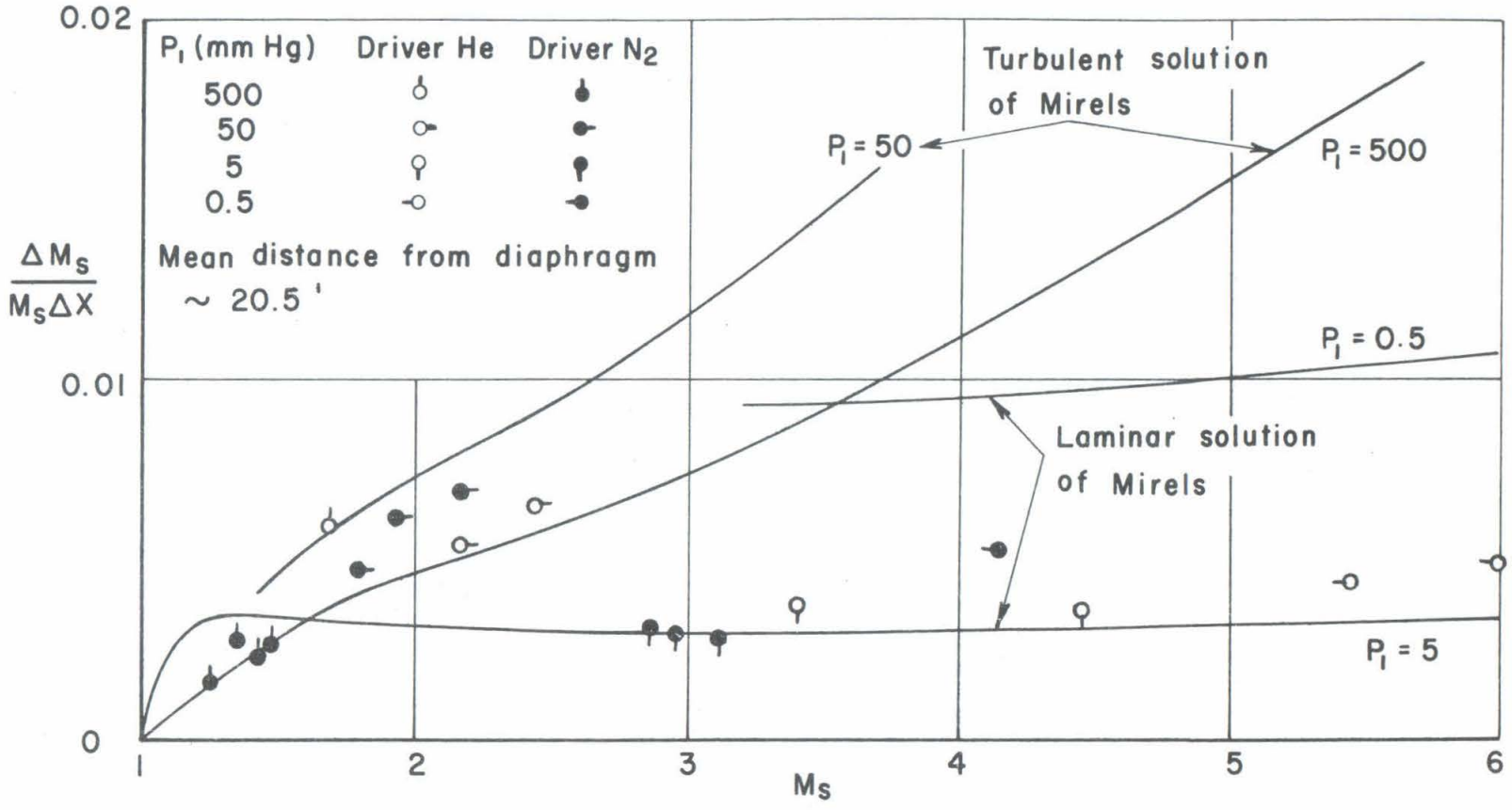


FIG. 28 - SHOCK WAVE ATTENUATION PER FOOT IN AIR FOR THE ROUND TWO INCH SHOCK TUBE

# DISTRIBUTION LIST

United States Army

U. S. Army Research Office (Durham)
Box CM, Duke Station
Druham, North Carolina
Attention: Information Processing Office
20 copies

Army Rocket and Guided Missile Agency
U. S. Army Ordnance Missile Command
Redstone Arsenal
Alabama
Attention: Technical Library
Attention: Mr. John Morrow
ORDXR-RMO

Commander
Army Ballistic Missile Agency
Redstone Arsenal
Alabama
Attention: ORDAB-IPL

Los Angeles Ordnance District
55 South Grand Avenue
Pasadena 2, California
Attention: Colonel P. H. Scordas
Attention: Mr. E. L. Stone
Attention: Mr. Typaldos, ORDEV-00

Chief of Ordnance
Department of the Army
ORDTB - Ballistic Section
The Pentagon
Washington 25, D. C.
Attention: Mr. George Stetson

Office of the Chief of Research and
Development
Department of the Army
Army Research Office
Washington 25, D. C.
Attention: Chief, Research Support Division

Commanding Officer
Diamond Ordnance Fuze Laboratories
Washington 25, D. C.
Attention: ORDTL 012

U. S. Army Ordnance
Ballistic Research Laboratories
Aberdeen Proving Ground
Maryland
Attention: Dr. Joseph Sternberg, Chief
Exterior Ballistics Laboratory
Attention: Dr. Raymond Sedney
Exterior Ballistics Laboratory

Commanding General
White Sands Missile Range
New Mexico
Attention: Technical Library

United States Navy

Director
U. S. Naval Research Laboratory
Washington 25, D. C.

U. S. Naval Ordnance Laboratory
White Oak
Silver Spring, Maryland
Attention: Dr. R. Kenneth Lobb
Aeroballistics Program Chief
Attention: Dr. A. E. Seigel
Chief, Ballistics Department
Attention: Dr. R. E. Wilson
Associate Technical Director
(Aeroballistics)

U. S. Naval Weapons Laboratory
Dahlgren, Virginia
Attention: Technical Library

U. S. Navy Department
David Taylor Model Basin
Applied Mathematics Laboratory
Washington 7, D. C.
Attention: Dr. F. N. Frenkiel

United States Air Force
Air Research and Development Command

Aeronautical Research Laboratories
Air Force Research Division
Air Research and Development Command
United States Air Force
Wright-Patterson Air Force Base
Ohio
Attention: Mr. Fred L. Daum, RRLD
Attention: Dr. Karl Gottfried Guderley, RRLM
Attention: Dr. Roscoe H. Mills, RRLD
Attention: RRLL

Wright Air Development Division
Air Research and Development Command
United States Air Force
Wright-Patterson Air Force Base
Ohio
Attention: WADD (WWAD - Library)
Attention: WADD (WWFEA - Reports Unit)
Attention: WWRMDF-2, Mr. Philip P. Antonatos
Attention: WWRMDF

Air Force Office of Scientific Research
Air Research and Development Command
United States Air Force
Washington 25, D. C.
Attention: Mechanics Division; Milton Rogers, Chief
Attention: SRGL (2 copies)

Directorate of Research Analysis
Air Force Office of Scientific Research
Air Research and Development Command
United States Air Force
Holloman Air Force Base
New Mexico
Attention: SRLS, Dr. Gerhard R. Eber

Air Force Ballistic Missile Division
Air Research and Development Command
United States Air Force
Air Force Unit Post Office
Los Angeles 45, California
Attention: Advanced Systems Division (WDTVV-3); Major E. W. Geniesse, Jr.
Attention: Penetration Division (WDTVV-4); 1/Lt. H. E. Hunter
Attention: AVCO Re-entry Vehicles Division (WDTVV-1); Capt. G. S. Lewis, Jr.

Air Research and Development Command
United States Air Force
Eglin Air Force Base
Florida
Attention: APGC (PGTRI, Technical Library)

Armed Services Technical Information Agency
Air Research and Development Command
United States Air Force
Arlington Hall Station
Arlington 12, Virginia
Attention: ASTIA (TIPCA)

National Aeronautics and Space Administration

NASA
Headquarters
1520 H Street, Northwest
Washington 25, D. C.
Attention: Dr. H. H. Kurzweg
Assistant Director of Research

NASA
George C. Marshall Space Flight Center
Huntsville, Alabama
Attention: Dr. Ernst D. Geissler, Director, Aeroballistics Division
Attention: M-AERO-A, Mr. Werner K. Dahm
Attention: Aeroballistics Division, M-AERO-E, Mr. T. G. Reed (3 copies)

NASA
Langley Research Center
Langley Field, Virginia
Attention: Librarian
Attention: Mr. Clinton E. Brown, Chief, Theoretical Mechanics Division, Bldg. 12
Attention: Dr. Adolf Busemann
Attention: Mr. Charles H. McLellan, 11-Inch Hypersonic Tunnel Section

NASA
Ames Research Center
Moffett Field, California
Attention: Library

NASA
Lewis Research Center
21000 Brookpark Road
Cleveland 35, Ohio
Attention: Library, Mr. George Mandel
2 copies

Miscellaneous Government Agencies

United States Atomic Energy Commission
P. O. Box 62
Oak Ridge, Tennessee
Attention: Library

U. S. Department of Commerce
National Bureau of Standards
Washington 25, D. C.
Attention: Dr. G. B. Schubauer
Chief, Fluid Mechanics Section

Universities and Non-Profit Organizations

Brown University
Division of Applied Mathematics
Providence 12, Rhode Island
Attention: Professor R. E. Meyer

Brown University
Division of Engineering
Providence 12, Rhode Island
Attention: Dr. Ronald F. Probstein

University of California at Berkeley
Aeronautical Sciences Department
Room 203, Mechanics Building
Berkeley 4, California
Attention: Professor S. A. Schaaf

University of California
Engineering and Mathematical
Sciences Library
Engineering II 8270
405 Hilgard Avenue
Los Angeles 24, California

University of California
Department of Engineering
Los Angeles 24, California
Attention: Professor A. F. Charwat
Attention: Professor John W. Miles

Case Institute of Technology
Department of Mechanical Engineering
University Circle
Cleveland 6, Ohio
Attention: Dr. G. Kuerti

Columbia University
Department of Mechanical Engineering
New York 27, N. Y.
Attention: Professor Robert A. Gross

Cornell University
Graduate School of Aeronautical Eng.
Ithaca, New York
Attention: Dr. William R. Sears
Attention: Library

University of Florida
Department of Aeronautical Eng.
Gainesville, Florida
Attention: Professor David T. Williams

Harvard University
Division of Eng. and App. Physics
Cambridge 38, Massachusetts
Attention: Dr. Howard W. Emmons

University of Illinois
Department of Aeronautical Engineering
Urbana, Illinois
Attention: Professor Harold O. Barthel
Attention: Dr. Allen I. Ormsbee

The Johns Hopkins University
Applied Physics Laboratory
8621 Georgia Avenue
Silver Spring, Maryland
Attention: Dr. L. L. Cronvich
Attention: Dr. F. K. Hill

The Johns Hopkins University
Department of Mechanics
Baltimore 18, Maryland
Attention: Dr. Francis H. Clauser
Attention: Dr. Stanley Corrsin
Attention: Professor L. S. G. Kovasznay

Lehigh University
Department of Physics
Bethlehem, Pennsylvania
Attention: Dr. Raymond J. Emrich

University of Maryland
Department of Aeronautical Engineering
College Park, Maryland
Attention: Professor S. F. Shen

University of Maryland
Institute for Fluid Dynamics and
Applied Mathematics
College Park, Maryland
Attention: Director
Attention: Professor J. M. Burgers
Attention: Professor Francis R. Hama
Attention: Professor S. I. Pai

Massachusetts Institute of Technology
Department of Aero and Astronautics
Aerophysics Laboratory
560 Memorial Drive
Cambridge 39, Massachusetts
Attention: Dr. Morton Finston

Massachusetts Institute of Technology
Department of Mathematics
Cambridge 39, Massachusetts
Attention: Professor C. C. Lin
Attention: Dr. George B. Whitham

Massachusetts Institute of Technology
Department of Mechanical Engineering
Cambridge 39, Massachusetts
Attention: Dr. A. H. Shapiro

Massachusetts Institute of Technology
Department of Aeronautical Engineering
Cambridge 39, Massachusetts
Attention: Professor E. Mollo-Christensen
Room 33-408
Attention: Dr. H. Guyford Stever

Massachusetts Institute of Technology
Department of Aeronautics and Astronautics
Cambridge 39, Massachusetts
Attention: Dr. Leon Trilling
Room 33-412

University of Michigan
Ann Arbor, Michigan
Attention: Engineering Library

University of Michigan
Willow Run Laboratories
P. O. Box 618
Ann Arbor, Michigan
Attention: BAMIRAC Library
Mr. Richard Jamron, Head
Information Handling Group

University of Michigan
Aeronautical Engineering Laboratories
North Campus
Ann Arbor, Michigan
Attention: Mr. James L. Amick

University of Michigan
Department of Aeronautical Engineering
Ann Arbor, Michigan
Attention: Dr. Arnold M. Kuethe

University of Michigan
Department of Aeronautical and
Astronautical Engineering
Ann Arbor, Michigan
Attention: Professor V. C. Liu
Attention: Professor William W. Willmarth

University of Michigan
Aeronautical and Astronautical
Engineering Laboratories
Aircraft Propulsion Laboratory
North Campus
Ann Arbor, Michigan
Attention: Professor J. A. Nicholls

University of Michigan
Department of Physics
Ann Arbor, Michigan
Attention: Dr. O. Laporte

University of Minnesota
Institute of Technology
Rosemount Aeronautical Laboratories
Rosemount, Minnesota
Attention: Mrs. Linda Caldon,
Librarian

New York University
Institute of Mathematics and Mechanics
53 Washington Square, South
New York 12, N. Y.
Attention: Library

North Carolina State College
Department of Mechanical Engineering
Raleigh, North Carolina
Attention: Professor R. M. Pinkerton

Northwestern University
The Technological Institute
Evanston, Illinois
Attention: Professor Ali Bulent Cambel

The Ohio State University
Department of Aeronautical and
Astronautical Engineering
2036 Neil Avenue
Columbus 10, Ohio
Attention: Professor John D. Lee
Attention: Professor Gavin L. VonEsch

Polytechnic Institute of Brooklyn
Aerodynamics Laboratory
527 Atlantic Avenue
Freeport, New York
Attention: Library
Attention: Professor Martin H. Bloom
Attention: Professor Antonio Ferri
Attention: Professor Paul A. Libby

Princeton University
School of Engineering
James Forrestal Research Center
Princeton, New Jersey
Attention: Library
Attention: Gas Dynamics Laboratory
Attention: Professor Sin-I Cheng
Attention: Dr. Luigi Crocco
Attention: Dr. Seymour Bogdonoff

Purdue University
School of Aeronautical and
Engineering Sciences
Wast Lafayette, Indiana
Attention: Aero. and Engineering
Sciences Library

Rensselaer Polytechnic Institute
Department of Aeronautical Engeering
Troy, New York
Attention: Library
Attention: Dr. Ting-Yi Li

University of Rochester
College of Engineering
Department of Mechanical Engineering
River Campus Station
Rochester 20, New York
Attention: Professor Martin Lessen

University of Southern California
Engineering Center
University Park
Los Angeles 7, California
Attention: Director
Attention: Dr. H. T. Yang

University of Southern California
Engineering Center
Aeronautical Laboratories Department
P. O. Box 1001
Oxnard, California
Attention: Mr. J. H. Carrington,
USCEC-ATL

Stanford University
Department of Aeronautical Engineering
Stanford, California
Attention: Professor Daniel Bershader
Attention: Dr. Milton Van Dyke

University of Texas
Defense Research Laboratory
P. O. Box 8029
Austin 12, Texas
Attention: Dr. M. J. Thompson

University of Virginia
Department of Physics
Charlottesville, Virginia
Attention: Dr. Jesse W. Beams

University of Washington
Department of Aeronautical Engineering
Seattle 5, Washington
Attention: Engineering Librarian
Attention: Professor R. E. Street

University of Wisconsin
Theoretical Chemistry Laboratory
P. O. Box 2127
Madison 5, Wisconsin
Attention: Dr. Joseph O. Hirschfelder

Yale University
Department of Mechanical Engineering
New Haven, Connecticut
Attention: Dr. Peter Wegener

Institute of the Aerospace Sciences
2 East 64th Street
New York 21, New York
Attention: Library

Industrial and Research Companies

Aeronautical Research Associates
of Princeton, Inc.
50 Washington Road
Princeton, New Jersey
Attention: Dr. Coleman duP. Donaldson

Aeronutronic
A Division of Ford Motor Company
Ford Road
P. O. Box 697
Newport Beach, California
Attention: Dr. L. L. Kavanau
Advanced Programs Staff

Aerospace Corporation, Inc.
Department of Theoretical Mechanics
Research Division
P. O. Box 95081
Los Angeles 45, California
Attention: Dr. Chieh-Chien Chang

Aerospace Corporation, Inc.
Aerodynamics and Propulsion Laboratory
P. O. Box 95085
Los Angeles 45, California
Attention: Dr. J. Logan, Director
2 copies

ARO, Inc.
Arnold Air Force Station
Tennessee
Attention: AEDC Library
Attention: Dr. B. H. Goethert
Director of Engineering
Attention: TS(T1)

ARO, Inc.
von Karman Gas Dynamics Facility
Arnold Air Force Station
Tennessee
Attention: Dr. J. Lukasiewicz, Chief
Attention: Mr. J. Leith Potter,
Manager, Research Branch

AVCO-Everett Research Laboratory
2385 Revere Beach Parkway
Everett 49, Massachusetts
Attention: Barbara A. Spence,
Technical Librarian

AVCO Research and Advanced
Development Division
201 Lowell Street
Wilmington, Massachusetts
Attention: Mr. A. Kahane
Assistant Technical Director
Attention: Dr. Frederick R. Riddell,
Tech. Ass't. to Pres. -S. Tec.

Boeing Airplane Company
Aero-Space Division
Seattle 24, Washington
Attention: Library 13-84

CONVAIR
A Division of General Dynamics Corp.
Astronautics Division
P. O. Box 1128
San Diego 12, California
Attention: Mr. K. J. Bossart, Tech. Dir.
Attention: Mr. W. B. Mitchell, 595-10

CONVAIR
A Division of General Dynamics Corp.
Scientific Research Laboratory
5001 Kearny Villa Road
San Diego 11, California
Attention: Mr. William H. Dorrance
Senior Staff Scientist
Mail Zone 1-162
Attention: Mr. Merwin Sibulkin
Staff Scientist

CONVAIR
A Division of General Dynamics Corp.
San Diego 12, California
Attention: Dr. H. Yoshihara
Chief of Fluid Dynamics Res.
Mail Zone 6-105

CONVAIR
A Division of General Dynamics Corp.
Aerospace Technology Section
P. O. Box 748
Fort Worth, Texas
Attention: Mr. R. C. Frost
Dept. 6-1
Mail Zone E63

CONVAIR
A Division of General Dynamics Corp.
Fort Worth, Texas
Attention: Mr. A. P. Madsen
Aerodynamics Group Eng.
Mail Zone E63
Attention: Mr. W. G. McMullen
Attention: Mr. Robert H. Widmer

CONVAIR
A Division of General Dynamics Corp.
Daingerfield, Texas
Attention: Mr. J. E. McMichael
Chief, Jet Engine Department

Cornell Aeronautical Laboratory, Inc.
P. O. Box 235
Buffalo 21, New York
Attention: Library
Attention: Dr. A. H. Flax
Attention: Mr. A. Hertzberg
Head, Aerodynamic Research

Douglas Aircraft Company, Inc.
Missiles and Space Systems
3000 Ocean Park Blvd.
Santa Monica, California
Attention: Library
Chief,
Aero/Astrodynamics Section
2 copies
Attention: Mr. R. J. Gunkel
Chief,
Aero/Astrodynamics Section

Douglas Aircraft Company, Inc.
827 Lapham Street
El Segundo, California
Attention: Dr. A. M. O. Smith

General Electric Company
Missile and Ordnance Systems Dept.
3198 Chestnut Street
Philadelphia 4, Pennsylvania
Attention: L. Chasen, Mgr. Libraries
Documents Library
Attention: Mr. P. J. Friel

General Electric Company
Space Sciences Laboratory
3750 D Street
Philadelphia, Pennsylvania
Attention: Mr. H. Lew

General Electric Company
Research Laboratory
P. O. Box 1088
Schenectady, New York
Attention: Dr. Henry T. Nagamatsu

Giannini Controls Corporation
1600 South Mountain Avenue
Duarte, California
Attention: Library

Grumman Aircraft Engineering Corp.
Bethpage, New York
Attention: Mr. Charles Tilgner, Jr.

Hughes Aircraft Company
Culver City, California
Attention: Mr. E. O. Marriott
Manager, Aerodynamics Dept.

Lockheed Aircraft Corporation
Missiles and Space Division
3251 Hanover Street
Palo Alto, California
Attention: Dr. W. A. Kozumplik
Head, Tech. Info. Center
Dept. 50-14, Bldg. 201

Lockheed Aircraft Corporation
Missiles and Space Division
Sunnyvale, California
Attention: Mr. R. N. Munson
Dept. 81-91

Lockheed Aircraft Corporation
Missiles and Space Division
P. O. Box 504
Sunnyvale, California
Attention: Mr. R. Smelt,
Chief Scientist

Lockheed Aircraft Corporation
Missile Systems Division
Sunnyvale, California
Attention: Mr. Maurice Tucker
Spacecraft and Missiles Research

Lockheed Aircraft Corporation
Missiles and Space Division
7701 Woodley Avenue
Van Nuys, California
Attention: Library

Lockheed Aircraft Corporation
Marietta, Georgia
Attention: Dr. W. F. Jacobs
Aerodynamics Dept. -72-07

Marquhardt Aircraft Company
P. O. Box 2013 - South Annex
Van Nuys, California
Attention: Technical Library

The Martin Company
Baltimore 3, Maryland
Attention: Mr. K. Jarmolow
Mail No. J-3033
Attention: Dr. Mark V. Morkovin
Mail No. J-3033

McDonnell Aircraft Corporation
Lambert-Saint Louis Municipal Airport
P. O. Box 516
St. Louis 66, Missouri
Attention: Mr. Kendall Perkins

The RAND Corporation
1700 Main Street
Santa Monica, California
Attention: Librarian
Attention: Dr. Carl Gazley, Jr.
Attention: Mr. E. P. Williams
Aero-Astronautics Dept.

Republic Aviation Corporation
Farmingdale, Long Island, New York
Attention: Engineering Library
Attention: Mr. R. W. Perry
Chief, Re-Entry Simulation Lab.
Applied Research and Dev.

Space Technology Laboratories, Inc.
P. O. Box 95001
Los Angeles 45, California
Attention: Technical Information Center
Document Procurement
Bldg. C, Room 2412
Attention: Dr. James E. Broadwell
Aerodynamics Research Section
Attention: Dr. C. B. Cohen
Attention: Dr. Luois G. Dunn, President
Attention: Dr. Andrew G. Hammitt, Head
Aerodynamics Research Section
Attention: Mr. Ernest I. Pritchard
Attention: Dr. George E. Solomon

Sperry Utah Engineering Laboratory
Division of Sperry Rand Corporation
322 North 21st Street West
Salt Lake City 16, Utah
Attention: Mr. Malcolm L. Matthews

Systems Corporation of America
1007 Broxton Avenue
Los Angeles 24, California
Attention: Dr. Paul D. Arthur

United Aircraft Corporation
Research Laboratories
East Hartford 8, Connecticut
Attention: Mr. John G. Lee

Internal

Mr. Paul E. Baloga
Dr. Julian D. Cole
Dr. Donald E. Coles
Dr. Anthony Demetriades
Dr. Toshi Kubota
Professor Lester Lees
Dr. H. W. Liepmann
Dr. Clark B. Millikan
Dr. Barry L. Reeves
Dr. Anatol Roshko

Dr. Frank Marble
Dr. S. S. Penner
Dr. W. D. Rannie
Dr. Edward Zukoski

Dr. Harry Ashkenas
Mr. George Goranson
Dr. James M. Kendall
Dr. John Laufer
Dr. Thomas Vrebalovich
Mr. Richard Wood

Aeronautics Library (2)
Hypersonic Files (3)
Hypersonic Staff and Research Workers (2